INSIGHTS INTO THE ACTION MECHANISM OF AZACYANINES: THEIR TOPOISOMERASE IIα INHIBITION POTENTIAL AND NUCLEIC ACID SELECTIVITY

A THESIS SUBMITTED TO
THE GRADUATE SCHOOL OF NATURAL AND APPLIED SCIENCES
OF
MIDDLE EAST TECHNICAL UNIVERSITY

BY

SERCAN GÜLOĞLU

IN PARTIAL FULLFILLMENT OF THE REQUIREMENTS
FOR
THE DEGREE OF MASTER OF SCIENCE
IN
BIOCHEMISTRY

MAY 2018

Approval of the thesis:

INSIGHTS INTO THE ACTION MECHANISM OF AZACYANINES: THEIR TOPOISOMERASE IIα INHIBITION POTENTIAL AND NUCLEIC ACID SELECTIVITY

submitted by **SERCAN GÜLOĞLU** in partial fulfillment of the requirements for the degree of **Master of Science in Biochemistry Department, Middle East Technical University** by,

Prof. Dr. Halil Kalıpçılar
Dean, Graduate School of **Natural and Applied Sciences** _____

Prof. Dr. Bülent İçgen
Head of Department, **Biochemistry Department** _____

Assoc. Prof. Dr. Özgül Persil Çetinkol
Supervisor, **Chemistry Department, METU** _____

Examining Committee Members:

Prof. Dr. Orhan Adalı
Biological Sciences Dept., METU _____

Assoc. Prof. Dr. Özgül Persil Çetinkol
Chemistry Dept., METU _____

Assoc. Prof. Dr. Ayşe Elif Erson Bensan
Biological Sciences Dept., METU _____

Assoc. Prof. Dr. Gülay Ertaş
Chemistry Dept., METU _____

Assoc. Prof. Dr. Çağla Sönmez
Mol. Bio. and Gen. Dept., Konya Food & Agriculture University _____

Date: _____

I hereby declare that all information in this document has been obtained and presented in accordance with academic rules and ethical conduct. I also declare that, as required by these rules and conduct, I have fully cited and referenced all materials and results that are not original to this work.

Name, Last name :

Signature :

ABSTRACT

INSIGHTS INTO THE ACTION MECHANISM OF AZACYANINES: THEIR TOPOISOMERASE IIα INHIBITION POTENTIAL AND NUCLEIC ACID SELECTIVITY

Güloğlu, Sercan
M.Sc., Department of Biochemistry
Supervisor: Assoc. Prof. Dr. Özgül Persil Çetinkol

May 2018, 117 pages

Topoisomerase II alpha (Topo IIα) is one of the essential enzymes in cell viability. It is required for cell cycle progression due to its role in regulating the topological constraints during DNA replication and transcription. Due to its role, Topo IIα became one of the extensively exploited targets in chemotherapy, and there is an on-going research in design of small molecules targeting topoisomerase's catalytic activity at different stages using different mechanisms.

Within the scope of this thesis first, the effects of five azacyanine derivatives on Topoisomerase IIα enzyme (Topo IIα) at molecular level have been assessed by using an in-vitro Topoisomerase Drug Screening kit. Three of the azacyanines (Azamethyl, Azaethyl and Azaisobutyl) used were benzimidazole derivatives differing from each

other in terms of the alkyl chain length on the benzimidazole ring and two of them were benzothiazoles (Aza4 and Aza5). Second, the affinity and selectivity of these compounds towards different nucleic acid sequences and structures have been investigated by using competition dialysis method. Our primary goal was to accentuate azacyanines as probable Topo IIα inhibitors, and provide some mechanistic explanations for their effects.

Our results revealed that three of the five azacyanine molecules investigated in here decreases the catalytic activity of Topo IIα. Detailed investigation of the effect of Azamethyl on Topo IIα revealed that the effect on Topo IIα was concentration dependent, such that the higher Azamethyl concentrations led to stronger effect as determined by the intensity of the DNA bands in ethidium bromide (EtBr) stained agarose gels. Moreover, when used at the same concentrations (50.0 μM), Azamethyl showed stronger effect than Etoposide which is a well-known Topo IIα inhibitor being used in chemotherapy. Even better, the efficiency of 50.0 μM Azamethyl was higher than 500.0 μM Etoposide.

To shed light onto the mechanism of Topo IIα catalytic activity change, we further investigated the affinity and selectivity of azacyanines towards different nucleic acid sequences and structures via competition dialysis. We included three more azacyanines (Azapropyl, Azabutyl and Azaisopropyl) in our competition dialysis setup to understand the effect of the chain length and branching on the benzimidazole ring in nucleic acid binding affinity and selectivity. Our results revealed that the azacyanines were highly selective towards triple helical nucleic acid structure poly(dA).$[poly(dT)]_2$. More importantly, their affinity and selectivity towards poly(dA).$[poly(dT)]_2$ was decreasing with the increasing linear alkyl chain length, and increasing branching. The order of affinity was Azamethyl > Azaethyl > Azapropyl > Azabutyl > Azaisobutyl > Azaisopropyl.

Altogether, the findings presented in here demonstrate the potential of azacyanines to inhibit Topo IIα's catalytic activity.

Keywords: Azacyanine, Catalytic Activity Change, Topoisomerase II Alpha, Selectivity, Nucleic Acid Structure, Competition Dialysis.

ÖZ

AZASİYANİNLERİN ETKİ MEKANİZMASI: TOPOİZOMERAZ IIα ENGELLEME POTANSİYELİ VE NÜKLEİK ASİT SEÇİCİLİĞİ

Güloğlu, Sercan
Yüksek Lisans, Biyokimya Bölümü
Danışman: Doç. Dr. Özgül Persil Çetinkol

Mayıs 2018, 117 sayfa

Topoizomeraz II alfa (Topo IIα) hücre yaşamında görev alan temel enzimlerden birisidir. DNA replikasyonu ve transkripsiyonu sırasında DNA'nın topolojik kısıtlamalarının çözülmesini sağladığı için hücre döngüsü ilerleyişinde gerekli bir enzimdir. Bu rolü sebebi ile Topo IIα kemoterapide sıkça kullanılan bir hedeftir ve topoizomeraz enziminin katalitik aktivitesini değişik mekanizmalar ile farklı adımlarda etkileyebilecek küçük moleküllerin dizaynı konusunda devam eden birçok bilimsel çalışma bulunmaktadır.

Bu tez kapsamında, ilk olarak beş farklı azasiyanin türevinin Topo IIα üzerindeki etkisi moleküler düzeyde in-vitro Topoizomeraz tarama kiti ile incelenmiştir. Kullanılan üç azasiyanin molekülü (Azametil, Azaetil ve Azaisobütil)

benzimidazol türevi olup benzimidazol halka yapısındaki alkil zinciri uzunlukları ve dallanması bakımından birbirlerinden farklılık göstermektedirler. Diğer iki azasiyanin molekülü (Aza4 ve Aza5) ise benzotiyazol türevidir. İkinci olarak, bu tez kapsamında azasiyanin moleküllerinin farklı tip nükleik asit sekanslarına ve yapılarına olan ilgisi ve seçiciliği rekabetçi diyaliz yöntemi kullanılarak incelenmiştir. Bu çalışmanın asıl amacı azasiyanin moleküllerinin Topo IIα üzerine olabilecek muhtemel etkilerini açığa çıkartabilmek ve bu etkiler üzerine mekanistik bir açıklama ortaya koyabilmektir.

Elde etiğimiz sonuçlar, incelenen bu beş azasiyanin molekülünden üçünün Topo IIα enziminin katalitik aktivitesini azalttığını göstermiştir. Ayrıntılı incelemelerde, etidyum bromür (EtBr) boyalı agaroz jellerindeki bantların yoğunluğuna bakılarak Azametil molekülünün kullanılan konsantrasyona bağlı olarak TopoIIα enziminin katalitik aktivitesine negatif olarak etki ettiği görülmüştür. Özellikle aynı konsantrasyonlarda (50.0 µM) kullanıldığında Azametil molekülünün Etoposid molekülüne göre çok daha etkili olduğu saptanmıştır. Etoposid molekülü kemoterapide kullanılan ve etkisi kanıtlanmış bir Topo IIα inhibitörüdür. Daha da önemlisi, 50.0 µM Azametil molekülünün 500.0 µM Etoposid molekülünden bile daha etkili bir şekilde Topo IIα'nın katalitik aktivitesini düşürdüğü gözlemlenmiştir.

Topo IIα'nın katalitik aktivitesinin değişmesine ışık tutmak amacı ile azasiyanin moleküllerinin farklı nükleik asit sekanslarına ve yapılarına karşı olan ilgisi ve seçiciliği rekabetçi diyaliz yöntemi kullanılarak araştırılmıştır. Daha önce çalışılmamış üç azasiyanin molekülü (Azapropil, Azabütil ve Azaizopropil) de zincir uzunluğunun ve halka yapısının nükleik asitlere bağlanmadaki etkisini incelemek üzere rekabetçi diyaliz düzeneğine eklenmiştir. Sonuçlarımız azasiyanin moleküllerinin üçlü yapı sarmal yapı oluşturan poly(dA).$[poly(dT)]_2$ nükleik asit yapısına yüksek afinite ve seçicilik ile bağlandığını göstermiştir. Daha da önemlisi bu ilgi ve seçicilik benzimidazol halka yapısındaki artan zincir uzunluğu ve zincirin dallanma özelliğine göre azalma göstermiştir. Moleküllerin poly(dA).$[poly(dT)]_2$ üçlü DNA yapısına karşı olan ilgileri aşağıdaki sıraya göre gerçekleşmiştir. Azametil > Azaetil > Azapropil > Azabütil > Azaisobütil > Azaisopropil.

Burada sunulan bulgular azasiyanin moleküllerinin muhtemel Topo IIα katalitik inhibitörü olabilme potansiyellerine ışık tutmaktadır.

Anahtar kelimeler: Azasiyanin, Katalitik Aktivite Değişikliği, Topoizomeraz II Alfa, Seçicilik, Nükleik Asit Yapısı, Rekabetçi Diyaliz.

TO

SCIENCE

&

HUMANITY

ACKNOWLEDGEMENTS

I would like to express my deepest gratitude to my supervisor Assoc. Prof. Dr. Özgül Persil Çetinkol for her guidance, encouragements, support, and endless patience.

I would like to thank Prof. Dr. Ahmet M. Önal and his lab members for their help with the fluorescence experiments. I would also like to thank Assoc. Prof. Dr. Gülay Ertaş for her support throughout agarose gel experiments. Moreover, I would like to thank Prof. Dr. Orhan Adalı and Assoc. Prof. Dr. Çağdaş Devrim Son for their support during enzyme storage and handling.

I am also immensely grateful to my committee members Prof. Dr. Orhan Adalı, Assoc. Prof. Dr. Ayşe Elif Erson Bensan, Assoc. Prof. Dr. Gülay Ertaş, and Assoc. Prof. Dr. Çağla Sönmez.

This thesis could not be completed without the support of our lab team. I am therefore sincerely thankful to all my lab mates especially Fahriye Nur Alper and Ayça Küçükakdağ for their kind friendship and huge support throughout this project. I also thank Simge Kelekçi, Gözdem Çavdar, Serra Tütüncü, İpek Hazal Önen, and Aynur Özel for their help and friendship. Special thanks to Dr. Mehrdad Forough for his kind friendship and comments on this manuscript.

I would like to thank all administrative, academic, and technical staff of Department of Chemistry and Department of Biology, METU, for their support during my education.

I gratefully acknowledge Scientific and Technological Research Council of Turkey (TUBITAK) for financial support via project number 216Z074 and 116Z219. Moreover, Middle East Technical University funds BAP-08-11-2016-026 should also be acknowledged for financial support.

TABLE OF CONTENT

ABSTRACT v

ÖZ viii

ACKNOWLEDGEMENTS xii

TABLE OF CONTENTS xiii

LIST OF TABLES xvii

LIST OF FIGURES xviii

ABBREVIATIONS xxi

CHAPTERS 1

1.INTRODUCTION 1

1.1. DNA Structures 1

1.1.1. Triplex DNA and DNA/RNA Hybrids 3

1.1.2. Quadruplex DNA Structures 6

1.1.3. Targeting DNA by Using Small Molecules 8

1.2. Topoisomerases 10

1.2.1. Classification of Topoisomerases 10

1.2.2. Topoisomerase I 11

1.2.3. Topoisomerase II 13

1.2.4. Working Principle of Topoisomerase II 14

1.2.5. Biological Functions of Topoisomerase II 15

1.2.5.1. Topoisomerase II During DNA Replication 16
1.2.5.2. Topoisomerase II During Chromosome Segregation 16
1.2.5.3. Topoisomerase II During Transcription 17
1.2.5.4. Topoisomerase II in Neuronal Cells 19
1.2.5.5. Topoisomerase II in Recombination, Checkpoints, and DNA Repair 19
1.2.6. Topoisomerases as Targets in Cancer Treatment 21
1.2.7. Targeting Topoisomerases Using Small Molecules 21
1.2.7.1. Examples of Small molecules Targeting Topoisomerases 21
1.2.7.2. Cell Response to Topoisomerase Targeting Small Molecules..24
1.3. Effects of Azacyanines in Yeast Cells 25
1.4. Thesis Focus 28

2.POSSIBLE EFFECTS OF AZACYANINE DERIVATIVES ON TOPOISOMERASE II ALPHA (TOPO IIα) 29
2.1. Introduction 29
2.2 Materials and Methods 31
2.3. Results and Discussion 33
2.3.1. Determination of the Optimal Concentration of Azamethyl for Topoisomerase II Alpha Inhibition.....33
2.3.2. Determination of the Effects of Different Azacyanines on Topoisomerase II Alpha 37
2.4. Conclusions 39

3.SELECTIVITY OF AZACYANINES TOWARDS NUCLEIC ACID STRUCTURES 41
3.1. Introduction 41
3.2 Materials and Methods 43
3.3. Results and Discussion 45
3.3.1. Azamethyl 45
3.3.2. Azaethyl 49
3.3.3. Azapropyl 52
3.3.4. Azabutyl 55
3.3.5. Azaisopropyl 58
3.3.6. Azaisobutyl 61
3.3.7. Aza4 64
3.3.8. Aza5 67
3.4. Conclusions 70

4.THESIS CONCLUSION 73
4.1. Azamethyl, Aza4, and Aza5 Catalytically Inhibit Topo IIα 73
4.2 Azamethyl, Aza4, and Aza5 Bind to Triplex and Quadruplex Nucleic Acid Structures with High Affinity and Selectivity 74
4.3. Concluding Remarks 75

REFERENCES 77

APPENDICES

A.PREPARATION OF BUFFERS AND STOCK SOLUTIONS 91

B.OLIGONUCLEOTIDES USED IN COMPETITION DIALYSIS 97

C.CONSTRUCTION OF STANDARD CURVES 101

C.1. Standard Curve Preparation 101

C.2. Standard Curve for Azamethyl 104

C.3. Standard Curve for Azaethyl 105

C.4. Standard Curve for Azapropyl 106

C.5. Standard Curve for Azabutyl 108

C.6. Standard Curve for Azaisopropyl 109

C.7. Standard Curve for Azaisobutyl 110

C.8. Standard Curve for Aza4 112

C.9. Standard Curve for Aza5 113

D.STATISTICAL ANALYSIS 115

LIST OF TABLES

TABLES

Table 1. Extinction coefficients of azacyanines 32

Table 2. Competition dialysis results for Azamethyl 47

Table 3. Competition dialysis results for Azaethyl 50

Table 4. Competition dialysis results for Azapropyl 53

Table 5. Competition dialysis results for Azabutyl 56

Table 6. Competition dialysis results for Azaisopropyl 59

Table 7. Competition dialysis results for Azaisobutyl 62

Table 8. Competition dialysis results for Aza4 65

Table 9. Competition dialysis results for Aza5 68

Table B.1. Oligonucleotides used throughout the competition dialysis experiments 98

Table C.1. Preparation of samples for the standard curve construction 102

Table C.2. Equations derived from standard curves for each azacyanine molecule ... 114

Table D.1. Statistical analysis results of competition dialysis experiments 116

LIST OF FIGURES

FIGURES

Figure 1. DNA structures observed in the cell 2

Figure 2. Possible triplex structures in the cell 4

Figure 3. Different forms of G-quadruplexes 6

Figure 4. Possible locations of G-quadruplex structures in the cell 7

Figure 5. Working principle of Topoisomerase I 12

Figure 6. Functions of Topoisomerase II 14

Figure 7. Working principle of Topoisomerase II 15

Figure 8. Topo II action during transcription 18

Figure 9. Some Topo I poisons 23

Figure 10. Some Topo II poisons 24

Figure 11. Synthetic Topo II poison: Amsacrine 24

Figure 12. Chemical structure of azacyanines 27

Figure 13. Common Topoisomerase II catalytic inhibitors and poisons 30

Figure 14. Proposed reaction mechanisms for Topoisomerase IIα kDNA based drug screening kit 31

Figure 15. Agarose gel electrophoresis results for the effect of Azamethyl on Topo IIα 35

Figure 16. Agarose gel electrophoresis results obtained by analyzing the gel image given in Figure 15 36

Figure 17. Agarose gel electrophoresis results for different azacyanines on Topo IIα 38

Figure 18. Agarose gel electrophoresis results obtained by analyzing the gel image given in Figure 17 39

Figure 19. Average fluorescence spectra of Azamethyl. 46

Figure 20. Competition Dialysis results for Azamethyl 48

Figure 21. Average fluorescence spectra of Azaethyl. 49

Figure 22. Competition Dialysis results for Azaethyl 51

Figure 23. Average fluorescence spectra of Azapropyl 52

Figure 24. Competition Dialysis results for Azapropyl 54

Figure 25. Average fluorescence spectra of Azabutyl. 55

Figure 26. Competition Dialysis results for Azabutyl 57

Figure 27. Average fluorescence spectra of Azaisopropyl. 58

Figure 28. Competition Dialysis results for Azaisopropyl 60

Figure 29. Average fluorescence spectra of Azaisobutyl 61

Figure 30. Competition Dialysis results for Azaisobutyl 63

Figure 31. Average fluorescence spectra of Aza4. 64

Figure 32. Competition Dialysis results for Aza4 66

Figure 33. Average fluorescence spectra of Aza5 67

Figure 34. Competition Dialysis results for Aza5 69

Figure C.1. Standard curve construction for Azamethyl 104

Figure C.2. Standard curve construction for Azaethyl 105

Figure C.3. Standard curve construction for Azapropyl 106

Figure C.4. Standard curve construction for Azabutyl 108

Figure C.5. Standard curve construction for Azaisopropyl.....109
Figure C.6. Standard curve construction for Azaisobutyl 110
Figure C.7. Standard curve construction for Aza4.....112
Figure C.8. Standard curve construction for Aza5.....113

ABBREVIATIONS

ANOVA	Analysis of variance
ATM	Ataxia telangiectasia mutated
ATP	Adenosine triphosphate
ATR	ATM Rad3 related
Aza4	Azacyanine 4
Aza5	Azacyanine 5
Azabutyl	Azacyanine butyl
Azaethyl	Azacyanine ethyl
Azaisobutyl	Azacyanine isobutyl
Azaisopropyl	Azacyanine isopropyl
Azamethyl	Azacyanine methyl
Azapropyl	Azacyanine propyl
BPES	Buffered phosphate EDTA with sodium chloride
bp	Base pair
C_b	Bound molecule concentration
C_f	Free molecule concentration
C_t	Total molecule concentration
CD	Circular dichroism
ChIP	Chromatin immunoprecipitation
CIC	Catalytic inhibitory compound
cm	Centimeter

c-Myc	MYC proto oncogene
CPT	Camptothecin
DAPI	4’,6-Diamidino-2-phenylindole, dihydrochloride
Da	Dalton
Decaten.	Decatenated deoxyribonucleic acid products
DMSO	Dimethyl sulfoxide
DNA	Deoxyribonucleic acid
dsDNA	Double stranded deoxyribonucleic acid
dsRNA	Double stranded ribonucleic acid
EDTA	Ethylenediamine tetra acetic acid
ε	Epsilon (for extinction coefficient)
EtBr	Ethidium bromide
g	Gram
G segment	Gate segment
IDT	Integrated -DNA technologies
IFP	Interfering topoisomerase poisons
kDNA	Catenated deoxyribonucleic acid
L	Liter
λ	Lambda
M_1	Molarity of the first solution
M_2	Molarity of the second solution
M	Molar
m	Weight of the chemical
mL	Milliliter
mM	Millimolar
Mg	Magnesium

min	Minutes
m-AMSA	Amsacrine
µg	Microgram
µL	Microliter
µM	Micromolar
NaCl	Sodium chloride
$Na_2EDTA.2H_2O$	Disodium ethylenediamine tetraacetate dehydrate
NaH_2PO_4	Sodium phosphate monobasic
Na_2HPO_4	Disodium hydrogen phosphate
nm	Nanometer
NMR	Nuclear magnetic resonance
Plk-1	Polo-like kinase-1
RNA	Ribonucleic acid
ROS	Reactive oxygen species
SDS	Sodium dodecyl sulfate
ssDNA	Single stranded deoxyribonucleic acid
ssRNA	Single stranded ribonucleic acid
TAE	Tris acetate EDTA
Tel24	$[d(TTGGG(TTAGGG)_3A)]$
TFO	Triplex forming oligonucleotide
T segment	Trans passing segment
Topo I	Topoisomerase 1
Topo IIα	Topoisomerase 2 alpha
Topo IIβ	Topoisomerase 2 beta
UTR	Untranslated region
UV-Vis	Ultraviolet visible

V_1	Volume of the first solution
V_2	Volume of the second solution
VP-16	Etoposide

CHAPTER 1

INTRODUCTION

1.1. DNA Structures:

Deoxyribonucleic acid (DNA), which is the carrier of genetic information, plays a central role in life. It is the main player in replication and transcription, and therefore responsible for the development and maintenance of life. DNA that is mainly condensed inside the nucleus is mostly in B form, Watson-Crick DNA. It is made up of two anti-parallel polynucleotide strands that wind around each other with a right-handed twist, forming the double helical structure. In double helical structure, the bases occupy the inside of the helix and the sugar-phosphate chains face to the outside. Its conformation provides a direct and easy access to replication and transcription related proteins like polymerases. Furthermore, B-form DNA is the most compatible form for packaging the long polymer inside the nucleus due to its tight bending capability. Its stability, flexibility and dynamic conformation are thought to be the main reasons behind the selection of DNA as the genetic material instead of ribonucleic acid (RNA). (Travers & Muskhelishvili, 2015).

After the discovery of right-handed double helical structure of B-form DNA by Watson and Crick in 1953 (Watson & Crick, 1953) there have been many revolutions in our understanding of the DNA structure and function.

Besides B-form DNA, other kinds of DNA structures such as A-DNA, Z-DNA, i-motifs, hairpins, bulges, stem-loops, pseudoknots, cruciforms, triplexes, and G-

quadruplexes have been discovered (Bachurin, Kletskii, Burov, & Kurbatov, 2018) (Figure 1). All of these structures that mostly have non-canonical (non-Watson-Crick) base pairing arrangements are found to play distinctive crucial roles in cell cycle regulation. Especially triple helical (triplex) and quadruplex structures received great attention in the last two decades due to their likely roles in gene expression and uncontrolled cell division associated with formation of cancerous tumors (H. Han & Hurley, 2000; Van Dyke & Nelson, 2013). It has been shown that triplex and quadruplex structures also have essential roles such as protecting DNA from degradation and keeping promoters silent (Rigo, Palumbo, & Sissi, 2017; Toscano-Garibay & Aquino-Jarquin, 2014).

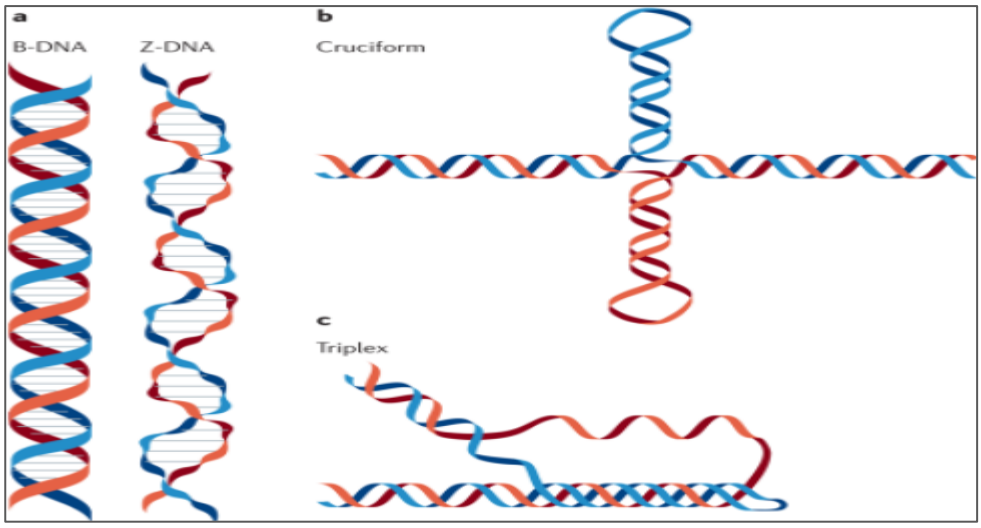

Figure 1. DNA structures observed in the cell. a.B-form DNA and Z-form DNA. b. Cruciform. c. Triplex. (Bochman, Paeschke, & Zakian, 2012). Reprinted from (*Nat. Rev. Genet.*), Vol.13, Copyright (2012) with permission from (Springer Nature).

Triplex structures are generally formed by the placement of a third strand in the major groove of the double helical structure. Four stranded G-quadruplex structure are generally formed by the association of guanine rich strands. (Bissler, 2007; Gacy *et al*., 1998; Hanahan & Weinberg, 2011).

1.1.1. Triplex DNA and DNA/RNA Hybrids:

Although triple helical structures are known for a long time, it took quite some time to realize their importance. In triple helix formations basically a third strand, so called triplex-forming oligonucleotide (TFO), binds to a duplex DNA structure via non-canonical Hoogsteen base pairing (Frank-Kamenetskii & Mirkin, 1995). Triple helical structures are mostly classified as purine motifs or pyrimidine motifs. In a purine motif, purine rich TFO binds to the purine strand of the duplex via reverse-Hoogsteen base pairing in an antiparallel orientation. On the other hand, in the pyrimidine motif, pyrimidine rich TFO binds to the purine strand of the duplex via Hoogsteen base pairing in a parallel orientation (Bing *et al*., 2017). DNA itself and RNAs such as long non-coding RNAs, promoter-associated RNAs, promoter inhibiting RNAs, promoter RNAs, small interfering RNAs, and micro RNAs are all considered as potential TFOs (Toscano-Garibay & Aquino-Jarquin, 2014) (Figure 2).

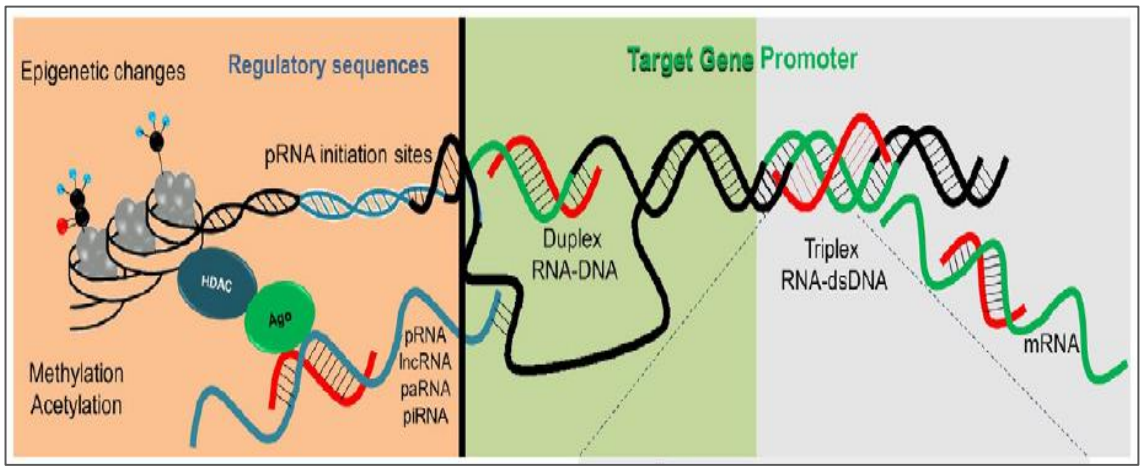

Figure 2. Possible triplex structures in the cell. (Toscano-Garibay & Aquino-Jarquin, 2014). Reprinted from (*Biochim. Biophys. Acta*), Vol.1839, Copyright (2014) with permission from (Elsevier).

Triplex forming oligonucleotides gained great attention in the last two decades with respect to controlling gene expression. Oligonucleotides can be used for controlling gene expression via antisense approach, which is composed of different strategies such as antisense and antigene strategies (Helene, Thuong, & Harel, 1992; Rakoczy, 2001). In the antisense strategy, oligonucleotides can be used to target messenger RNAs therefore downregulating protein production. On the other hand, in the antigene strategy, oligonucleotides can be used as triplex forming oligos (TFOs) by binding specific sequences on DNA thereby inhibiting the transcription of the gene (Helene *et al*., 1992; Rakoczy, 2001). As for controlling the gene expression, it has been shown that triple helices are related to gene silencing (Toscano-Garibay & Aquino-Jarquin, 2014), DNA damage, and DNA repair mechanisms (Ni *et al*., 2018). Therefore, triplex formation can be used in silencing the oncogenes to prevent tumor growth.

Furthermore, there are also several in-vitro studies, published recently, showing the emerging roles of triplex nucleic acid structures in various areas such as biosensors, sequence specific labeling, DNA based nanostructures, and RNA biology (Chen *et al*., 2015; Conrad, 2014; M. S. Han, Lytton-Jean, & Mirkin, 2006; Hu, Cecconello, Idili, Ricci, & Willner, 2017).

Nevertheless, triplex structures are generally unstable compared to their corresponding duplex structures because of the weaker Hoogsteen base pairing. Since their stability is essential in impeding gene expression and/or regulation, stabilizing such structures has become a major focus in rational drug design research. One way to increase the stability of these structures is to design small molecules that tightly and selectively bind to them. Despite many different types of stabilizing small molecules present there is still a need for better and more effective triplex binding molecules (Chaires *et al*., 2003; Escudé *et al*., 1998; M. S. Han *et al*., 2006).

On the other hand, the formation of stable triplex sequences in-vivo could be harmful for normal cells. It has been shown that polypurine-polypyrimidine mirror repeats (triplex forming sequences) could give rise to various diseases by causing mutations or altering gene expression (Bissler, 2007). There are a number of inherited as well as acquired diseases associated with the potential formation of stable triple helical structures due to the presence of trinucleotide repeats such as Friedreich's ataxia, Tuberosis sclerosis complex, Autosomal dominant polycystic kidney disease, and Follicular lymphoma (Bissler, 2007).

Among these diseases Friedreich's ataxia, is an autosomal recessive disease which exhibits progressive degeneration of nerve tissues located in the spinal cord and nerves in the legs and arms. The gene, responsible for this disease, is located on chromosome 9 and normally contains 7-22 GAA repeats. However, in Friedreich's ataxia patients number of repeats increases abruptly, to hundreds or thousands. These increased numbers of repeats are in return cause the formation of hinged DNA (H-DNA) that interferes with the gene expression. This process gives rise to reduced

number of frataxin protein which is a mitochondrial protein that controls cellular iron homeostasis. Reduced number of frataxin, then, causes reduced muscle activity (Bissler, 2007; Frank-Kamenetskii & Mirkin, 1995).

1.1.2. Quadruplex DNA Structures:

It is known that the formation of quadruplex structures is dependent on guanine nucleotides. Planar arrangement of four guanine bases forms G-quartets, where the stacking of these G-quartets results in the formation of the G-quadruplex structures (Bing *et al*., 2017). There are structurally different quadruplexes based on the number of guanine bases and the number of strands involved in the formation of the structure (Figure 3).

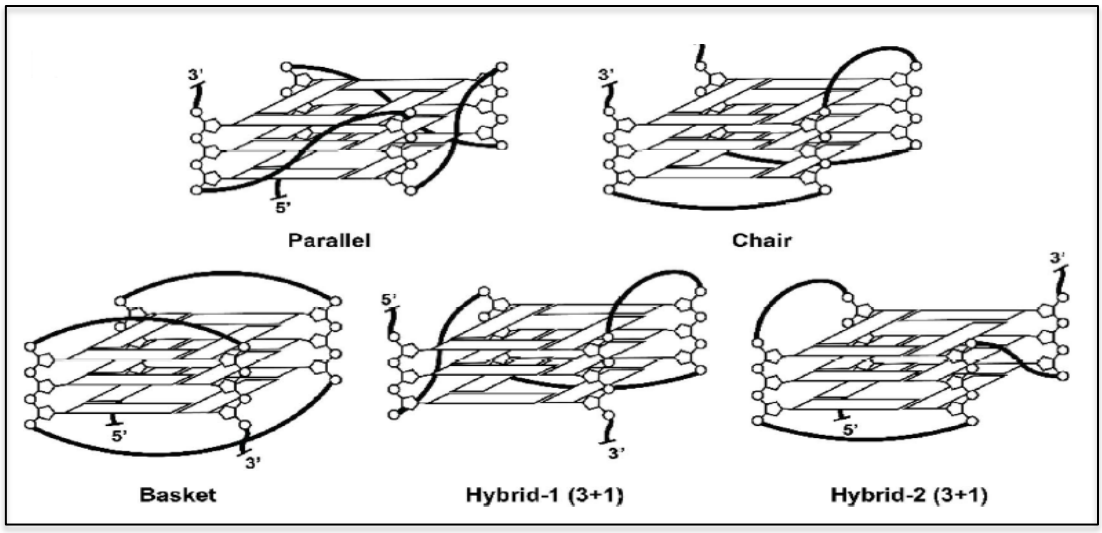

Figure 3. Different forms of G-quadruplexes.(Harkness & Mittermaier, 2017). Reprinted from (*Biochim. Biophys. Acta*), Vol.1865, Copyright (2017) with permission from (Elsevier).

The formation of G-quadruplex structures in-vitro is well established and the propensity of guanine rich sequences to form G-quadruplex structures in-vivo is well accepted. Genome-wide bioinformatic analyses revealed that the guanine rich sequences are particularly present at the end of the chromosomes, telomeres, and in promoter regions such as the ones seen in c-myc gene (Rigo *et al*., 2017) (Figure 4).

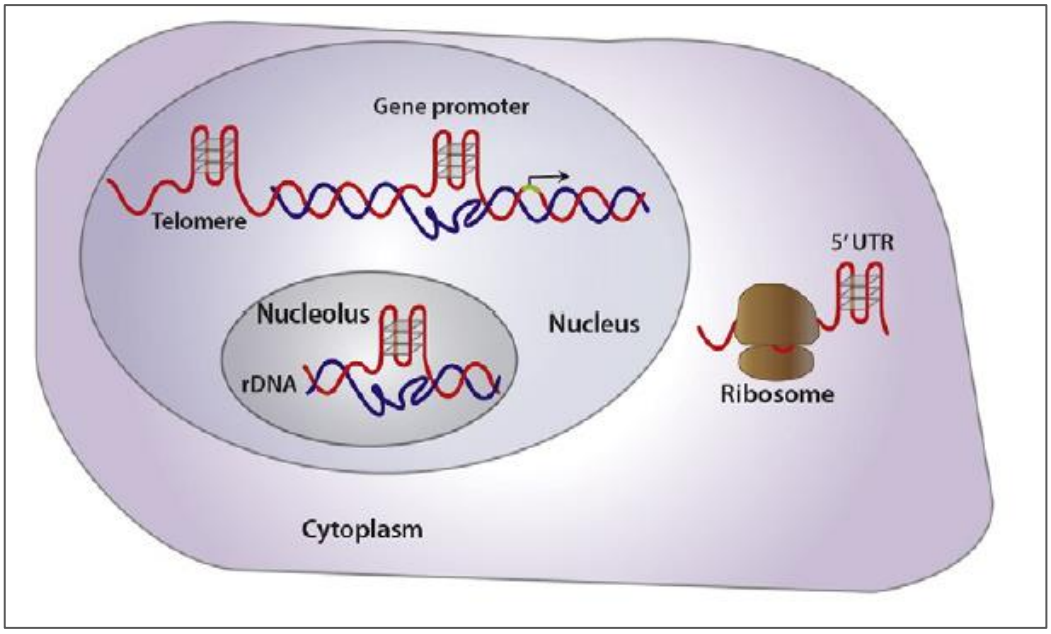

Figure 4. Possible locations of G-quadruplex structures in the cell. (Rigo *et al*., 2017). Reprinted from (*Biochim. Biophys. Acta*), Vol.1861, Copyright (2017) with permission from (Elsevier).

Guanine rich sequences are believed to play very important roles in regulation of many cellular functions such as telomere maintenance, transcription regulation, and translational & post-translational regulation of RNAs (Bing *et al*., 2017). For instance, roles of guanine rich sequences at the end of the telomeres include prevention of

chromosome fusions which would otherwise give rise to genomic instability and prevention of degradation of chromosome ends. Furthermore, guanine rich sequences at transcription start sites are believed to control the gene expression (Rigo *et al*., 2017). Another function of guanine rich sequences appears in RNA biology. G-quadruplex structures on RNA molecules could have many roles such as translation regulation, 3'end formation, transcription termination, RNA localization, splicing regulation, and ribonucleoprotein formation (Fay, Lyons, & Ivanov, 2017).

Due their possible roles in gene expression and gene regulation, guanine rich sequences are one of the most sought after structures in cancer treatment. For instance, it is proposed that driving the formation of quadruplex structures and stabilizing them in guanine rich oncogenes such as c-Myc, could be enough to halt the over-expression of these genes in cancer cells (Siddiqui-Jain, Grand, Bearss, & Hurley, 2002)

1.1.3. Targeting DNA by Using Small Molecules:

Nucleic acids play essential roles in various biological processes like gene storage, transcription, replication etc. Therefore, one can regulate many biological processes by targeting the nucleic acid structures in-vivo. This approach forms the basis of the most conventional drug design studies (M. Wang, Yu, Liang, Lu, & Zhang, 2016). Nucleic acids are the most preferred targets compared to proteins and protein-like factors mainly due to their upstream roles. Additionally, the existence of alternative nucleic acid structures, namely duplex, triplex, and quadruplex makes them desirable targets for various drugs in the treatment of several diseases (M. Wang *et al*., 2016).

Wang *et al*. summarized the importance and the recent advances in developing small molecules that target nucleic acid structures. Small molecules could interfere with biological processes by binding to the nucleic acid structures, and altering either their structure or their interactions with other proteins and/or nucleic acid structures. For instance, the binding of a small molecule to a DNA sequence could block the enzyme binding, such as topoisomerase or DNA polymerase, to that very same sequence by blocking the recognition of the sequence by these proteins due to a

change triggered in DNA's conformation upon small molecule binding (M. Wang *et al*., 2016).

There are numerous examples of small molecules targeting duplex DNA using different modes of binding. For instance, psoralen, aflatoxin B, N^4C-ethyl-N^4C, mitomycin C, and N^2G-ethyl-N^2G target DNA duplex by forming covalent bonds with the DNA structure. On the other hand, while netropsin, distamycin, DAPI, berenil, pentamidine, and Hoechst 33258 are targeting DNA duplex by binding to the minor groove, neomycin, nogalamycin, and neocarzinostatins are targeting DNA duplex by binding to the major groove via non-covalent interactions. Additionally, daunomycin, adriamycin, ditercalinium, and cryptolepine which are known as intercalators are also targeting DNA duplex via non-covalent interactions, mainly by stacking between base pairs. Furthermore, there are molecules targeting DNA duplex via multiple binding modes such as PBD-BIMZ and PBD-naphthalimide (M. Wang *et al*., 2016).

On the other hand, there are also numerous studies targeting triplex nucleic acid structures. For example, benzopyridoindole derivatives such as benzo[e]pyridoindole (BePI) and benzo[g]pyridoindole (BgPI) have been demonstrated as successful triplex stabilizing small molecules. Moreover, coralyne, a berberine alkaloid, is a well-known natural product that stabilizes triplex structures. Other studies also showed the binding and selectivity of naphtylquinoline, bis-amidoantraquinones, and amidoglycosides towards triplex DNA structures (Fox & Darby, 2004). Additionally, neomycin-pyrene computational modelling also demonstrated that that these small molecules target triplex DNA structures through both groove binding and intercalation (M. Wang *et al*., 2016).

Quadruplex DNA structures are also targets for small molecules as mentioned before. For instance, distamycin A, daunomycin, RHPS4, Tmpyp4, Telomestatin, and BRACO 19 targets quadruplex structures (M. Wang *et al*., 2016). Moreover, it had been recently shown that -newly synthesized small molecule- CX-5461, which is a

polymerase I derived rRNA inhibitor, has the ability of stabilizing G-quadruplex structures on DNA (Xu *et al*., 2017).

1.2. Topoisomerases:

Throughout DNA transcription, replication, and recombination several proteins and enzymes play crucial roles. During these processes unwinding DNA is a prerequisite for proteins to enter to the site. However, unwinding DNA subsequently creates some topological problems since unwinding one site would give rise to overwinding elsewhere on the DNA. This topological problem is solved by topoisomerase enzymes. They are responsible from linearizing and/or releasing the torsion on the DNA. By doing so other proteins can enter to the site and required process may continue. Linearizing DNA by topoisomerases, however, is a very complex mechanism involving DNA cleavage, DNA relaxation, and finally religation of the phosphate backbone in order to restore the integrity of the DNA continuity (Winkler, 2011). Detailed molecular mechanisms are given in the following sections.

1.2.1. Classification of Topoisomerases:

Topoisomerases are classified mainly into two groups as Type I (Topo I) and Type II (Topo II) based on their ability to cleave only one or both of the DNA strands respectively. In other words, while Type I topoisomerases introduce single strand breaks, Type II topoisomerases introduce double strand breaks (Champoux, 2001; J. C. Wang, 1998). Odd numbered enzymes (e.g. “I” or “III”) generally fall into type I topoisomerases, whereas evenly numbered enzymes (e.g. “II” or “IV”) generally fall into type II topoisomerases. There are also many sub classifications of topoisomerases where letters “A”, “B”, or “C” indicate the subtype. Subtypes usually differ from each other in amino acid sequence, structure, and/or function (Vos, Tretter, Schmidt, & Berger, 2011).

There are six functionally different topoisomerases encoded by the human genome which are organized into three main groups; type I (type Ia and type Ib), type II (type

IIa and type IIb), and type III (type IIIa and type IIIb) (Pommier, 2013). All of these enzymes have distinctive roles in the cell. Moreover, while topoisomerase type I and type II enzymes are abundant in the nucleus, topoisomerase type III enzyme is abundant in mitochondria. The distinctive roles of Topo I and Topo II enzymes in the cell are explained in detail below.

1.2.2. Topoisomerase I:

Type I topoisomerase enzyme helps fork movement during relaxation of DNA and all higher eukaryotes contain at least one type I topoisomerase enzyme. Type I topoisomerases are further divided into two sub-families; type Ia which relaxes only the negatively supercoiled DNA and type Ib which relaxes both the negatively and positively supercoiled DNA (Goto, Laipis, & Wang, 1984; Liu & Miller, 1981). Mammalian cells have type Ib sub-family. Type Ib topoisomerases share no homology with the other type of topoisomerases and are functionally distinct from type Ia topoisomerases (Uday Bhanu & Kondapi, 2010).

Topoisomerase I (Topo I) has essential roles for the normal development of the cell (Morham, Kluckman, Voulomanos, & Smithies, 1996). It simply relaxes supercoiled DNA thus ease the entrance of other enzymes and/or proteins into the required site. Unless Topo I works properly, helical constraints of the supercoiled DNA may hinder DNA replication or/and transcription processes (Gilmour, Pflugfelder, Wang, & Lis, 1986; J. Wu, Phatnani, Hsieh, & Greenleaf, 2010). It has been shown that inactivation of Topo I reduced the transcription rate of *Saccharomyces cerevisiae* and disturbed the development of *Drosophila melanogaster* (Uday Bhanu & Kondapi, 2010).

The working principle of Topo I is illustrated in Figure 5. It is based on trans-esterification reaction that occurs between the tyrosine residue located in the topoisomerase's active site (tyrosine 723 in humans) and 3' phosphodiester backbone of the DNA. Then rotation of free 5' hydroxyl end over the intact DNA strand takes place. After the relaxation of the duplex, 5' hydroxyl end acts as a nucleophile and reverse trans-esterification occurs towards the phosphotyrosil bond. Topo I is liberated

after DNA re-ligation and catalyzes another nicking, closing, relaxation cycle elsewhere in the genome (Pommier & Cherfils, 2005). After relaxation, DNA or RNA polymerases will continue with replication or transcription (Barros *et al*., 2013; Uday Bhanu & Kondapi, 2010).

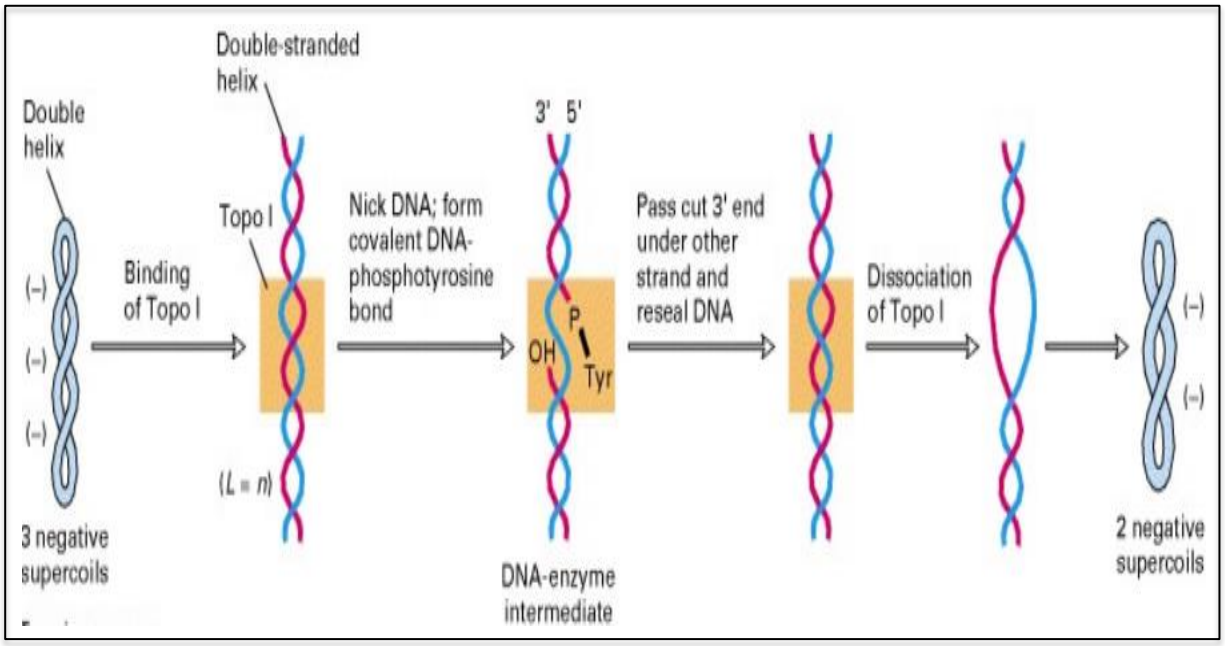

Figure 5. Working principle of Topoisomerase I (Lodisch *et al*., 2000).

However, despite the importance in relieving the torsional stress, Topo I also possesses serious dangers to the cells. It can trigger genomic instability when encounters with a non-B DNA structure or might interfere with continuing gene expression. As a result of interference, negatively supercoiled strands might accumulate at one site and eventually promote the formation of R-loops and/or stable non-B DNA structures like quadruplexes. This action, at the end, has the capability of interfering with DNA replication and provide highly toxic double strand breaks (N. Kim & Jinks-

Robertson, 2017). Thus, targeting Topo I and/or interfering with its activity can be used in the treatment regime of cancer to kill the malignant cells.

1.2.3. Topoisomerase II:

Topoisomerase II enzymes (Topo II) are believed to play a role in DNA replication, chromosome condensation, chromosome segregation, transcription, DNA repair, and neuronal activities although some of these roles are controversial (J. Nitiss, 2009; Vos *et al*., 2011). In mammalian cells, there are two Topo II isozymes (type IIα and type IIb) while in other eukaryotic cells there is only one Topo II (J. L. Nitiss, 2009).

As mentioned before, in order to solve the topological problems in DNA, introduction of DNA strand breaks is obligatory. Topoisomerases provide a safe way for DNA breaks by protecting the cut edges of the breaks. Topo II's function seems more important in this aspect because it creates double strand breaks while Topo I creates single strand breaks, which can be compensated by other strand of the DNA. If the cut site is not protected by the enzyme after Topo II cleavage, mutations might arise due to the unrepaired double strand break. Topoisomerase II enzymes function in two different ways; decatenation of catenated DNA and/or relaxation of supercoiled DNA (Figure 6).

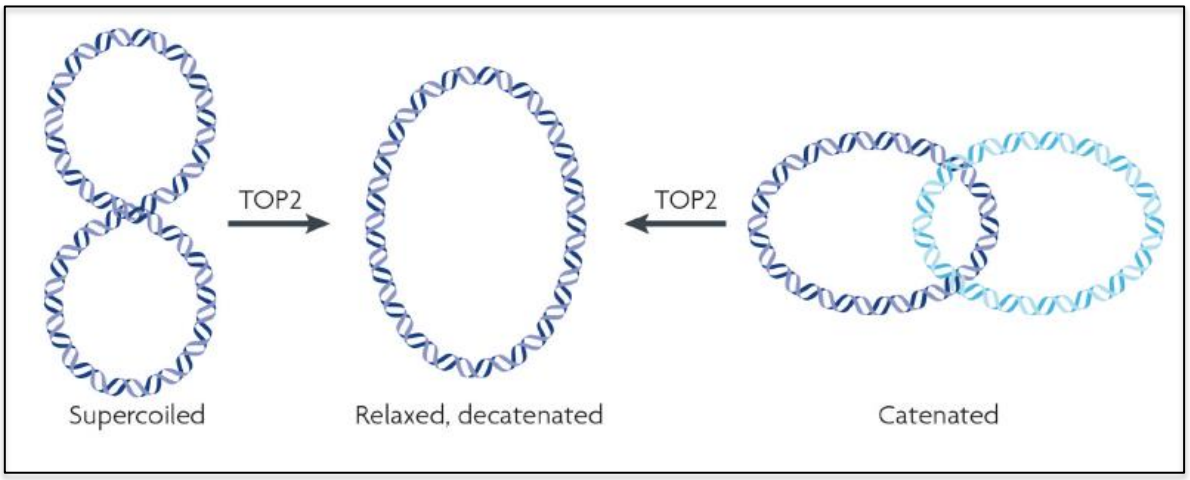

Figure 6. Functions of Topoisomerase II (J. Nitiss, 2009). Reprinted from (*Nat. Rev. Cancer*), Vol.9, Copyright (2009) with permission from (Springer Nature).

1.2.4. Working Principle of Topoisomerase II:

Topoisomerase II enzymes are homodimeric where each subunit breaks one DNA strand to create a double strand break. As illustrated in Figure 7, Topo II interacts with two strands of DNA to complete the passage. It introduces a double stranded break in one DNA strand which is called as G segment (gate segment), and then passes the other DNA strand, which is called the T segment, through the break. T segment is passed through the G segment by the enzyme via ATP dependent reaction. Then the break in G segment is resealed (J. Nitiss, 2009).

Enzyme cleavage of G strand is achieved in the presence of Mg^{2+} by forming a phosphotyrosine linkage between each of the DNA single strands. On the other hand, it produces a free tyrosine in each subunit of the enzyme. Then a closed clamp is formed by ATP binding to the enzyme. This closed clamp captures T segment and passes it through the break in the G segment. After the passage, T segment leaves the enzyme through the carboxy terminus. ATP hydrolysis occurs twice during the whole process. First ATP is used to assist in strand passage. The second ATP is used to re-open the

clamp. G segment may be released after the process or, if it is necessary, enzyme may go through another catalytic cycle without dissociating the G segment (Figure 7). This mechanism of Topo II provides some advantages like protection of DNA ends of the break and the ability of quick and efficient religation of DNA breaks (J. Nitiss, 2009).

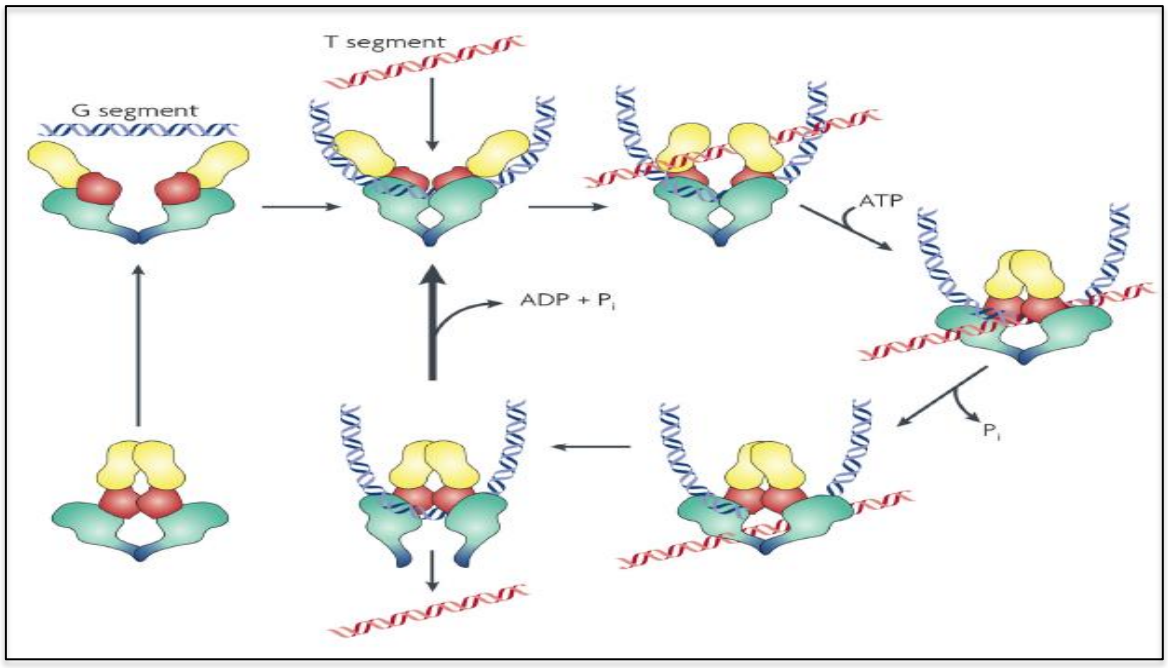

Figure 7. Working principle of Topoisomerase II (J. Nitiss, 2009). Reprinted from (*Nat. Rev. Cancer*), Vol.9, Copyright (2009) with permission from (Springer Nature).

1.2.5. Biological Functions of Topoisomerase II:

As mentioned above, Topo II enzyme has a vital role in several processes during cell cycle and metabolism. The role of Topo II in some of these specific processes are discussed in detail below (Ferguson & Baguley, 1994; J. Nitiss, 2009; Vos *et al*., 2011).

1.2.5.1. Topoisomerase II During DNA Replication:

DNA replication is a semi-conservative process which occurs via unwinding of two DNA strands followed by the replication of each strand. In the absence of a functional topoisomerase in the replication fork, positively supercoiled DNA accumulates. The accumulation of DNA results in several topological problems and ultimately blocks the replication. Early stages of replication only require Topo I activity to relax the DNA. But in the later stages of replication when two replication forks impinge on each other, Topo I cannot fit into the replication site to relax the DNA. At this stage where two interlinked catenanes present, Topo II activity is required for decatenation of the dimer (J. Nitiss, 2009; Vos *et al*., 2011). Topo II action during the replication elongation includes catenation of pre-catenane structures (Lucas, Germe, Chevrier-Miller, & Hyrien, 2001).

Type II topoisomerases are composed of two subtypes; Topo IIα and Topo IIβ. It is believed that human Topo IIα has different functions than Topo IIβ and other type II topoisomerases at lower eukaryotic cells. It is observed that Topo II relaxes positively supercoiled DNA more actively than negatively supercoiled DNA (McClendon, Rodriguez, & Osheroff, 2005). Since it is the positively supercoiled DNA that is accumulating during the replication fork movement, Topo IIα is hypothesized to play a more crucial role then Topo IIβ. Yet, several studies have proven this hypothesis. Li *et. al*. had shown that the phosphorylation of Topo IIα during S-phase is a prerequisite for the replication process (H Li, Wang, & Liu, 2008). Moreover, it has been shown that while Topo IIβ knockout cells can be recovered and continue with the replication, Topo IIα knocked down cells failed to continue with the replication (J. Nitiss, 2009)

1.2.5.2. Topoisomerase II During Chromosome Segregation:

During mitosis, duplicated chromosomes must be segregated from each other once the replication is completed. Topoisomerases aid during this process by compacting DNA and holding sister chromatids together during chromosome line up at

the center of the cell. Afterwards sister chromatids are separated from each other by topoisomerase action. Although catenated DNA is a problem for early replication process, at chromosome segregation step, catenated sister chromatid generation helps for proper chromosome lining at the center of the cell. DNA compaction via catenation, performed by topoisomerases, facilitates the chromosome segregation (J. Nitiss, 2009; Vos *et al*., 2011).

It was once believed that catenated DNAs were the sole reasons behind the staying of sister chromatids together. But it had been clearly shown that the specialized proteins called cohesins are the main players in keeping sister chromatids together (Diaz-Martinez, Gimenez-Abian, & Clarke, 2008; Losada & Hirano, 2005). It had been observed that even though the cohesins are essential for the sister chromatid cohesion, their absence is partly tolerated (Huang, Milutinovich, & Koshland, 2005; Michaelis, Ciosk, & Nasmyth, 1997). One possible explanation for this situation is the maintenance of cohesion with catenated DNA formation.

Another relation of topo II enzyme with the chromosome segregation is its association with the factors like aurora B kinase and the polo-like kinase (Plk-1) which are responsible for centromere formation and segregation (Coelho *et al*., 2008; H Li *et al*., 2008). Although these interactions are not well understood, co-localization of topo II with Plk-1 and aurora kinase B might be important for centromere resolution (Vos *et al*., 2011).

1.2.5.3. Topoisomerase II During Transcription:

During transcription, RNA polymerase action gives rise to localized positively supercoiled DNAs ahead of transcription bubble (Liu & Wang, 1987; H. Y. Wu, Shyy, Wang, & Liu, 1988) (Figure 8). If these positively supercoiled strands are left unchecked, stable R loop (RNA-DNA hybrids) formation might be observed (Marc Drolet, Bi, & Liu, 1994). Since the formation of such structures cause genomic instability, the cell growth will be impaired due to the formation of DNA breaks (M Drolet *et al*., 1995; Tuduri *et al*., 2009).

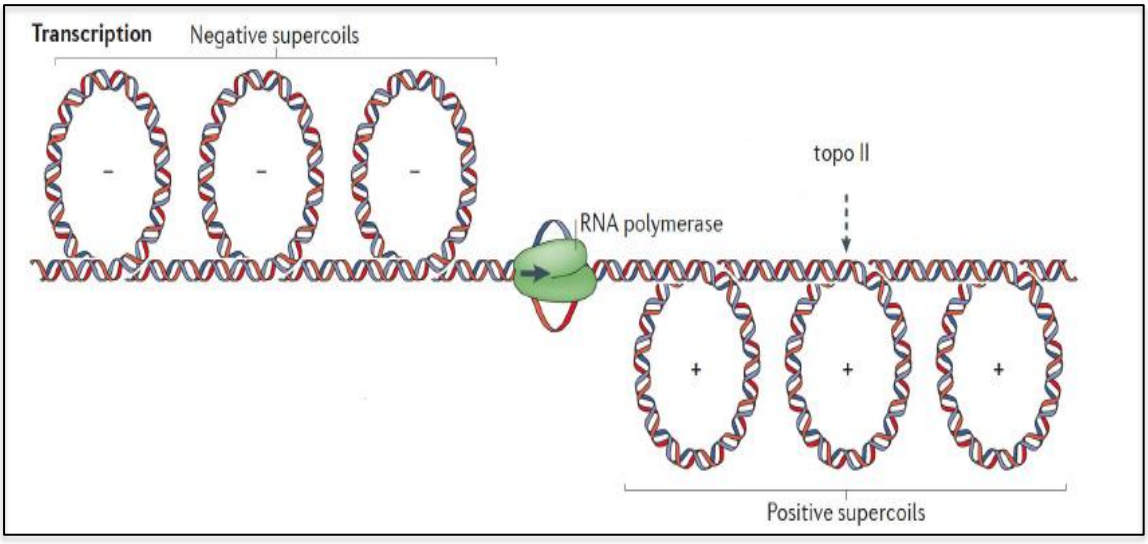

Figure 8. Topo II action during transcription (Vos *et al*., 2011). Reprinted from (*Nat. Rev. Mol. Cell Biol.*), Vol.12, Copyright (2011) with permission from (Springer Nature).

Although it has been shown that topo I enzymes work more actively at transcription site to remove the negative supercoils, a sub-type of topo II enzyme, topo IIβ has been observed at many promoter sites of highly transcribed genes (J. Nitiss, 2009; Vos *et al*., 2011). Ju *et al*. showed topo IIβ localization on the promoter of genes which were activated by nuclear hormone receptors by means of chromatin immunoprecipitation (ChIP) experiments (Ju *et al*., 2006; Ju & Rosenfeld, 2006). The finding in their studies was the co-localization of topo IIβ with DNA repair related proteins (PARP, Ku70/Ku86, and DNA dependent protein kinase) at the transcription initiation site. This type of localization and function is different than the function of topo IIβ in double stranded DNA breakage. It is believed that topo IIβ is recruited to promoters for its enzymatic function. Nevertheless, the absolute function and the

underlying mechanism of topo IIβ during transcription still needs to be elucidated (J. L. Nitiss, 2009)

1.2.5.4. Topoisomerase II in Neuronal Cells:

Topo IIβ had been also found to have a unique role in certain neuronal cells. No other type of topoisomerase has been found to have such a role (J. L. Nitiss, 2009). Topo IIβ had been established as one of the crucial enzymes for the neural development (Lyu & Wang, 2003; Yang, Li, Prescott, Burden, & Wang, 2000). Experiments in these studies were based on the loss of function of topo IIβ. Mice with homozygous deleted topo IIβ genes were inviable because of several neuronal deficits related to motor neuron failures. Microarray analysis of the same mice showed, approximately 1-4% of expressed genes were different. Furthermore, scientists showed that the localization of topo IIβ on various genes that are mostly related to developmentally regulated genes. Together these findings showed the importance of topo IIβ on neural cell development both directly and indirectly (J. L. Nitiss, 2009).

1.2.5.5. Topoisomerase II in Recombination, Checkpoints, and DNA Repair:

Various types of topoisomerases in the cell give rise to double stranded DNA (dsDNA) breaks. These dsDNA breaks in a way, impacts different mechanisms in the cell such as cell cycle checkpoint response activation, meiotic recombination, and DNA repair (J. Nitiss, 2009; Vos *et al*., 2011).

Several other topoisomerase like proteins accompany topoisomerase enzymes throughout these processes. For example: topo IIβ-A subunit homolog, Spo 11, creates dsDNA breaks during homologous recombination (Bergerat *et al*., 1997; Keeney, Giroux, & Kleckner, 1997; Pecia *et al*., 2002). After formation of dsDNA break by Spo11, protein must be detached from the DNA to prevent mutations (Neale, Pan, & Keeney, 2005). At this point, double strand break repair proteins like Rad50-Mre11-Nbs1 (MRN) complex (Keeney, 2008; Neale *et al*., 2005), Rad51 and Dmc1-like factors (Baudat, Manova, Yuen, Jasin, & Keeney, 2000; W. Li & Ma, 2006), and

nuclease Sae2/CtIP (Hartsuiker *et al*., 2009) remove Spo11 from the DNA in an independent mechanism from ATM (ataxia telangiectasia mutated) and ATR (ATM Rad3-related), which are the most known repair pathways.

As a consequence of their role on introducing strand breaks, topoisomerases can also promote DNA repair mechanism. Cliby *et al*. showed ATM and ATR pathway activation upon Topo I caused breakage (Cliby, Lewis, Lilly, & Kaufmann, 2002). Moreover Treszezamsky *et al*. showed BRCA1 and BRCA2 pathway activation after topoisomerase II caused dsDNA breaks (Treszezamsky *et al*., 2007). All of these pathways are known to have a role both in cell cycle arrest and DNA repair mechanism. Several other studies showed that SUMOylation and ubiquitinylation mediated destruction of topoisomerase enzymes, in which they inadvertently trapped with DNA in a covalent complex. Once the topoisomerase is destroyed, repairing enzymes such as Tdp1 and Tdp2 help to repair the covalent tyrosine-DNA adducts. In other words, the activation of the checkpoint response and DNA repair is dependent on both the type of the breakage and the enzymes involved in the process. However, the exact mechanism is not elucidated in detail yet (Vos *et al*., 2011).

There are also several studies showing the role of Topo II in cell cycle arrest. In one study, it had been shown in yeast cells that whereas a complete depletion of Topo II did not lead to cell cycle delay during mitosis, expression of the inactive Topo II led to a mitotic delay (Baxter & Diffley, 2008). This observation suggests that Topo II presence is needed to trigger the cell cycle arrest (Andrews *et al*., 2006). On the contrary, in another study, it had been observed that removal of Topo II via Tet-off system caused a mitotic delay but the depletion of Topo IIα via siRNA system did not induce mitotic delay (Hongchang Li, Wang, & Liu, 2008). The latter experiment suggests that knockdown of Topo IIα was insufficient to induce DNA repair which supports the conclusion of Andrews *et al.* (Andrews *et al*., 2006).

1.2.6. Topoisomerases as Targets in Cancer Treatment:

Although topoisomerase enzymes are very important for cell viability, any corruption on their DNA cleavage activity would give rise to mutagenic DNA breaks which may eventually lead to cell death. Scientists exploited this situation to deliberately kill malignant cells via topoisomerase inhibition in cancer therapy since 1980s. Several proteins, small molecules, and protein-like factors that can inhibit topoisomerase activity had been discovered. The mode of action of these molecules varies greatly. One kind attenuates the DNA binding activity of these enzymes, another attenuates the enzyme's ability to cleave DNA (Vos *et al*., 2011).

1.2.7. Targeting Topoisomerases Using Small Molecules:

1.2.7.1. Examples of Small molecules Targeting Topoisomerases:

There are two broad classes of topoisomerase targeting small molecules based on their mode of action: "inhibitors" affect the enzyme activity and "poisons" stabilize DNA-enzyme complex. Whereas the effects of inhibitors are reversible, the effects of poisons are irreversible. And therefore poisons are considered to be more toxic for cells than inhibitors (Nitiss, 2009).

There are several molecules used for decades in significant therapeutics to inhibit the topoisomerase activity but their mechanisms of action have only been understood rather recently. For example; Camptothecin and its derivatives like Topotecan and irinotecan (Figure 9) affect Topo Iβ by intercalating between the active site of the enzyme and the cleaved DNA ends, thus blocking DNA religation and relaxation of supercoils. Therefore, they are classified as Topo Iβ poisons (Barros *et al*., 2013; Staker *et al*., 2002). Another example is Fluoroquinolones, whose targets are gyrase and Topo IV in bacteria, are used as antibiotics. Additionally, semisynthetic podophyllotoxin derivatives such as Etoposide and Teniposide (Figure 10) are being used as chemotherapeutic agents. Etoposide is a Topo II poison which binds between 5' and 3' end of a broken DNA and prevents the resealing and the releasing of the strand (Laponogov *et al*., 2010). Other examples are novo- and chlorobiocins (Lewis *et al*.,

1996; Tsai *et al*., 1997), radicicol (Corbett & Berger, 2006), and bisdioxopiperazines (Classen, Olland, & Berger, 2003). They all block the ATPase activity of the enzyme. Moreover, simocyclinone D8 affects DNA binding (Edwards *et al*., 2009) and NTBI GSK299423 affects DNA cleavage (Bax *et al*., 2010) .

In addition to aforementioned examples, m-AMSA (Amsacrine) (Figure 11) needs particular attention. Because it is the first synthetic compound which targets topoisomerase II (Hornedo & Van Echo, 1985). Its working principle is based on intercalation and blocking the movement of DNA-enzyme complex (Ketron, Denny, Graves, & Osheroff, 2012). Its discovery led scientists to explore new, less toxic synthetic compounds for topoisomerase inhibition.

Together these findings not only highlight the variety of topoisomerase targeting molecules but also show the abundance of molecular scaffolds capable of topoisomerase inhibition (Vos *et al*., 2011).

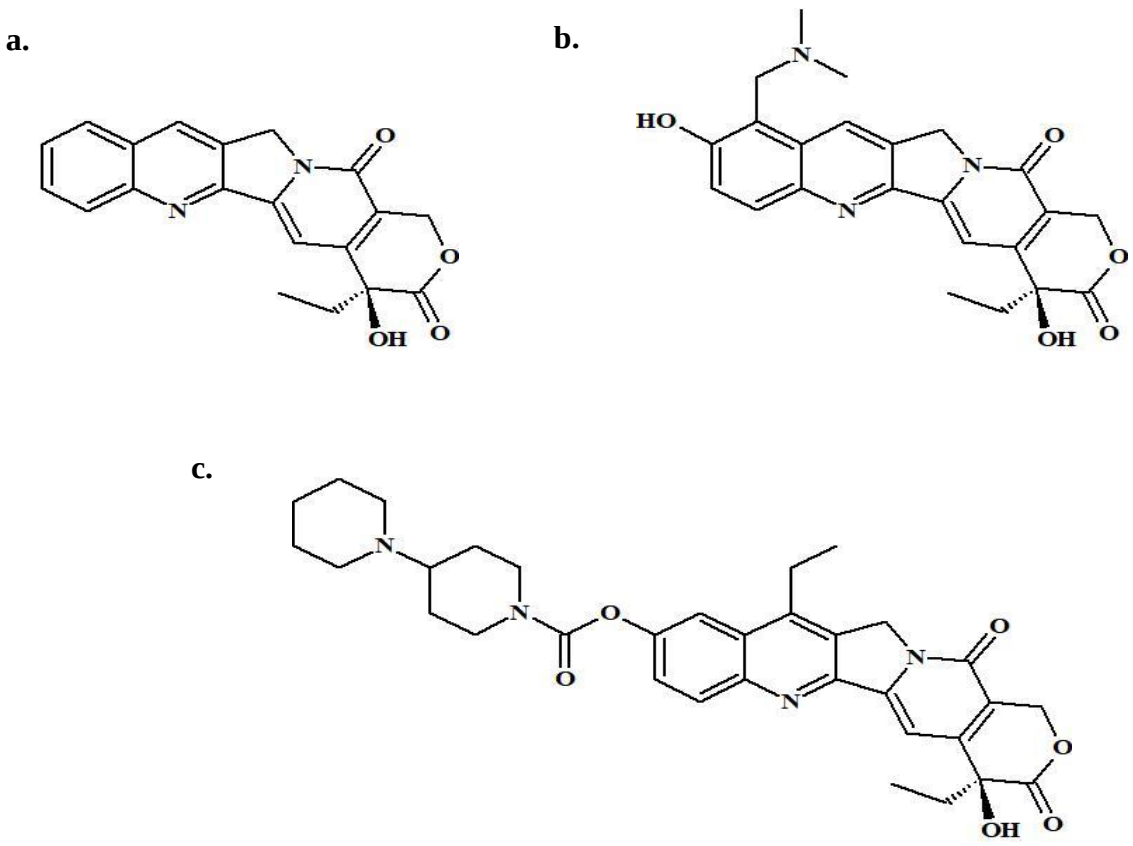

Figure 9. Some Topo I poisons. **a**.camptothecin. **b**.topotecan. **c**.irinotecan.

a.

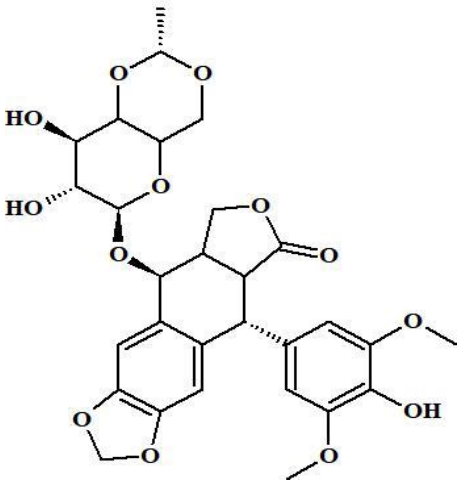

b.

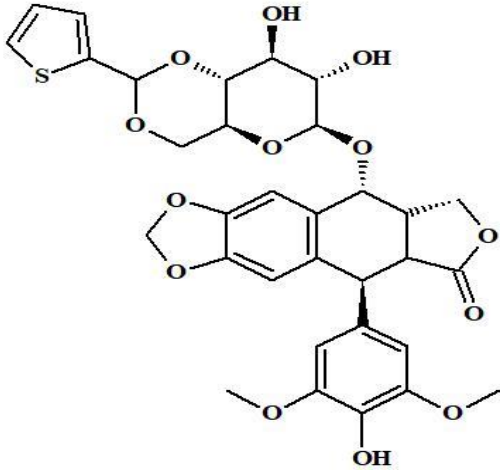

Figure 10. Some Topo II poisons. **a**.etoposide. **b**.teniposide.

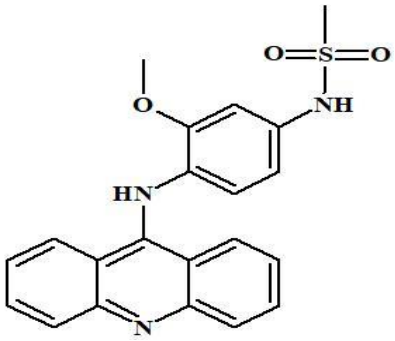

Figure 11. Synthetic Topo II poison: Amsacrine.

1.2.7.2. Cell Response to Topoisomerase Targeting Small Molecules:

In most of the cells, accumulation of mutations, ubiquitinylation, SUMOylation, and the formation of reactive oxygen species (ROS) is observed upon the intake of a topoisomerase inhibitor or poison. All of these changes occurring inside the cell lead to

mitotic delay, induce DNA repair mechanisms and ultimately induce cell death due to unrepaired DNA breaks (Vos *et al*., 2011).

For instance, in bacteria, it had been observed that some fluoroquinolones (Topo IV poison) promote cell death by inducing ROS production (Dwyer, Kohanski, Hayete, & Collins, 2007; Kohanski, Dwyer, Hayete, Lawrence, & Collins, 2007). Interestingly, some other fluoroquinolones like moxifloxacin and PD161144 were shown to kill cells even though the ROS cascade is blocked (oxygen absence). This result suggests that there might be other pathways for anti-topoisomerase action (X. Wang, Zhao, Malik, & Drlica, 2010).

In eukaryotes, both Topo I and Topo II poisons induce ubiquitinylation and SUMOylation (Vos *et al*., 2011). These processes are needed to initiate repair response as described earlier. Repair response mechanism acts to decrease the effect of the poison on topoisomerase. One way to mitigate the effect of the repair response mechanism is to administer the repair response mechanism inhibitor concurrently with the poison. For instance, it had been shown that fibroblasts of mice lacking PARP-1, one of the crucial enzymes in repair mechanism, are found to be more sensitive to topo II inhibitor (C-1305) (Węsierska-Gądek, Schloffer, Gueorguieva, Uhl, & Skladanowski, 2004). In another study, it had been shown that doxorubicin's (topo II inhibitor) activity in liver cells was enhanced by ANI which is a PARP inhibitor (Muñoz-Gámez *et al*., 2011).

1.3. Effects of Azacyanines in Yeast Cells:

Azacyanines (Figure 12 a, b, and c) were first synthesized by Kurth *et.al*. as ion channel inhibitors (Haddadin, Kurth, & Olmstead, 2000). The interactions of these azacyanines named as Azamethyl (named as Aza3 in previous studies), Aza4 and Aza5 with different DNA structures had also been established by lateral studies. By using NMR, UV-Vis and CD spectroscopy, it had been shown that these molecules bind selectively to G-quadruplex forming human telomeric sequence (tel24) over duplex DNA sequences (Çetinkol, Engelhart, Nanjunda, Wilson, & Hud, 2008). They had also

been able to induce the formation of the poly(A) self-structure in-vitro (Çetinkol & Hud, 2009).

Moreover, it has been shown that these azacyanines were able to induce genomic instability in yeast cells. In his thesis, Kim showed that azacyanine derivatives (Azamethyl, Aza4, and Aza5) induce chromosomal fragility in yeast cells. He hypothesized that this might be due to the stabilization of triple helical structures formed by $(GAA)_n$ triplex repeats. Moreover, it has been shown that increased chromosome fragility, caused by azacyanines, induced DNA repair surveillance system and caused G2/M phase arrest. It is also emphasized that azacyanines inhibit cell growth in a dose dependent manner (Kim, 2009).

However, there is no study, up to date, showing neither azacyanines' high affinity towards triple helical structures nor their selectivity towards different nucleic acid structures. Though their chemical structure resembles especially to the intercalators mentioned above, meaning that they might have a potential to target several structures in a cell such as DNA, RNA, and/or DNA-RNA hybrids in addition to their complexes such as DNA-topoisomerase complexes. Therefore, inspired by these findings mentioned above we hypothesized that the observed effects of azacyanines in yeast cells might be due to their binding ability to different nucleic acid structures, especially to triplex and quadruplex structures and/or topoisomerase II alpha.

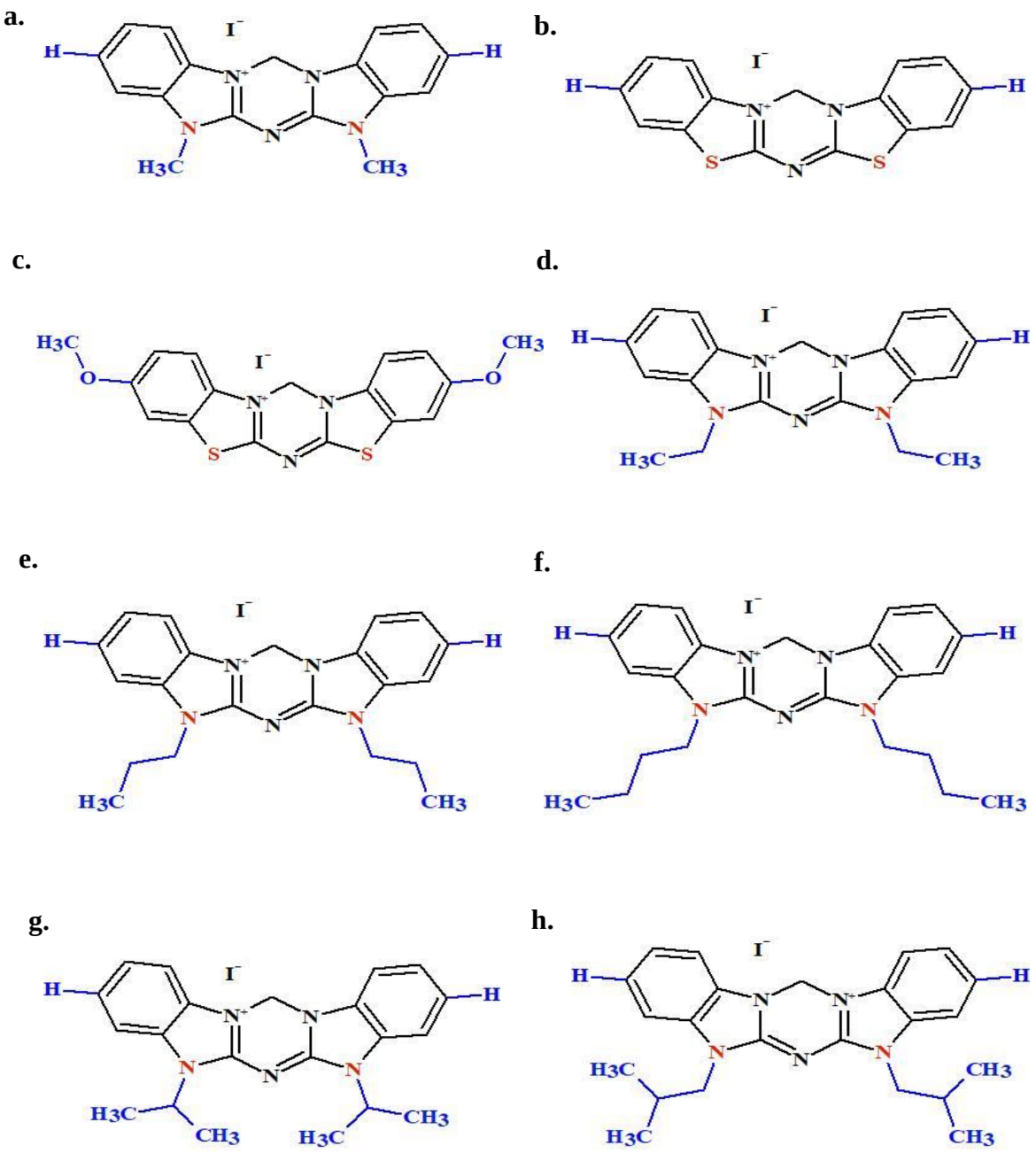

Figure 12. Chemical structure of azacyanines. **a**. Azamethyl. **b**. Aza4. **c**. Aza5. **d**. Azaethyl. **e**. Azapropyl. **f.** Azabutyl. **g**. Azaisopropyl. **h**. Azaisobutyl.

1.4.Thesis Focus:

This thesis focuses on the effect of several azacyanines on topoisomerase IIα and their selectivity towards different nucleic acid structures. Our main goal is to have a grasp on the mechanism of action of azacyanines observed in the yeast cells (Kim, 2009). Chemical structures of azacyanines used in our studies are given in Figure 12.

Here first, we focused on the effect of azacyanines on Topoisomerase II alpha enzyme (Topo IIα) which is the main expressed type II topoisomerase in the mammalian cells. Recently, a number of studies about synthetic topoisomerase inhibitors showed successful inhibition of Topo IIα. Since azacyanines (Figure 12) share similar aromatic ring structures with these molecules namely camptothecin, topotocen, irinotecan, etoposide, teniposide, and amsacrine (Figures 9-11), we hypothesized that the cell cycle arrest observed in yeast cells might be due to their ability to inhibit Topo IIα (Kim, 2009).

Secondly, we focused on revealing the binding affinity and selectivity of these azacyanines towards different nucleic acid structures via using competition dialysis to test Kim's hypothesis on their binding ability to triple helical structures. Our goal was to shed light to the effect of azacyanines on genome instability observed in yeast cells via understanding their interactions with different DNA structures (Kim, 2009).

As a whole, at the end of this thesis, we aim to propose some alternative mechanisms on toxic effects of these azacyanine molecules in cells and reveal their potential as possible topoisomerase inhibitors and chemotherapeutic agents.

CHAPTER 2

POSSIBLE EFFECTS OF AZACYANINE DERIVATIVES ON TOPOISOMERASE II ALPHA (TOPO IIα)

2.1. Introduction:

Topoisomerase II alpha (Topo IIα) has long been utilized as a target in chemotherapeutic applications in clinical oncology. Usage of small molecules as therapeutic agents such as etoposide and doxorubicin (classified asTopo IIα poisons) to target Topo IIα due to their toxicity is one of the most commonly applied practices. Topo IIα poisons' main function is to stabilize the Topo IIα-DNA complex, and eventually lead to apoptosis due to the accumulation of DNA damage. Though, it should also be noted that the utilization of such Topo IIα poisons bears also the risk of secondary malignancies and cardiotoxicity (Lipshultz *et al*., 2010; Vrooman *et al*., 2011).

In addition to Topo IIα poisons, there are several other small molecules identified as catalytic inhibitors. Catalytic inhibitors inhibit Topo IIα enzyme at different stages of its catalytic cycle without stabilizing the DNA-Topo enzyme complex (Figure 13) (Bau, Kang, Austin, & Kurz, 2013; Larsen, Escargueil, & Skladanowski, 2003; Pommier, 2013).

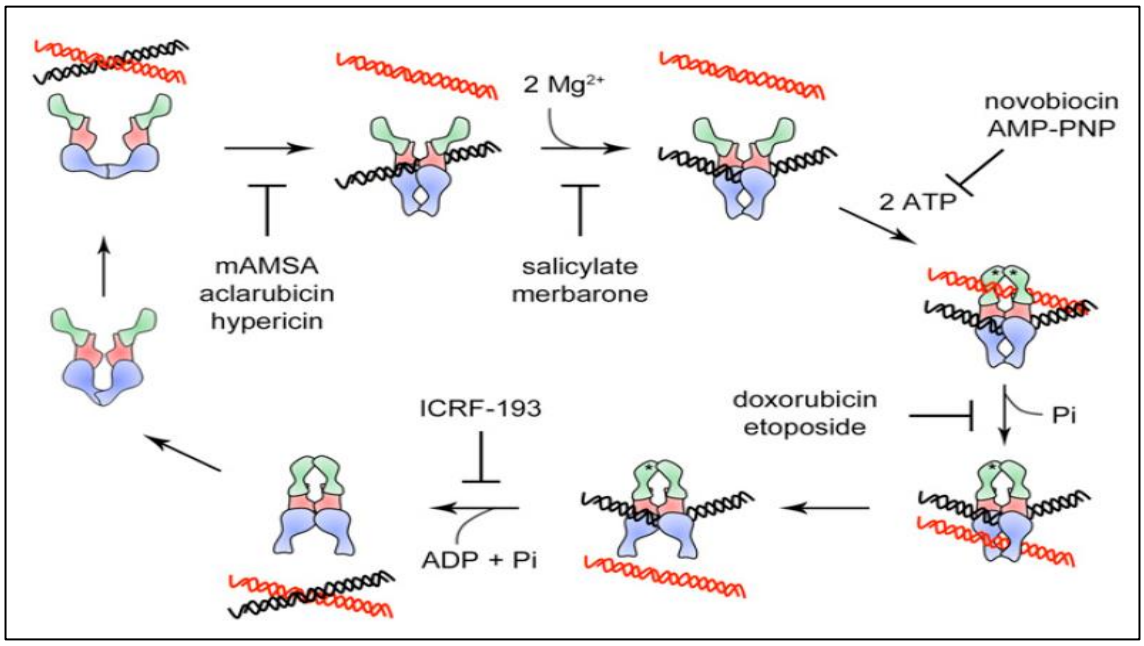

Figure 13. Common Topoisomerase II catalytic inhibitors and poisons (Bau *et al*., 2013).

Based on the structural similarity, such as the extended aromatic ring system with the positive charge, of many topoisomerase II inhibitors to our azacyanines (Figures 9-12), we hypothesized that our molecules might also have the capability of inhibiting Topo IIα.

We utilized a kit from TopoGEN Inc. (Buena Vista, USA) which is optimized for revealing the catalytic inhibition efficiency of small molecules. The proposed reaction mechanisms with the catenated DNA (kDNA) substrate provided by the supplier are given in Figure 14. We have investigated the effect of Azamethyl, Aza4 and Aza5 on Topo IIα, which were shown to trigger cell cycle arrest in yeast cells (Kim, 2009). In addition to these three molecules we have included Azaethyl and Azaisobutyl compounds in our assay in order to understand the effect of small

molecule structure, mainly the effect of chain length and branching on the benzimidazole ring, on inhibition efficiency. After the incubation of the compounds with the enzyme (Topo IIα) and substrate (catenated DNA), the inhibition efficiency of azacyanines were assessed via agarose gel electrophoresis.

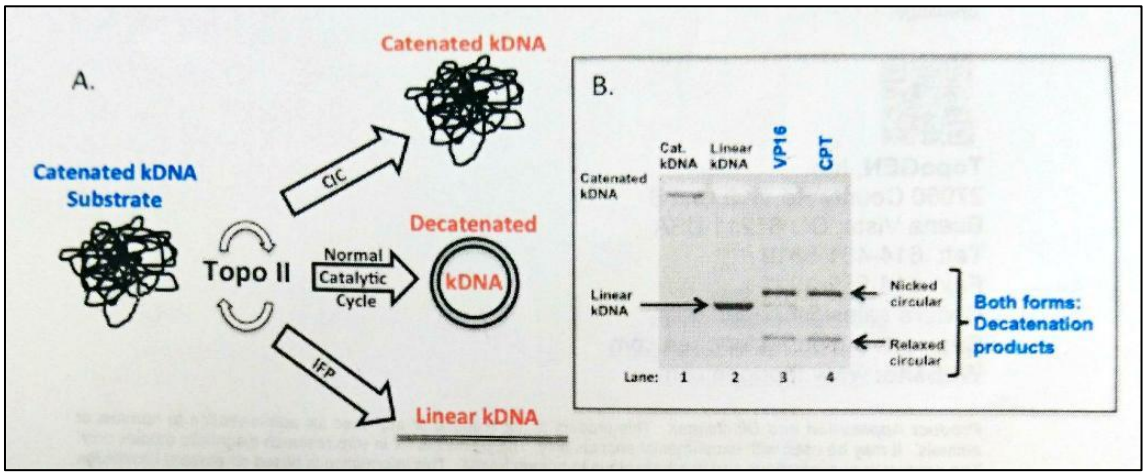

Figure 14. Proposed reaction mechanisms for Topoisomerase IIα kDNA based drug screening kit. kDNA: catenated DNA (substrate), VP-16 (Etoposide): proved topo II poison, CPT (Camptothecin): proved topo I inhibitor. Image taken from manufacturer's user manual (TopoGEN Inc., Catalog no: TG1019-2).

2.2. Materials and Methods:

All the small molecules were synthesized and characterized in our lab according to previously published protocols (Haddadin *et al.*, 2000). Stock solutions of azacyanines were prepared by dissolving in DMSO (Sigma Aldrich, M81802) and further diluted with Tris-HCl therefore the effect of DMSO on the enzyme was minimized. Preparation of 10.0 mM Tris-HCl is described in detail in Appendix A. The

concentrations of the stock solutions were determined using calculated extinction coefficient values given in Table 1 (the Beer-Lambert's Law: absorbance = extinction coefficient x path length x concentration) via UV-Vis spectrometer. Millipore de-ionized water was used throughout all of the experiments.

Table 1. Extinction coefficients of azacyanines.

Name of the compounds	Extinction Coefficient ($M^{-1}.cm^{-1}$)
Azamethyl	343 nm – 45,700
Aza4	387 nm – 24,240
Aza5	407 nm – 25,000
Azaethyl	343 nm – 44,700
Azaisobutyl	343 nm – 44,700
Azapropyl	343 nm – 43,300
Azabutyl	343 nm – 44,000
Azaisopropyl	343 nm – 45,100

Topoisomerase II Drug Screening Kit (kDNA based) (TG1019-2) was purchased from TopoGEN Inc. (Buena Vista, USA). Experiments were conducted as instructed by the supplier. Briefly, required amount of ingredients (water, buffer, DNA, test compound, and enzyme) were pooled together in an eppendorf tube on ice followed by 37°C, 40 minutes incubation. The reactions were stopped by addition of 10% SDS at 37°C and followed by the addition of Proteinase K and 30 minutes incubation at 37°C to digest the enzyme. Afterwards loading dye was added to each sample and the samples were loaded into 1% agarose gel with EtBr. Agarose gels were prepared in 1xTAE buffer as described before (Lee, Costumbrado, Hsu, & Kim, 2012). Samples were poured to Thermo Fischer Owl Easycast B2 mini gel electrophoresis system and then run for 180 minutes at 100 Volt. At the end of the electrophoresis, gels were

stained with EtBr and de-stained in water. Gels were visualized using BioRad XR Molecular Gel Imager. Details of preparation of 50X TAE buffer, 1%agarose gel, and EtBr solution are given in Appendix A.

2.3. Results and Discussion:

2.3.1. Determination of the Optimal Concentration of Azamethyl for Topoisomerase II Alpha Inhibition:

We started our investigations on the effect of azacyanines on Topo IIα by determining the effect of different concentrations of Azamethyl on Topo IIα along with the proven Topo II poison Etoposide (VP-16) (Liu, 1989). Here all the reaction mixtures, unless said otherwise, include the substrate, 200.0 ng kDNA (catenated DNA) and 5.0 units of Topo IIα.

The result of our initial screening is given in Figure 15. In lane 1, kDNA, which was our substrate in our assay, was used as a control. Linearized and decatenated DNA products were also used as control markers in lanes 2 and 5 respectively. Lane 3 and 4 were our positive control 50.0 μM and 500.0 μM VP-16 respectively. VP-16 is expected to decrease the enzyme activity in a concentration dependent manner. In lane 6, a "blank" well that only includes the solvent DMSO and the buffer (Tris-HCl) was also used as a control in order to see the effect of our solutions on Topo IIα activity. Here the ratio of DMSO:Tris-HCl was 1:9 which was the ratio used in preparation of positive control VP-16 samples in lanes 3 and 4. Lane 7, a "no drug" well, was another control which only includes the reaction mixture without any inhibitor. Here, we expect to see the full enzyme activity on our substrate. Lanes 8-11 had different concentrations of Azamethyl added to the reaction mixture.

As shown in Figure 15, our enzyme was active under the reaction conditions and our solution used in the preparation of VP-16 and azacyanines had little effect on our enzyme's activity (Lanes 6 and 7). Our substrate, kDNA by itself barely enters the gel (Lane 1). But in the presence of Topo IIα (Lanes 6 and 7), several bands were observed due to the formation of decatenated kDNA products by Topo IIα. Decatenated

bands in lanes 3,4, and 6-11are not at the same alignment with the decatenated DNA marker because of the long running time (3 hours) and should not be considered as a linear band. VP-16 is clearly inhibiting Topo IIα in a dose dependent manner (Lanes 3 and 4). The intensity of the decatenated DNA bands was decreased in the presence of 50.0 μM VP-16. The measured intensities of the decatenated DNA bands were given in Figure 16. Here, the intensities of decatenated DNA bands in all samples were normalized to the intensity of the decatenated DNA band belonging to the sample that has full Topo IIα activity in the absence of any inhibitor (lane 7- no drug). The intensity decreased to 0.63 in the presence of 50.0 μM VP-16 (lane 3) compared to the lane 7 which was taken as 1.00. The intensity of the band decreased further to 0.20 in the presence of 500.0 μM VP-16. Our compound, Azamethyl, showed incredible catalytic activity decrease compared to VP-16. The intensities of the bands were 0.75, 0.26, 0.12 and 0.01 in the presence of 1.0 μM, 10.0 μM, 50.0 μM and 100.0 μM Azamethyl respectively. It is clear that Azamethyl decreases the catalytic activity of Topo IIα in a concentration dependent manner. However, at this point, we cannot classify its inhibition efficiency as a Topo IIα poison, since we did not observe the band belonging to the linear DNA in the presence of Azamethyl. The linear band formation, even though it was weak, was observed in the presence low concentrations of VP-16. More importantly, our results revealed that the effect of Azamethyl on Topo IIα was stronger compared to VP-16. Even at 50.0 μM concentration Azamethyl's efficiency was greater than 500.0 μM of VP-16.

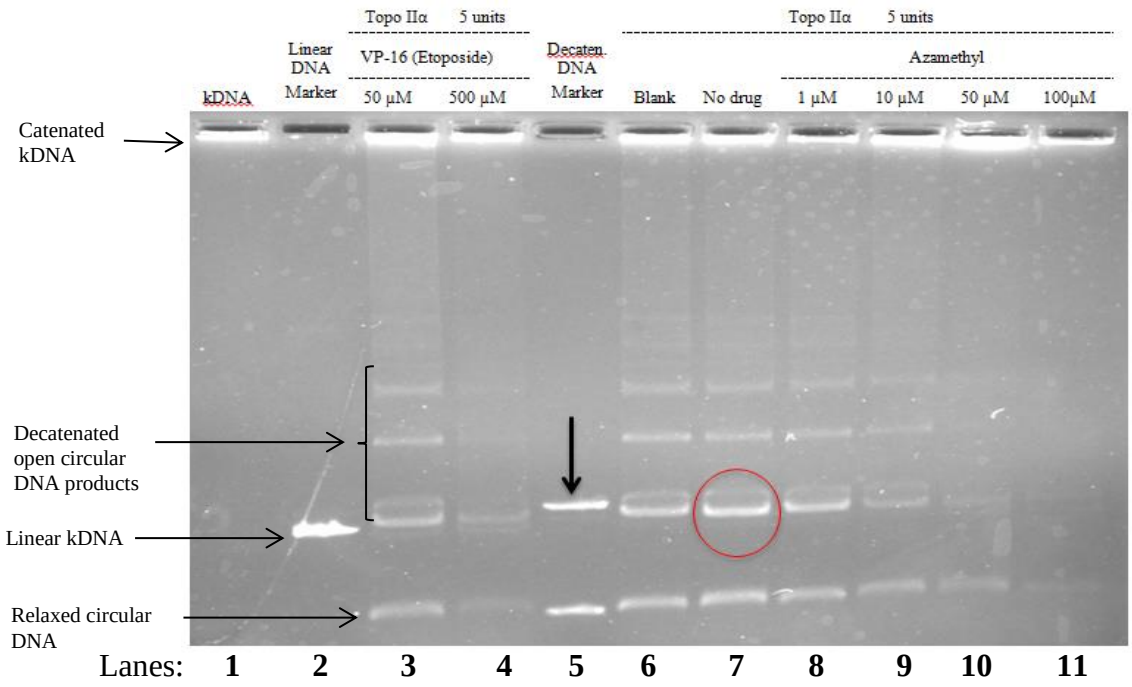

Figure 15. Agarose gel electrophoresis results for the effect of Azamethyl on Topo IIα. Lane 1: "kDNA", catenated DNA substrate, Lane 2: "Linear DNA marker" Topo IIα poison indicator, Lane 3 and 4: Topo IIα and kDNA in the presence of "VP-16" (Etoposide) which is a proven Topo IIα poison, Lane 5: "Decaten. DNA marker", decatenated DNA products as an indicator of the enzyme activity, Lane 6: "Blank" only drug solvents (DMSO:Tris-HCl - 1:9), Lane 7: "no drug" includes only the enzyme Topo IIα. Lane 8-11: Topo IIα and kDNA in the presence of "Azamethyl" which is the tested drug. Gel conditions: 1%agarose in 1xTAE buffer; 100 V; 180 minutes run. Black arrow indicates the band that is the main indicator of the enzyme activity. Red circle: all intensities are normalized according to this band.

	Normalized Intensities (relative to red circled band in figure 15)
VP-16-50 µM (lane 3)	0.63
VP-16-500 µM (lane 4)	0.20
Blank (lane 6)	0.85
No drug (lane 7)	1.00
Azamethyl-1 µM (lane 8)	0.75
Azamethyl-10 µM (lane 9)	0.26
Azamethyl-50 µM (lane 10)	0.12
Azamethyl-100 µM (lane 11)	0.01

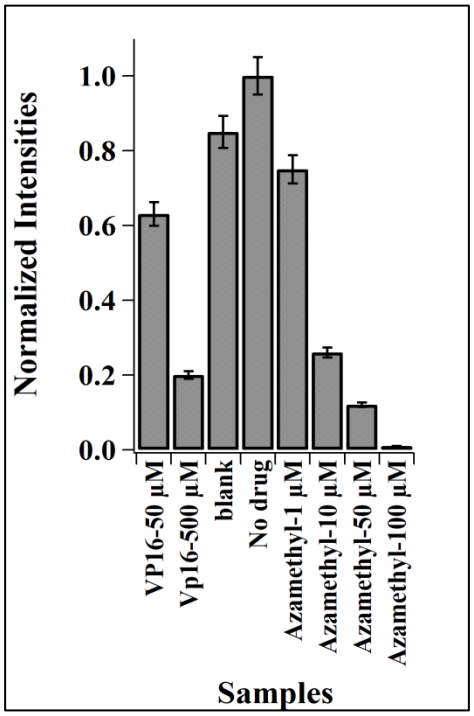

Figure 16. Agarose gel electrophoresis results obtained by analyzing the gel image given in Figure 15. Left table is the normalized intensity values. Normalization was performed relative to our negative control (no drug sample) that only includes the substrate (kDNA) and the enzyme (Topo IIα). The contents of the samples were given in Figure 15. Error bars represent 5% of the normalized intensities. Intensities measured by Image Lab, Version 5.2.1 (BioRad Laboratories).

2.3.2. Determination of the Effects of Different Azacyanines on Topoisomerase II Alpha:

Once we have seen that Azamethyl was decreasing the catalytic activity of Topo IIα, we decided to investigate the effects of other azacyanines also on Topo IIα. We included Aza4 and Aza5 in our assay since these two molecules were studied by Kim in his studies along with Azamethyl (Kim, 2009). In addition, we included two Azamethyl analogs named as Azaethyl and Azaisobutyl to understand the effect of alkyl chain length and branching on Topo IIα catalytic activity. Once again, we have included VP-16 as our positive control. Since the efficiency of Azamethyl was strong at 50.0 μM concentration, here we tested all the drugs efficiencies at that concentration on 5 units of Topo IIα. Again we have included kDNA as our substrate along with linearized and decatenated DNA markers. No drug lane and the blank lane (DMSO:Tris-HCl, 1:9) were also used as our negative controls.

Our results given in Figure 17 clearly demonstrated that Azamethyl, Aza4 and Aza5 can decrease the catalytic activity of Topo IIα. The intensity of the decatenated DNA decreased in the presence of Azamethyl, Aza4 and Aza5. The measured intensities given in Figure 18 were 0.16, 0.26 and 0.37 respectively. We did not observe the formation of the linear band in the presence of Azamethyl, Aza4 and Aza5 thus cannot classify them as poisons. Decatenated bands in lanes 3, 5-11are not at the same alignment with the decatenated DNA marker because of the long running time (3 hours) and should not be considered as a linear band. To our surprise, Azaethyl and Azaisobutyl did not show any change on Topo IIα catalytic activity. (Figures 17 and 18). On the contrary, the activity of Topo IIα seemed to increase slightly in the presence of Azaethyl and Azaisobutyl. The intensities of the decatenated DNA band were measured as 1.20 and 1.21 in the presence of Azaethyl and Azaisobutyl, respectively.

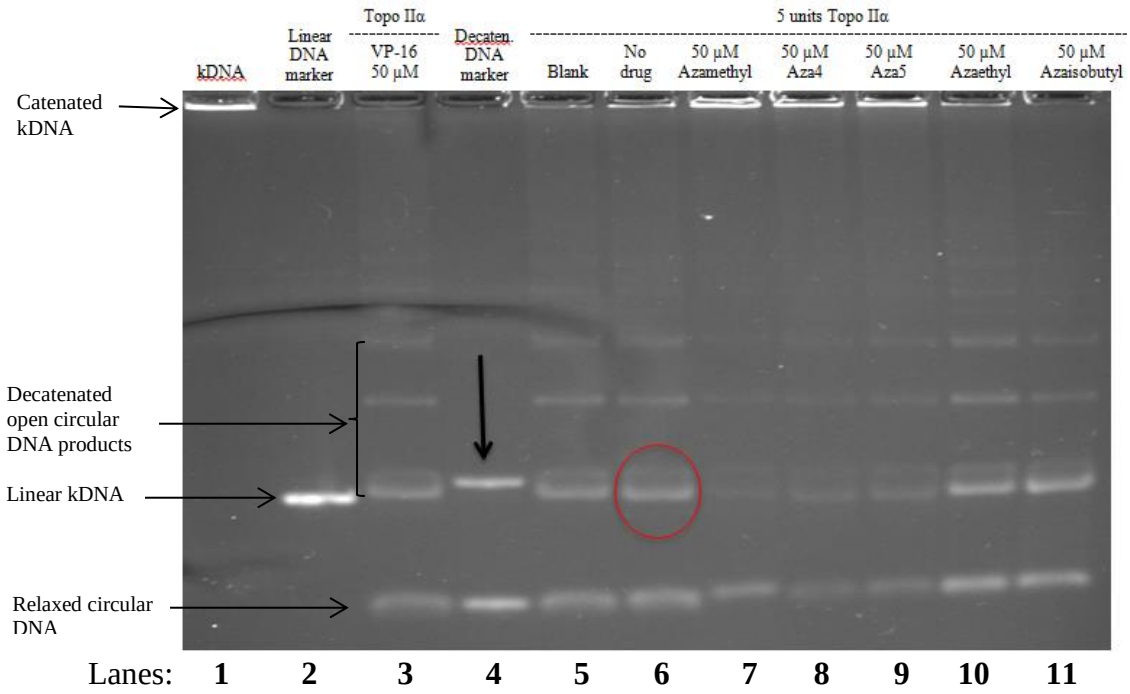

Figure 17. Agarose gel electrophoresis results for different azacyanines on Topo IIα. Lane 1: "kDNA", catenated DNA substrate, Lane 2: "Linear DNA marker", Lane 3: kDNA and Topo IIα in the presence of "VP-16" (Etoposide) which is a proven Topo IIα poison, Lane 4: "Decaten. DNA marker", decatenated DNA products as an indicator of the enzyme activity, Lane 5: "Blank" only drug solvents (DMSO:Tris-HCl - 1:9), Lane 6: "no drug" includes only the enzyme Topo IIα. Lane 7-11: kDNA and Topo IIα in the presence of 50.0 µM azacyanine derivatives. Lane 7: "Azamethyl", Lane 8: "Aza4", Lane 9: "Aza5", Lane 10: "Azaethyl", Lane 11: "Azaisobutyl". Gel conditions: 1%agarose in 1xTAE buffer; 100 V; 180 minutes run. Black arrow indicates the band that is the main indicator of the enzyme activity. Red circle: all intensities are normalized according to this band.

	Normalized Intensities (relative to red circled band in figure 17)
VP-16-50 µM (lane 3)	0.87
Blank (lane 5)	0.84
No drug (lane 6)	1.00
Azamethyl-50 µM (lane 7)	0.16
Aza4-50 µM (lane 8)	0.26
Aza5-50 µM (lane 9)	0.37
Azaethyl-50 µM (lane 10)	1.20
Azaisobutyl-50 µM (lane 11)	1.21

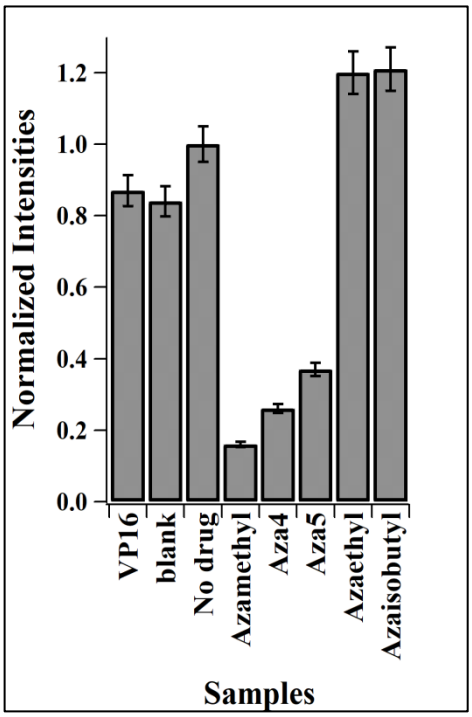

Figure 18. Agarose gel electrophoresis results obtained by analyzing the gel image given in Figure 17. Left table is the normalized intensity values. Normalization was performed relative to our negative control (no drug sample) that only includes the substrate (kDNA) and the enzyme (Topo IIα). The contents of the samples were given in Figure 17. Error bars represent 5% of the normalized intensities. Intensities measured by Image Lab, Version 5.2.1 (BioRad Laboratories).

2.4.Conclusions:

Our results revealed that Azamethyl, Aza4 and Aza5 cause to decrease in Topo IIα's catalytic activity, while Azaethyl and Azaisobutyl do not.

Among the molecules investigated in here, Azamethyl showed the highest decrease in TopoIIα's catalytic activity. The effect of Azamethyl on Topo IIα was concentration dependent, such that there was a slight decrease on catalytic activity of Topo IIα even in the presence of 1.0 μM Azamethyl. More importantly, our results revealed that Azamethyl is more powerful than the proven Topo IIα poison, Etoposide (VP-16). While the topoisomerase was 63% active in the presence of 50.0 μM VP-16, its activity was only 12% in the presence of 50.0 μM Azamethyl. To our surprise, 50.0 μM Azamethyl showed stronger effect than 500.0 μM VP-16. We have also tested the effect of Azaethyl, Azaisobutyl, Aza4 and Aza5 at 50.0 μM small molecule concentration. Our results revealed that while Aza4 and Aza5 also decrease the catalytic activity of Topo IIα, Azaethyl and Azaisobutyl do not show such ability. On the contrary, to our surprise the activity of Topo IIα seemed to increase slightly in the presence of Azaethyl and Azaisobutyl. The interactions of these molecules with Topo IIα need to be investigated in detail in order to be able to explain such an increase. However, we think that the underlying cause might be related to the interactions of these molecules with the DNA rather than TopoIIα. As will be explained in chapter 3, azacyanines have the capability of binding to different nucleic acids. Therefore if Azaethyl and Azaisobutyl do not interfere with the Topo IIα, they might be binding to decatenated DNA products and this could cause the increased intensities.

Results obtained here provide us an alternative explanation on how azacyanines might be affecting the cells in addition to the observations by Kim (Kim, 2009). It is now clear that Azamethyl, Aza4, and Aza5 decreases Topo IIα enzyme's catalytic activity. This might be one of the reasons behind the cell cycle arrest observed by Kim (Kim, 2009). They might be interfering with the enzyme at different steps of its catalytic cycle. For example, they might be interfering with the binding of the enzyme to DNA, stabilizing the non-covalent DNA-enzyme complex, or inhibiting ATP binding to the enzyme (Larsen *et al.*, 2003). Yet, at which stage of its catalytic cycle that our small molecules interfere with Topo IIα needs to be elucidated further.

CHAPTER 3

SELECTIVITY OF AZACYANINES TOWARDS NUCLEIC ACID STRUCTURES

3.1. Introduction:

For more than 40 years, mainly because of the participation of small molecules as therapeutic drugs, designing of small molecules that have the ability to bind nucleic acids has been an active area (Waring & Wakelin, 2003). Targeting nucleic acid structures (DNA and/or RNA) with small molecules gives an opportunity for the genetically originated diseases' treatment (Martinez & Chacon-Garcia, 2005; Thurston, 1999). Particularly, small molecule binding to non-canonical nucleic acid structures such as triplex and quadruplexes has been a major focus for rational drug design. However, designing molecules that can bind to nucleic acid structures tightly and selectively is the first step to understand such interactions (Hurley, 1989; Mergny & Helene, 1998; Thurston, 1999).

Small molecules, upon binding to certain nucleic acid structures, change the conformation and therefore could either stabilize or destabilize these structures and cause problems such as impaired gene expression patterns and/or mutations (Bissler, 2007). This subsequently induces DNA repair systems and drives cells to cell cycle arrest and could even lead to cell death. Their stabilization ability, have been widely used in drug design for several treatments such as cancer to get rid of undesired cells (M. Wang *et al.*, 2016). Moreover, selectivity of various other small molecules towards

specific nucleic acid sequences had been shown with different studies (Chaires *et al.*, 2003; Ren & Chaires, 1999; Chaires, 1998).

Selectivity of Azamethyl, Aza4, and Aza5 to quadruplex structures along with duplex DNA structures and poly(A) had been reported previously (Çetinkol *et al.*, 2008; Çetinkol & Hud, 2009). Additionally, Kim investigated the effects of these molecules in-vivo using yeast cells, expressing GAA•TTC repeat sequences. It had been revealed that all the molecules were blocking the DNA synthesis, inducing chromosome fragility and inhibiting cell growth in these yeast cells in a dose dependent manner. Based on his results, Kim hypothesized that the observed results might be due to the binding of these molecules to triple helical structures. He even suggested that these molecules can form the basis for the development of novel antitumor drugs that bind to triple helical structures tightly and act via the inhibition of cellular proliferation (Kim, 2009).

In Chapter 2, we have observed that Azamethyl, Aza4, and Aza5 catalytically inhibit Topo IIα. Yet at which catalytic step do they inhibit the enzyme's activity is not known. Therefore, we hypothesized that if azacyanines have the capability of binding to different nucleic acid structures; they might be affecting the enzyme at the first step of its catalytic activity, which is the binding of the enzyme to DNA as shown in Figure 7. Azacyanines might be interfering with the DNA and thus changing the conformation of the DNA. This might be preventing the enzyme binding to DNA and thus inhibiting the enzyme activity.

Here, using competition dialysis method, we have investigated the selectivity of azacyanines towards various nucleic acid structures. We have also included Azaethyl, Azapropyl, Azaisopropyl, Azabutyl and Azaisobutyl in addition to Azamethyl, Aza4, and Aza5, in our competition dialysis experiments to see the effect of alkyl chain length and branching of benzimidazole ring on nucleic acid binding affinity and selectivity.

3.2. Materials and Methods:

Competition dialysis experiments were conducted as previously described (Chaires *et al*., 2003; Ragazzon, Garbett, & Chaires, 2007; Ren & Chaires, 1999). Components and preparation of the buffers used throughout the experiments are given in Appendix A and the oligonucleotides used in the experiments are given in Appendix B. Construction of standard curves are given in Appendix C.

The oligonucleotide samples were prepared as described in Ren & Chaires, 1999. Briefly, oligonucleotides including poly(dA), poly(dT), poly(dA).poly(dT), poly(dAdT).poly(dAdT), poly(rA).poly(rU), poly(dGdC).poly(dGdC) were purchased from Sigma-Aldrich (St. Louis, MO, USA). Natural DNA of *Micrococcus lysodeikticus* purchased from Sigma-Aldrich (St. Louis, MO, USA) was sonicated for 30 minutes (5 minutes sonication following 5 minutes rest) followed by phenol-chloroform extraction (Chaires, Dattagupta, & Crothers, 1982). 32 base long oligonucleotides including $(dA)_{32}$ and $(dT)_{32}$ and quadruplex sequences including Tel24 (5'- TTGGG[TTAGGG]$_3$A- 3') and 5'- $T_2G_{20}T_2$ -3' were purchased from Integrated DNA Technologies (IDT) (Coralville, IA, USA). Remaining oligonucleotides were produced by mixing the required nucleic acids as described below:

- Triplex DNA - poly(dA).[(poly(dT)]$_2$ was prepared by mixing poly(dA).poly(dT) and poly(dT) in a 1:1 equimolar ratio,
- Triplex DNA - $(dA)_{32}.[(dT)_{32}]_2$ was prepared by mixing $(dA)_{32}$ and $(dT)_{32}$ in a 1:2 equimolar ratio,
- Triplex RNA - poly(rA).[poly(rU)]$_2$ was prepared by mixing either poly(rA).poly(rU) and poly(rU) in a 1:1 equimolar ratio, or poly(rA) and poly(rU) in a 1:2 equimolar ratio
- Duplex DNA - $(dA)_{32}.(dT)_{32}$ was prepared by mixing $(dA)_{32}$ and $(dT)_{32}$ in a 1:1 equimolar ratio.

All the prepared oligonucleotides were annealed by heating at 95°C for 5 minutes in a water bath and then left overnight at room temperature for cooling down slowly to assure the formation of the proper secondary structure before used in competition dialysis experiments.

For each competition dialysis experiment, 0.5 mL of 75.0 µM of each oligonucleotide, in a monomeric unit (nucleotide, base pair, triplet, quartet), were put into Pierce (Thermofischer Scientific, USA) 7000 Da molecular weight cutoff dialysis cassettes. Then, cassettes were dialyzed against 500.0 mL of 1.0 µM of the selected ligand (Azamethyl, Azaethyl, Azapropyl, Azabutyl, Azaisobutyl, Azaisopropyl, Aza4, orAza5) solution for 24 hours. 1xBPES buffer (1.0 mM Na_2EDTA, 6.0 mM Na_2HPO_4, 2.0 mM NaH_2PO_4, and 185.0 mM NaCl); pH 7.0, was prepared (see Appendix A) as previously described (Ren & Chaires, 1999) and used in all experiments.

At the end of the dialysis period, aliquots were taken from each dialysis cassettes, and 1% (w/v) SDS was added to release the bound ligands from nucleic acids and to ensure that the ligands were free in the cassettes. Afterwards, the ligand concentrations in each cassette were determined via fluorescence spectroscopy (Varian, Cary Eclipse). Device setup was as following: Emission spectra collected: 325 to 675 nm, excitation wavelength: 324 nm, excitation and emission slits: 2.5 and 5.0, respectively. For each azacyanine derivative, standard curves were constructed using the same fluorescence spectrophotometer prior to competition dialysis (see Appendix C). This allowed us to determine the concentration of ligands by using fluorescence intensities. Appropriate corrections were made in calculating the ligand concentration in each cassette considering the dilution due to the added SDS and 1X BPES buffer. Two independent experiments were performed for each molecule.

The ratio of the bound ligand to free ligand concentration (C_b/C_f) was determined by: $C_b/C_f=(C_t/C_f)-1$ where C_t (total ligand concentration) is the concentration of the ligand in each dialysis cassette and C_f (free ligand concentration) is the concentration of the ligand in a positive control dialysis cassette (that only

includes 1X BPES buffer) which typically did not significantly vary from initial small molecule concentration that was 1.0 μM.

Descriptive statistics was used to analyze our competition dialysis results. SPSSv23.0.0.0 (IBM corp., Armonk, NY) was utilized for statistical analysis. Kruskal Wallis non-parametric test was performed for non-normal distributions. One-way ANOVA test was performed, with Bonferronni and Sidak post-hoc tests, for normal distributions (see Appendix D).

3.3. Results and Discussions:

3.3.1. Azamethyl:

At the end of the 24 hours long competition period, the concentration of Azamethyl was different in each dialysis cassette as indicated by the varying fluorescence intensities among the cassettes containing different nucleic acids as shown in Figure 19. And more importantly, the fluorescence intensities in certain cassettes were also highly different than the fluorescence intensity obtained for the control cassette that is only containing buffer solution. This means that Azamethyl was binding to certain nucleic acid structures and therefore diffusing into the cassettes that are containing these nucleic acid structures. Using the fluorescence intensities, the exact concentration of Azamethyl in each dialysis cassette was calculated as explained in Appendix C. In each trial, C_b/C_f for each cassette was calculated, and then C_b/C_f ratios for both of the replicate experiments were averaged out and recorded as the final result (Table 2). The final average C_b/C_f values for each nucleic acid structure were plotted as shown in Figure 20. Our statistical results were also given in Figure 20.

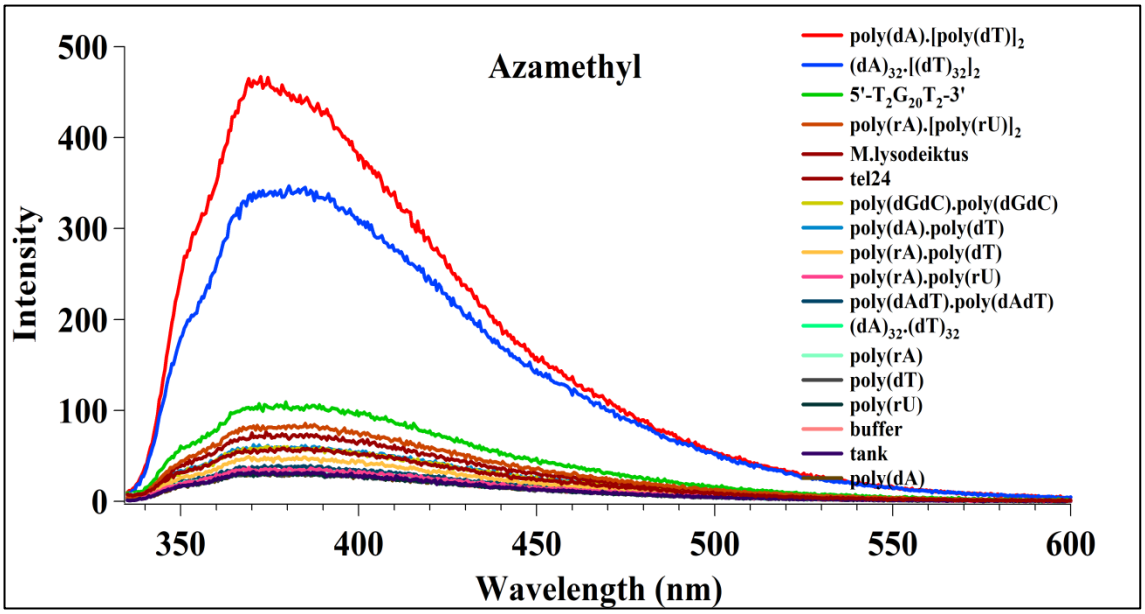

Figure 19. Average fluorescence spectra of Azamethyl. Measurements were obtained at the end of the 24 hours long competition dialysis against Azamethyl from dialysis cassettes containing different nucleic acid structures.

Table 2. Competition dialysis results for Azamethyl.

Oligonucleotides	Folds over buffer (C_b/C_f)			
	1st replicate	2nd replicate	Average	Standard deviation
poly(dA).[poly(dT)]$_2$ - triplex DNA	10.11	13.28	**11.69**	2.24
(dA)$_{32}$.[(dT)$_{32}$]$_2$ - triplex DNA	10.78	10.52	**10.65**	0.18
5'-T$_2$G$_{20}$T$_2$ – 3'- quadruplex DNA	2.51	2.54	**2.53**	0.03
poly(rA).[poly(rU)]$_2$ - triplex RNA	1.60	1.76	**1.68**	0.11
M.lysodeiktus - dsDNA	1.32	1.37	**1.34**	0.04
tel24 - quadruplex DNA	1.26	0.98	**1.12**	0.20
poly(dGdC).poly(dGdC) - dsDNA	1.14	0.95	**1.05**	0.13
poly(dA).poly(dT) - dsDNA	0.77	0.97	**0.87**	0.14
poly(rA).poly(dT) - DNA-RNA hybrid	0.48	0.56	**0.52**	0.06
poly(rA).poly(rU) - dsRNA	0.64	0.17	**0.40**	0.33
poly(dAdT).poly(dAdT) - dsDNA	0.27	0.21	**0.24**	0.04
(dA)$_{32}$.(dT)$_{32}$ - dsDNA	0.09	0.11	**0.10**	0.02
poly(rA) - ssRNA	0.13	0.08	**0.10**	0.04
poly(dT) - ssDNA	0.02	0.02	**0.02**	0.00
buffer	0.00	0.00	**0.00**	0.00
tank	0.03	-0.04	**-0.01**	0.05
poly(dA) - ssDNA	-0.01	-0.09	**-0.05**	0.05
poly(rU) - ssRNA	0.06	-0.03	**0.01**	0.06

The ratio of the bound ligand to free ligand concentration (C_b/C_f) was determined by: $C_b/C_f=(C_t/C_f)-1$ where C_t (total ligand concentration) is the concentration of the ligand in each dialysis cassette and C_f (free ligand concentration) is the concentration of the ligand in a positive control dialysis cassette (buffer) that only includes 1X BPES buffer which typically did not significantly vary from initial small molecule concentration that was 1.0 μM in the solution (tank).

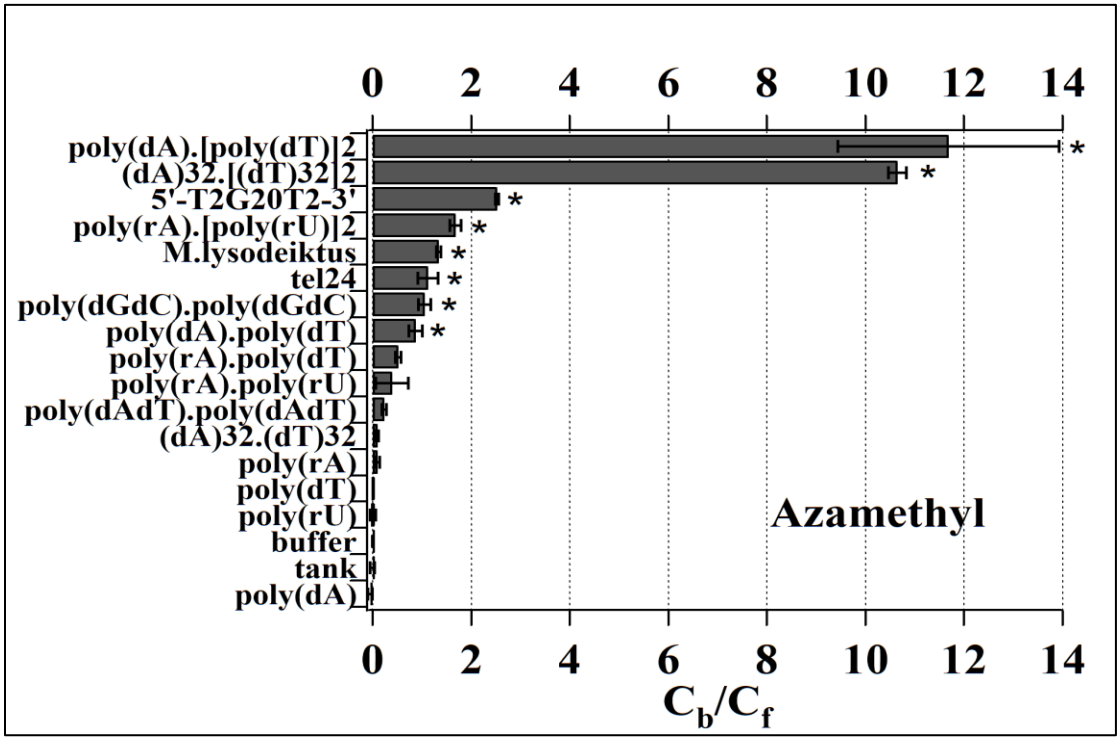

Figure 20. Competition Dialysis results for Azamethyl. *; p<0,05 from control by Kruskal Wallis non-parametric test. Error bars are ±1 standard deviations of the mean with a confidence level of 95%.

Our competition dialysis results revealed undoubtedly that Azamethyl is binding to triple helical structures of poly(dA).poly$[(dT)]_2$ and $(dA)_{32}.[(dT)_{32}]_2$ with high affinity and selectivity. The amount of Azamethyl collected in the dialysis cassettes containing poly(dA).poly$[(dT)]_2$ and $(dA)_{32}.[(dT)_{32}]_2$ was substantial compared to other samples. The average calculated C_b/C_f values were 11.69 and 10.65 with significance levels of p=0.012 and p=0.014 respectively according to non-parametric Kruskal–Wallis test. Azamethyl also showed significant binding to 5'-$T_2G_{20}T_2$ -3' quadruplex and poly(rA).$[poly(rU)]_2$ RNA triplex with C_b/C_f values of 2.53 and 1.68, respectively. Our results also revealed that, Azamethyl's affinity towards

double stranded structures was low with even lower affinity towards RNA structures compared to DNA structures. Furthermore, Azamethyl had no affinity towards single stranded nucleic acid structures under these conditions, where the obtained C_b/C_f values were within the experimental errors.

3.3.2. Azaethyl:

The fluorescence spectra of the samples against Azaethyl in each dialysis cassette were given in Figure 21. The concentration of Azaethyl was also different in each dialysis cassettes after 24 hours long competition dialysis. Then C_b/C_f was calculated, as mentioned in materials and methods, and C_b/C_f ratio for both of the replicate experiments were averaged out and recorded as the final result (Table 3). The average C_b/C_f values with the statistical analysis were plotted in Figure 22.

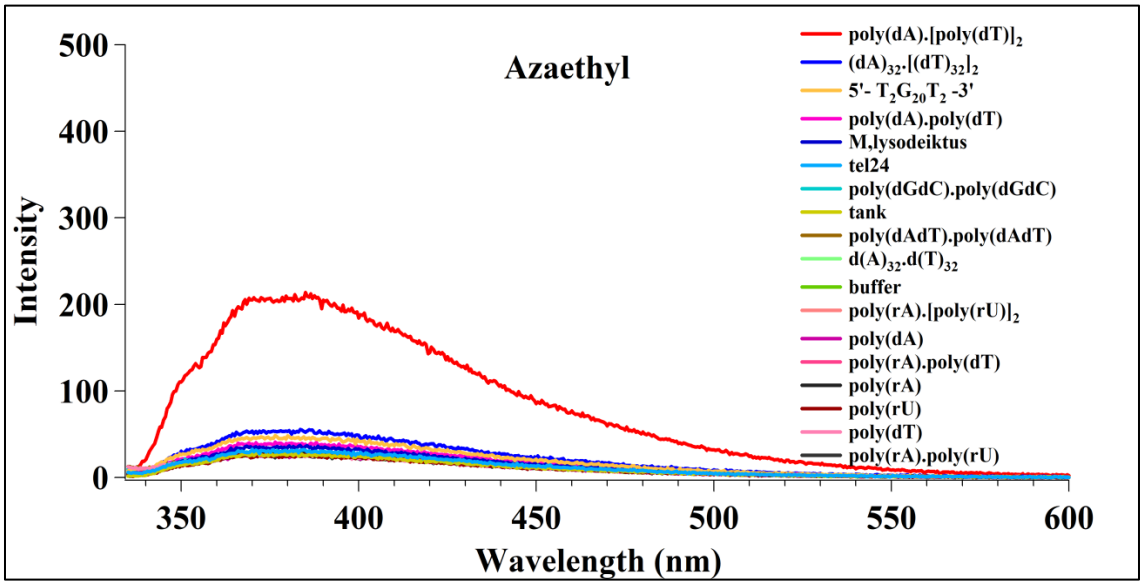

Figure 21. Average fluorescence spectra of Azaethyl. Measurements were obtained at the end of the 24 hours long competition dialysis against Azaethyl from dialysis cassettes containing different nucleic acid structures.

Table 3. Competition dialysis results for Azaethyl.

Oligonucleotides	Folds over buffer (C_b/C_f)			
	1st replicate	2nd replicate	Average	Standard deviation
poly(dA).[poly(dT)]$_2$ - triplex DNA	6.95	6.88	**6.92**	0.05
(dA)$_{32}$.[(dT)$_{32}$]$_2$ - triplex DNA	1.75	1.00	**1.37**	0.53
5'-T$_2$G$_{20}$T$_2$ – 3'- quadruplex DNA	0.88	0.72	**0.80**	0.11
poly(rA).[poly(rU)]$_2$ - triplex RNA	-0.02	-0.01	**-0.02**	0.01
M.lysodeiktus - dsDNA	0.49	0.32	**0.40**	0.12
tel24 - quadruplex DNA	0.24	0.15	**0.19**	0.06
poly(dGdC).poly(dGdC) - dsDNA	0.20	0.13	**0.17**	0.05
poly(dA).poly(dT) - dsDNA	0.36	0.42	**0.39**	0.04
poly(rA).poly(dT) - DNA-RNA hybrid	0.08	-0.02	**0.03**	0.08
poly(rA).poly(rU) - dsRNA	0.00	-0.08	**-0.04**	0.05
poly(dAdT).poly(dAdT) - dsDNA	0.04	0.03	**0.03**	0.01
(dA)$_{32}$.(dT)$_{32}$ - dsDNA	0.00	0.02	**0.01**	0.01
poly(rA) - ssRNA	-0.03	-0.03	**-0.03**	0.00
poly(dT) - ssDNA	0.00	-0.04	**-0.02**	0.03
buffer	0.00	0.00	**0.00**	0.00
tank	0.04	0.03	**0.04**	0.01
poly(dA) - ssDNA	-0.03	-0.02	**-0.03**	0.01
poly(rU) - ssRNA	-0.07	-0.04	**-0.05**	0.02

The ratio of the bound ligand to free ligand concentration (C_b/C_f) was determined by: $C_b/C_f=(C_t/C_f)-1$ where C_t (total ligand concentration) is the concentration of the ligand in each dialysis cassette and C_f (free ligand concentration) is the concentration of the ligand in a positive control dialysis cassette (buffer) that only includes 1X BPES buffer which typically did not significantly vary from initial small molecule concentration that was 1.0 µM in the solution (tank).

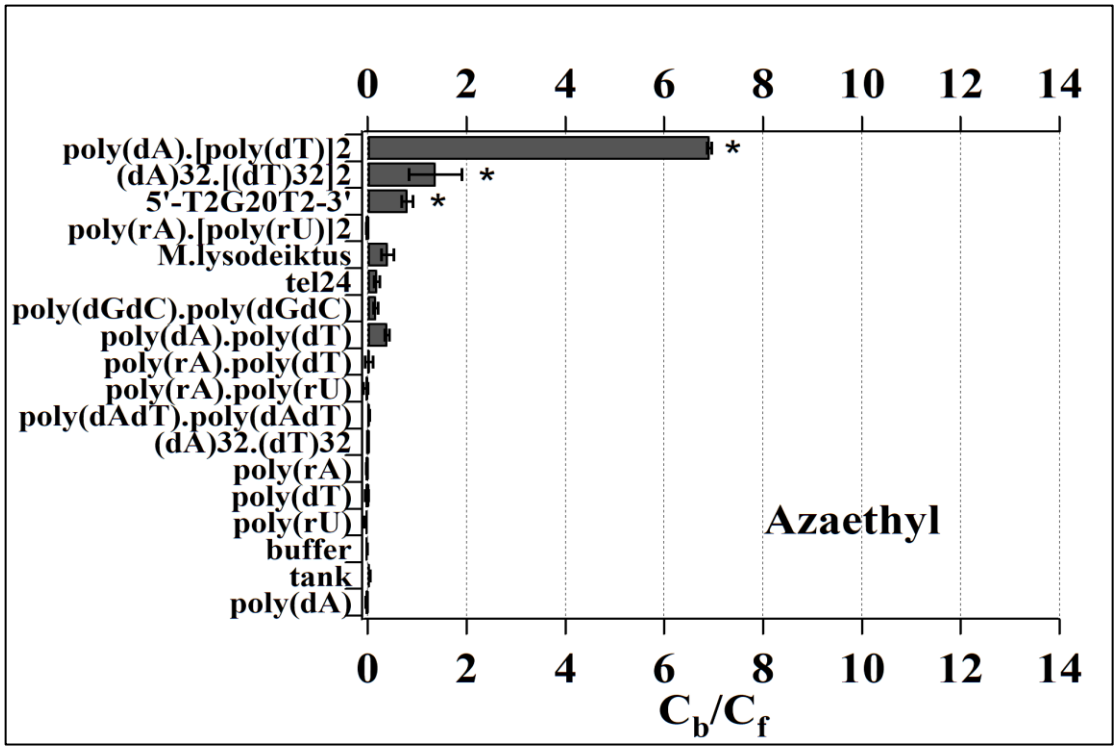

Figure 22. Competition Dialysis results for Azaethyl. *; p<0,05 from control by Kruskal Wallis non-parametric test. Error bars are ±1 standard deviations of the mean with a confidence level of 95%.

Azaethyl also showed significant selectivity, though not as dramatic as Azamethyl's, towards poly(dA)[poly(dT)]$_2$ and (dA)$_{32}$[(dT)$_{32}$]$_2$ triplex DNA structures with average C_b/C_f values of 6.92 and 1.37 and significance levels of p=0.026 and p=0.033, respectively, according to non-parametric Kruskal–Wallis test. Other than its binding to poly(dA)[poly(dT)]$_2$ and (dA)$_{32}$[(dT)$_{32}$]$_2$ triplex DNA structures, its binding to 5'-T$_2$G$_{20}$T$_2$-3' quadruplex was also significant according to our statistical analysis (p=0.044). Its binding was found to be nonsignificant to any other sequences.

3.3.3. Azapropyl:

The fluorescence spectra of the samples in each dialysis cassette were depicted in Figure 23. The concentration of Azapropyl was also different in each dialysis cassettes after 24 hours long competition. The calculated C_b/C_f values for both of the replicate experiments were given in Table 4 along with the average C_b/C_f values. The average C_b/C_f values with the statistical analysis were also plotted in Figure 24.

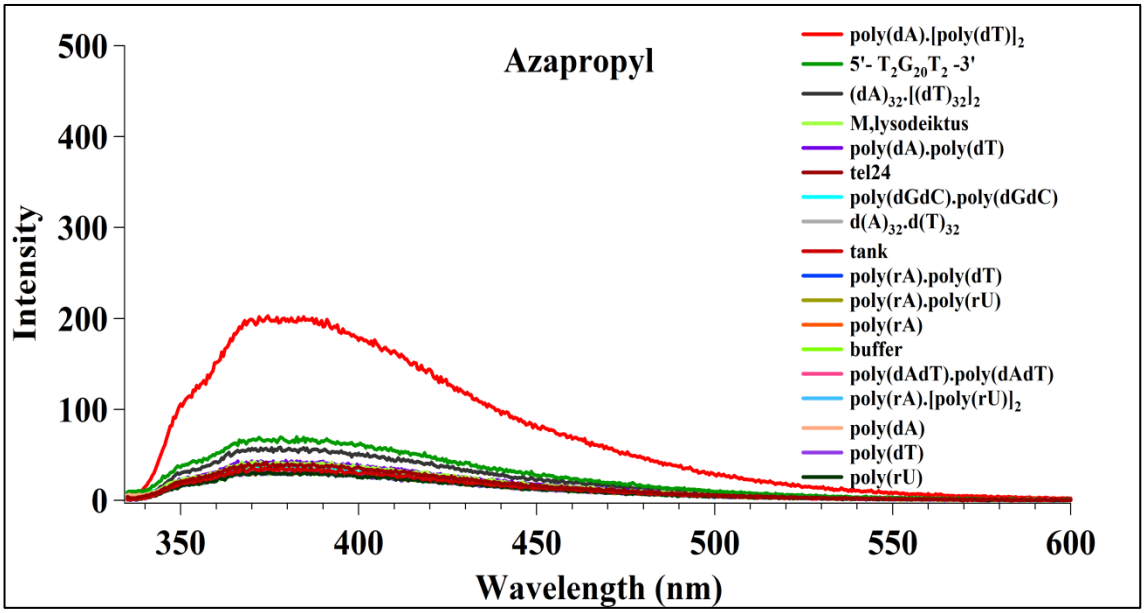

Figure 23. Average fluorescence spectra of Azapropyl. Measurements were obtained at the end of the 24 hours long competition dialysis against Azapropyl from dialysis cassettes containing different nucleic acid structures.

Table 4. Competition dialysis results for Azapropyl.

Oligonucleotides	Folds over buffer (C_b/C_f)			
	1st replicate	2nd replicate	Average	Standard deviation
poly(dA).[poly(dT)]$_2$ - triplex DNA	4.62	5.73	**5.18**	0.78
(dA)$_{32}$.[(dT)$_{32}$]$_2$ - triplex DNA	0.65	0.85	**0.75**	0.14
5'-T$_2$G$_{20}$T$_2$ – 3'- quadruplex DNA	1.27	1.30	**1.28**	0.02
poly(rA).[poly(rU)]$_2$ - triplex RNA	0.13	-0.01	**0.06**	0.10
M.lysodeiktus - dsDNA	0.39	0.35	**0.37**	0.03
tel24 - quadruplex DNA	0.24	0.25	**0.25**	0.01
poly(dGdC).poly(dGdC) - dsDNA	0.21	0.15	**0.18**	0.04
poly(dA).poly(dT) - dsDNA	0.32	0.35	**0.33**	0.02
poly(rA).poly(dT) - DNA-RNA hybrid	0.05	0.06	**0.05**	0.01
poly(rA).poly(rU) - dsRNA	-0.05	0.05	**0.00**	0.06
poly(dAdT).poly(dAdT) - dsDNA	-0.02	0.00	**-0.01**	0.01
(dA)$_{32}$.(dT)$_{32}$ - dsDNA	0.10	0.11	**0.10**	0.00
poly(rA) - ssRNA	-0.02	0.01	**0.00**	0.03
poly(dT) - ssDNA	0.05	-0.05	**0.00**	0.07
buffer	0.00	0.00	**0.00**	0.00
tank	0.16	0.08	**0.12**	0.05
poly(dA) - ssDNA	0.08	-0.03	**0.03**	0.08
poly(rU) - ssRNA	0.03	-0.05	**-0.01**	0.05

The ratio of the bound ligand to free ligand concentration (C_b/C_f) was determined by: $C_b/C_f=(C_t/C_f)-1$ where C_t (total ligand concentration) is the concentration of the ligand in each dialysis cassette and C_f (free ligand concentration) is the concentration of the ligand in a positive control dialysis cassette (buffer) that only includes 1X BPES buffer which typically did not significantly vary from initial small molecule concentration that was 1.0 μM in the solution (tank).

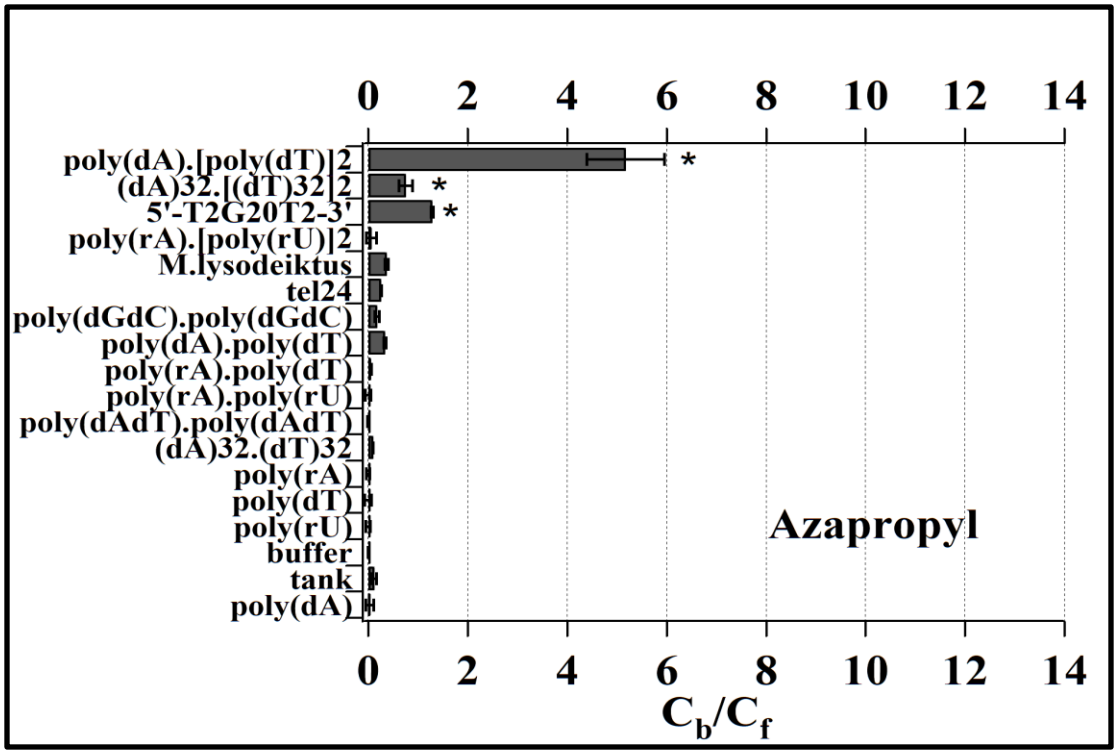

Figure 24. Competition Dialysis results for Azapropyl. *; p<0,05 from control by Kruskal Wallis non-parametric test. Error bars are ±1 standard deviations of the mean with a confidence level of 95%.

Our results have revealed that Azapropyl also shows the highest affinity towards poly(dA)[poly(dT)]$_2$ triplex DNA structure. However, its affinity to 5'-$T_2G_{20}T_2$-3' quadruplex sequence was higher than its affinity to $(dA)_{32}[(dT)_{32}]_2$ triplex DNA unlike Azamethyl and Azaethyl molecules. The obtained C_b/C_f values for poly(dA)[poly(dT)]$_2$, 5'-$T_2G_{20}T_2$-3', and $(dA)_{32}[(dT)_{32}]_2$ were 5.18 (p=0.024) and 1.28 (0.031), and 0.75 (p=0.041), respectively.

3.3.4. Azabutyl:

The fluorescence spectra of the Azabutyl samples obtained from dialysis cassettes after 24 hours of competition dialysis were displayed in Figure 25. Again, the concentration of Azabutyl was varied between different dialysis cassettes. The calculated C_b/C_f ratios for both of the replicate experiments were given in Table 5 and the average C_b/C_f values with the statistical analysis were plotted in Figure 26.

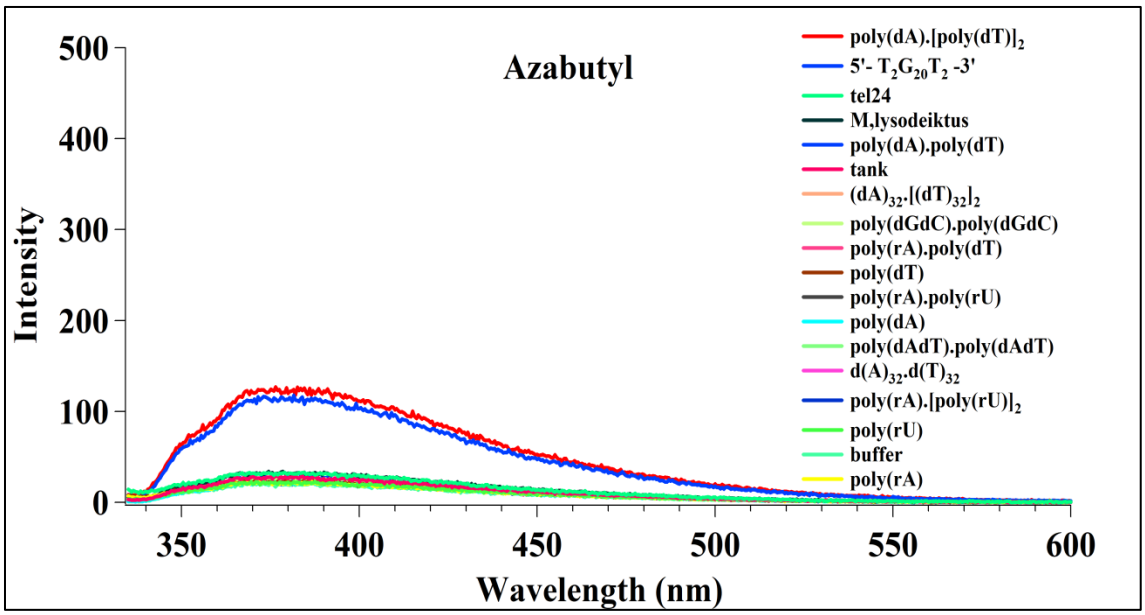

Figure 25. Average fluorescence spectra of Azabutyl. Measurements were obtained at the end of the 24 hours long competition dialysis against Azabutyl from dialysis cassettes containing different nucleic acid structures

Table 5. Competition dialysis results for Azabutyl.

Oligonucleotides	Folds over buffer (C_b/C_f)			
	1st replicate	2nd replicate	Average	Standard deviation
poly(dA).[poly(dT)]$_2$ - triplex DNA	4.36	5.53	**4.94**	0.82
(dA)$_{32}$.[(dT)$_{32}$]$_2$ - triplex DNA	0.31	0.31	**0.31**	0.00
5'-T$_2$G$_{20}$T$_2$ – 3'- quadruplex DNA	4.30	4.94	**4.62**	0.45
poly(rA).[poly(rU)]$_2$ - triplex RNA	0.04	0.03	**0.03**	0.00
M.lysodeiktus - dsDNA	0.71	0.57	**0.64**	0.10
tel24 - quadruplex DNA	0.64	0.61	**0.62**	0.02
poly(dGdC).poly(dGdC) - dsDNA	0.18	0.29	**0.23**	0.08
poly(dA).poly(dT) - dsDNA	0.26	0.37	**0.32**	0.08
poly(rA).poly(dT) - DNA-RNA hybrid	0.18	0.16	**0.17**	0.02
poly(rA).poly(rU) - dsRNA	0.04	0.11	**0.07**	0.05
poly(dAdT).poly(dAdT) - dsDNA	0.10	0.07	**0.09**	0.02
(dA)$_{32}$.(dT)$_{32}$ - dsDNA	0.13	0.07	**0.10**	0.05
poly(rA) - ssRNA	0.07	-0.02	**0.02**	0.07
poly(dT) - ssDNA	-0.01	0.16	**0.07**	0.12
buffer	0.00	0.00	**0.00**	0.00
tank	0.19	0.34	**0.26**	0.11
poly(dA) - ssDNA	0.00	0.10	**0.05**	0.07
poly(rU) - ssRNA	0.04	0.01	**0.03**	0.02

The ratio of the bound ligand to free ligand concentration (C_b/C_f) was determined by: $C_b/C_f=(C_t/C_f)-1$ where C_t (total ligand concentration) is the concentration of the ligand in each dialysis cassette and C_f (free ligand concentration) is the concentration of the ligand in a positive control dialysis cassette (buffer) that only includes 1X BPES buffer which typically did not significantly vary from initial small molecule concentration that was 1.0 μM in the solution (tank).

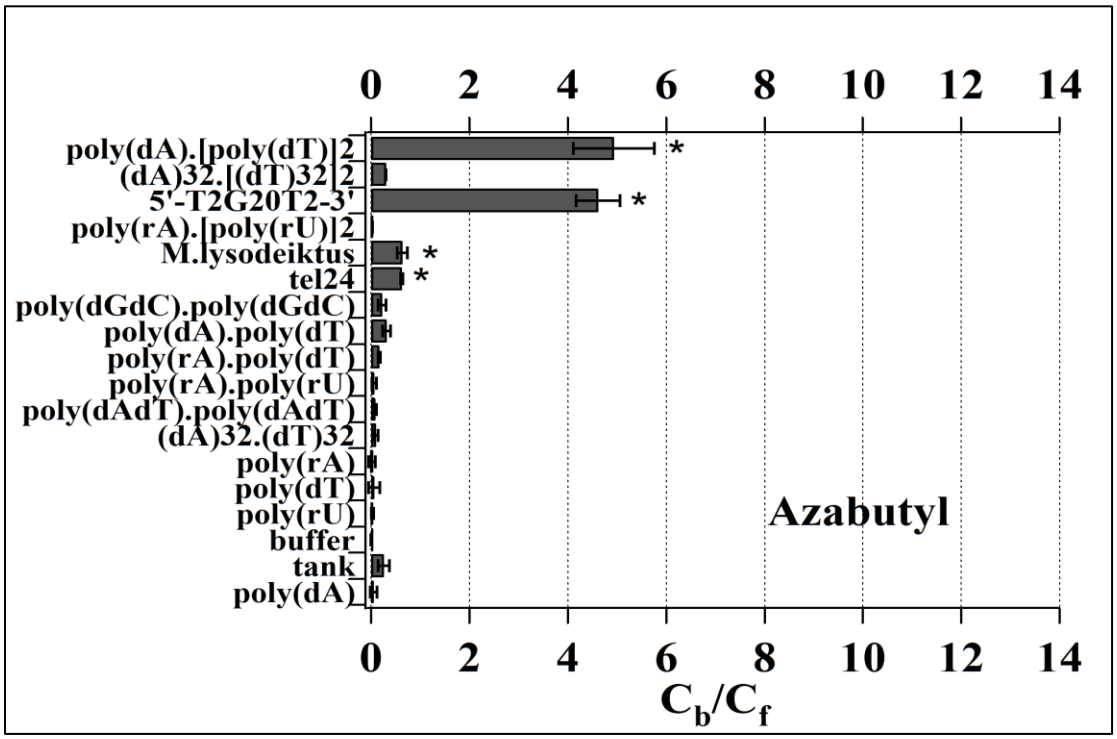

Figure 26. Competition Dialysis results for Azabutyl. *; p<0,05 from control by Kruskal Wallis non-parametric test. Error bars are ±1 standard deviations of the mean with a confidence level of 95%.

Azabutyl showed similar affinity towards poly(dA)[poly(dT)]$_2$ triplex and 5'-T$_2$G$_{20}$T$_2$-3' quadruplex with C_b/C_f values of 4.94 and 4.62, respectively. Interestingly, it did not show any significant affinity to (dA)$_{32}$[(dT)$_{32}$]$_2$ triplex. Such a result indicates that the affinity of the small molecules depends not only to the structure of the nucleic acid but also its length. Conversely, Azabutyl also showed statistically significant binding to *Micrococcus lysodeikticus* (C_b/C_f = 0.64 folds) and tel24 (C_b/C_f =0.62 folds) according to our analysis.

3.3.5. Azaisopropyl:

The fluorescence spectra of the Azaisopropyl samples recovered from dialysis cassettes were provided in Figure 27. The concentration of Azaisopropyl was only slightly different in each dialysis cassette as given in Table 6. Average C_b/C_f values given in Figure 28 were also not that different from each other.

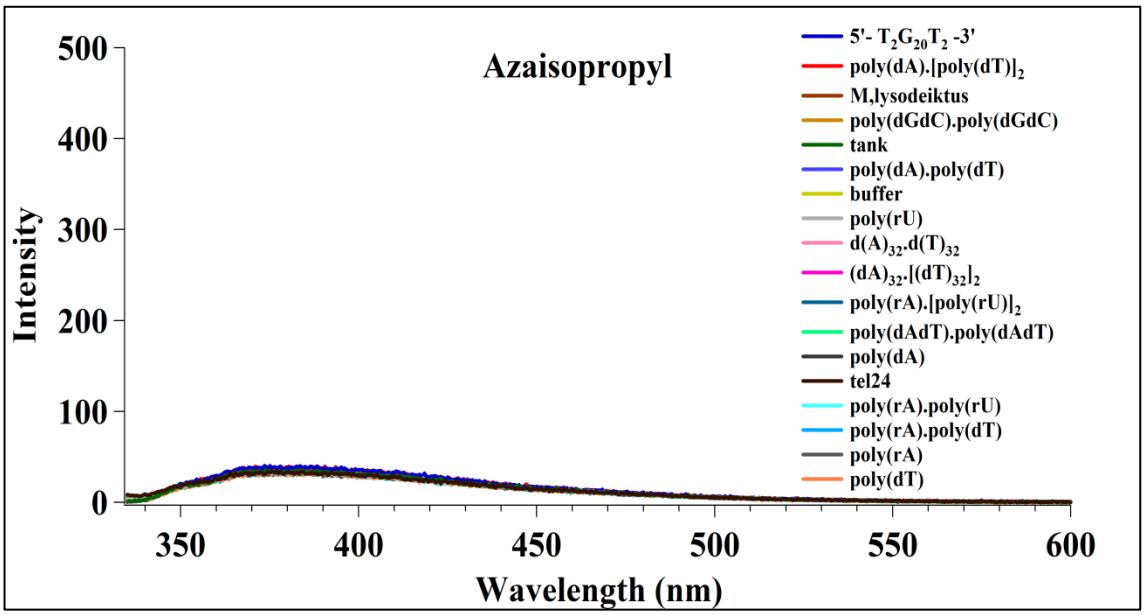

Figure 27. Average fluorescence spectra of Azaisopropyl. Measurements were obtained at the end of the 24 hours long competition dialysis against Azaisopropyl from dialysis cassettes containing different nucleic acid structures

Table 6. Competition dialysis results for Azaisopropyl.

Oligonucleotides	Folds over buffer (C_b/C_f)			
	1st replicate	2nd replicate	Average	Standard deviation
poly(dA).[poly(dT)]$_2$ - triplex DNA	0.22	0.13	**0.17**	0.06
(dA)$_{32}$.[(dT)$_{32}$]$_2$ - triplex DNA	0.13	-0.02	**0.05**	0.10
5'-T$_2$G$_{20}$T$_2$ – 3'- quadruplex DNA	0.26	0.14	**0.20**	0.08
poly(rA).[poly(rU)]$_2$ - triplex RNA	0.01	-0.02	**-0.01**	0.02
M.lysodeiktus - dsDNA	0.15	0.09	**0.12**	0.05
tel24 - quadruplex DNA	0.12	-0.03	**0.05**	0.11
poly(dGdC).poly(dGdC) - dsDNA	0.08	0.08	**0.08**	0.01
poly(dA).poly(dT) - dsDNA	0.06	0.03	**0.04**	0.02
poly(rA).poly(dT) - DNA-RNA hybrid	0.07	-0.06	**0.01**	0.09
poly(rA).poly(rU) - dsRNA	0.11	-0.04	**0.03**	0.11
poly(dAdT).poly(dAdT) - dsDNA	-0.03	-0.02	**-0.03**	0.00
(dA)$_{32}$.(dT)$_{32}$ - dsDNA	0.02	-0.02	**0.00**	0.02
poly(rA) - ssRNA	0.01	-0.06	**-0.03**	0.05
poly(dT) - ssDNA	0.02	-0.08	**-0.03**	0.07
buffer	0.00	0.00	**0.00**	0.00
tank	0.09	0.06	**0.07**	0.02
poly(dA) - ssDNA	0.05	-0.02	**0.01**	0.05
poly(rU) - ssRNA	-0.02	0.00	**-0.01**	0.01

The ratio of the bound ligand to free ligand concentration (C_b/C_f) was determined by: $C_b/C_f=(C_t/C_f)-1$ where C_t (total ligand concentration) is the concentration of the ligand in each dialysis cassette and C_f (free ligand concentration) is the concentration of the ligand in a positive control dialysis cassette (buffer) that only includes 1X BPES buffer which typically did not significantly vary from initial small molecule concentration that was 1.0 μM in the solution (tank).

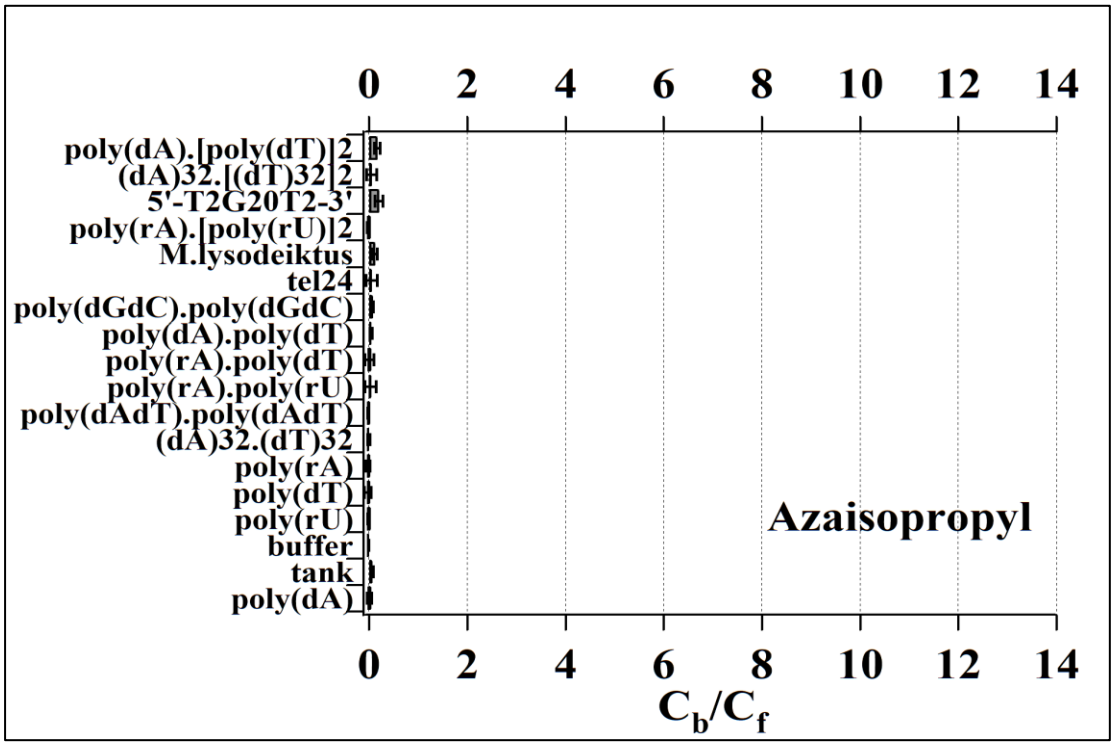

Figure 28. Competition Dialysis results for Azaisopropyl. *; p<0,05 from control by One-way ANOVA parametric test followed by Bonferronni and Sidak Post-Hoc tests. Error bars are ±1 standard deviations of the mean with a confidence level of 95%.

Azaisopropyl's behavior was significantly different than the azacyanines which bear a linear alkyl chain in their benzimidazole ring. It did not show any selectivity to any kind of nucleic acid structure. The amount of the Azaisopropyl concentration in dialysis cassettes containing different nucleic acid structures was no different than the control dialysis cassette containing only the buffer solution. Since the data showed normal distribution (Kolmogorov-Smirnov; p=0.200 and Shapiro-Wilk; p=0.620), we performed one-way ANOVA following Bonferroni and Sidak post-hoc tests in here,

and confirmed that the binding of Azaisopropyl to any of the nucleic acids structures was not statistically significant.

3.3.6. Azaisobutyl:

Average fluorescence spectra of Azaisobutyl samples obtained at the end of the 24 hours long competition dialysis from dialysis cassettes containing different nucleic acid structures were given in Figure 29. C_b/C_f values are given in Table 7 and statistical analysis of the samples was plotted in Figure 30.

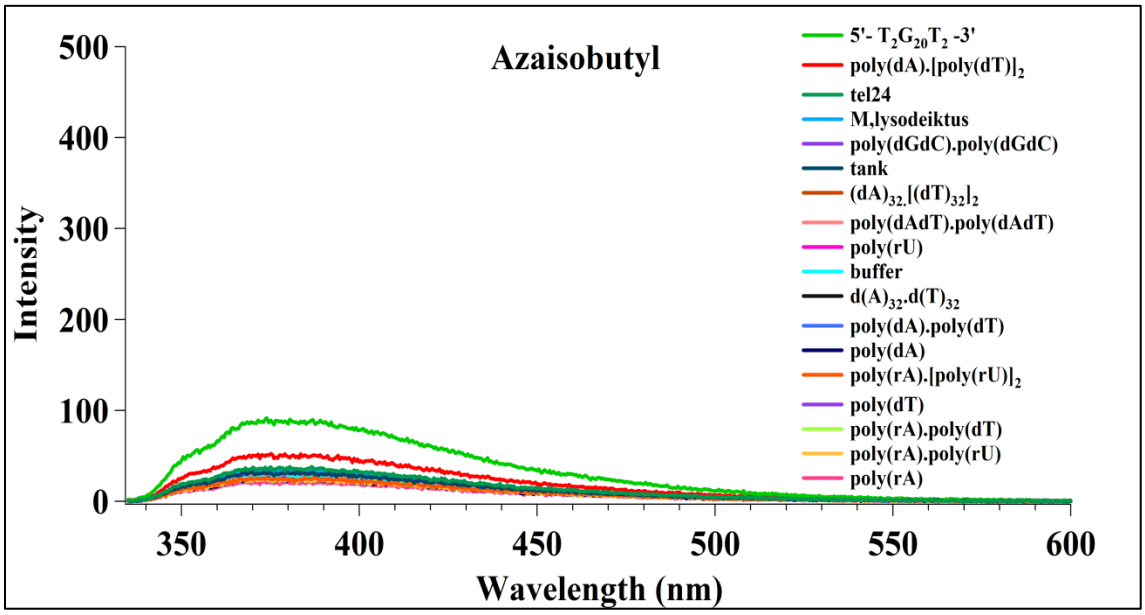

Figure 29. Average fluorescence spectra of Azaisobutyl. Measurements were obtained at the end of the 24 hours long competition dialysis against Azabutyl from dialysis cassettes containing different nucleic acid structures

Table 7. Competition dialysis results for Azaisobutyl.

Oligonucleotides	Folds over buffer (C_b/C_f)			
	1st replicate	2nd replicate	Average	Standard deviation
poly(dA).[poly(dT)]$_2$ - triplex DNA	1.16	0.97	**1.07**	0.13
(dA)$_{32}$.[(dT)$_{32}$]$_2$ - triplex DNA	0.58	0.02	**0.30**	0.39
5'-T$_2$G$_{20}$T$_2$ – 3'- quadruplex DNA	2.49	2.52	**2.50**	0.02
poly(rA).[poly(rU)]$_2$ - triplex RNA	0.05	-0.13	**-0.04**	0.13
M.lysodeiktus - dsDNA	0.31	0.28	**0.30**	0.02
tel24 - quadruplex DNA	0.24	0.29	**0.27**	0.04
poly(dGdC).poly(dGdC) - dsDNA	0.22	0.10	**0.16**	0.09
poly(dA).poly(dT) - dsDNA	0.51	-0.08	**0.21**	0.42
poly(rA).poly(dT) - DNA-RNA hybrid	0.02	-0.14	**-0.06**	0.11
poly(rA).poly(rU) - dsRNA	0.06	-0.17	**-0.06**	0.16
poly(dAdT).poly(dAdT) - dsDNA	0.02	0.01	**0.01**	0.00
(dA)$_{32}$.(dT)$_{32}$ - dsDNA	0.33	-0.06	**0.13**	0.28
poly(rA) - ssRNA	0.00	-0.32	**-0.16**	0.23
poly(dT) - ssDNA	0.10	-0.14	**-0.02**	0.17
buffer	0.00	0.00	**0.00**	0.00
tank	0.32	0.09	**0.20**	0.16
poly(dA) - ssDNA	0.04	-0.13	**-0.05**	0.11
poly(rU) - ssRNA	-0.12	0.01	**-0.06**	0.09

The ratio of the bound ligand to free ligand concentration (C_b/C_f) was determined by: $C_b/C_f=(C_t/C_f)-1$ where C_t (total ligand concentration) is the concentration of the ligand in each dialysis cassette and C_f (free ligand concentration) is the concentration of the ligand in a positive control dialysis cassette (buffer) that only includes 1X BPES buffer which typically did not significantly vary from initial small molecule concentration that was 1.0 µM in the solution (tank).

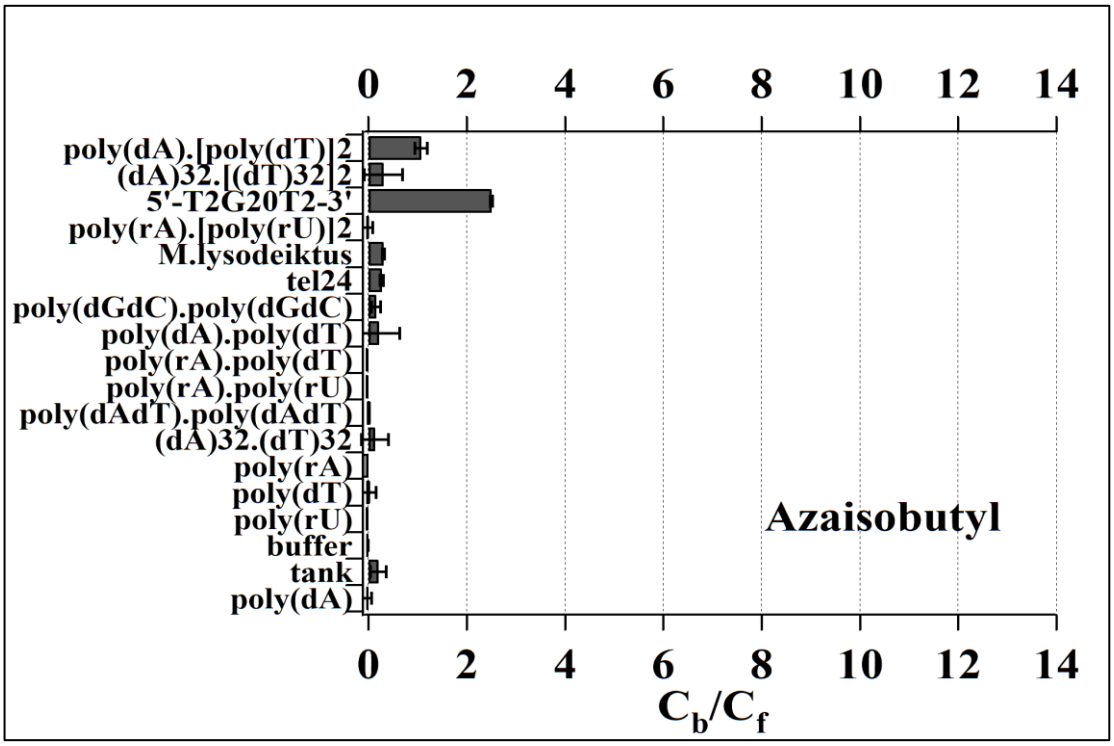

Figure 30. Competition Dialysis results for Azaisobutyl. *; p<0,05 from control by Kruskal Wallis non-parametric test. Error bars are ±1 standard deviations of the mean with a confidence level of 95%.

Our competition dialysis results for Azaisobutyl revealed that Azaisobutyl was not that different from Azaisopropyl in term of its binding affinity and selectivity towards different nucleic acid structures. It did not show any significant binding affinity to any of the structures we investigated as affirmed by the lack of a significant variation among C_b/C_f values (Table 7 and Figure 30). Azabutyl only showed slight binding to 5'-$T_2G_{20}T_2$-3' quadruplex sequence with C_b/C_f value 2.50, but our statistical analysis revealed the binding was not significant (p-value=0.198).

3.3.7. Aza 4:

The nucleic acid affinity and selectivity of Aza4 and Aza5, which are benzothiazole derivatives, was also investigated using competition dialysis. The fluorescence spectra of the Aza4 samples obtained from each dialysis cassette were shown in Figure 31. The C_b/C_f ratios for both of the trials along with the average C_b/C_f values were given in Table 8 and the average C_b/C_f values along with the statistical analysis were plotted in Figure 32.

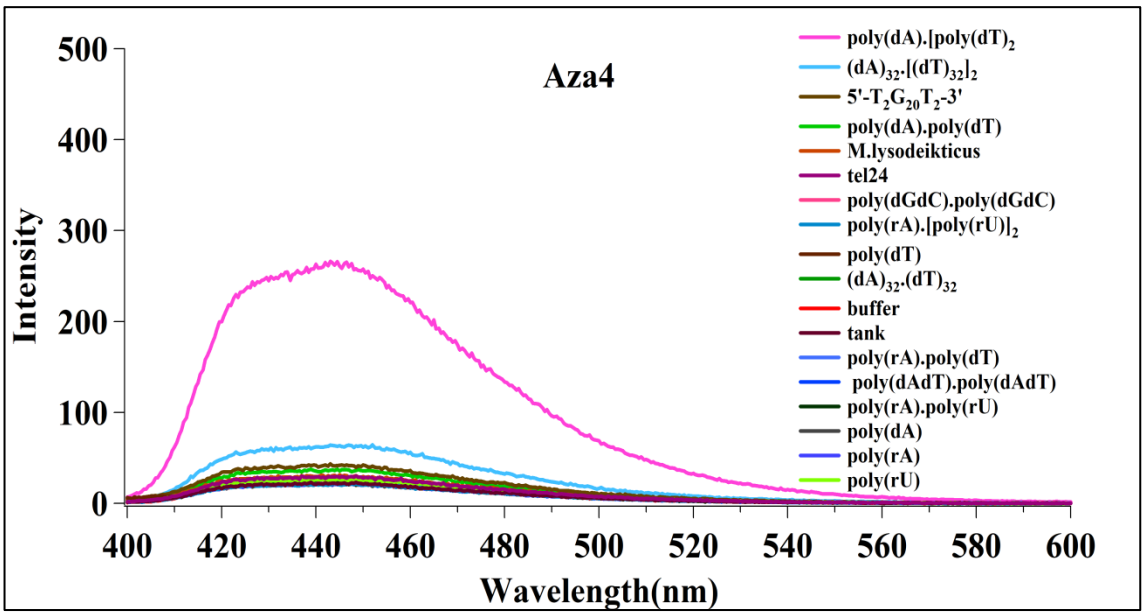

Figure 31. Average fluorescence spectra of Aza4. Measurements were obtained at the end of the 24 hours long competition dialysis against Aza4 from dialysis cassettes containing different nucleic acid structures

Table 8. Competition dialysis results for Aza4.

Oligonucleotides	Folds over buffer (C_b/C_f)			
	1st replicate	2nd replicate	Average	Standard deviation
poly(dA).[poly(dT)]$_2$ - triplex DNA	10.23	10.94	**10.59**	0.50
(dA)$_{32}$.[(dT)$_{32}$]$_2$ - triplex DNA	2.19	1.94	**2.06**	0.18
5'-T$_2$G$_{20}$T$_2$ – 3'- quadruplex DNA	0.97	0.88	**0.92**	0.06
poly(rA).[poly(rU)]$_2$ - triplex RNA	0.25	0.20	**0.23**	0.03
M.lysodeiktus - dsDNA	0.45	0.39	**0.42**	0.04
tel24 - quadruplex DNA	0.33	0.34	**0.33**	0.01
poly(dGdC).poly(dGdC) - dsDNA	0.18	0.19	**0.19**	0.01
poly(dA).poly(dT) - dsDNA	0.67	0.66	**0.66**	0.01
poly(rA).poly(dT) - DNA-RNA hybrid	0.00	0.01	**0.01**	0.01
poly(rA).poly(rU) - dsRNA	0.06	0.04	**0.05**	0.01
poly(dAdT).poly(dAdT) - dsDNA	0.05	0.02	**0.04**	0.02
(dA)$_{32}$.(dT)$_{32}$ - dsDNA	0.10	0.02	**0.06**	0.06
poly(rA) - ssRNA	0.01	-0.01	**0.00**	0.01
poly(dT) - ssDNA	0.05	0.02	**0.04**	0.02
buffer	0.00	0.00	**0.00**	0.00
tank	0.06	0.01	**0.04**	0.04
poly(dA) - ssDNA	0.06	-0.01	**0.02**	0.05
poly(rU) - ssRNA	0.03	-0.05	**-0.01**	0.06

The ratio of the bound ligand to free ligand concentration (C_b/C_f) was determined by: $C_b/C_f=(C_t/C_f)-1$ where C_t (total ligand concentration) is the concentration of the ligand in each dialysis cassette and C_f (free ligand concentration) is the concentration of the ligand in a positive control dialysis cassette (buffer) that only includes 1X BPES buffer which typically did not significantly vary from initial small molecule concentration that was 1.0 μM in the solution (tank).

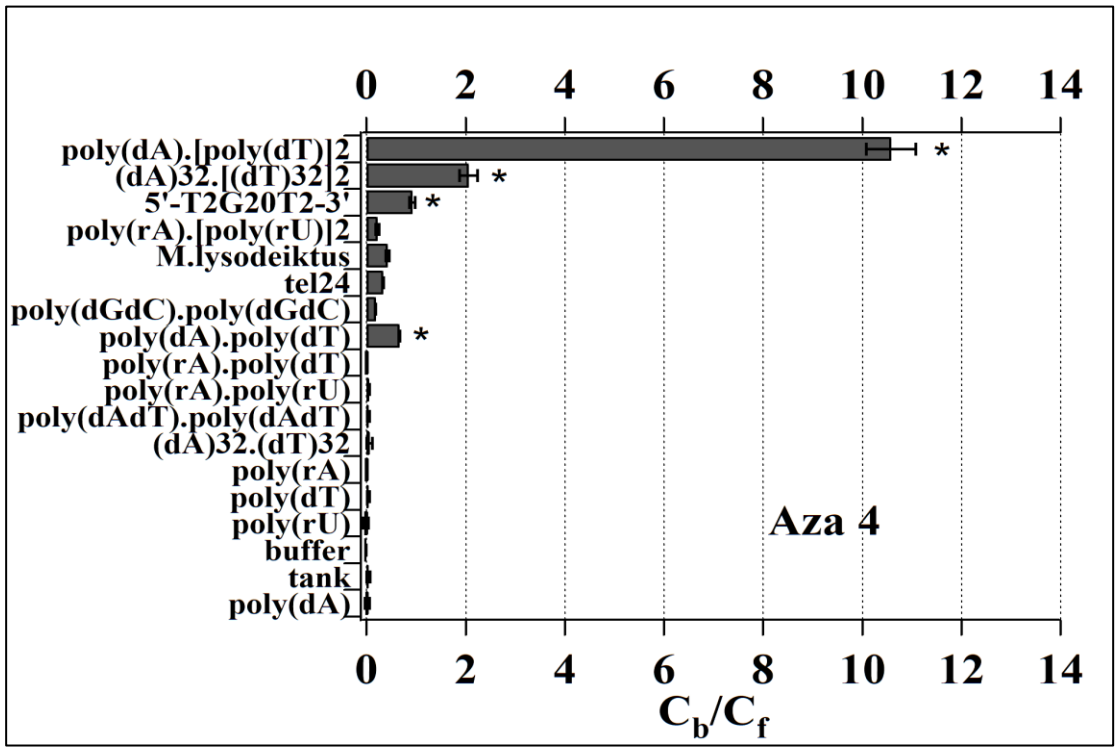

Figure 32. Competition Dialysis results for Aza4. *; p<0,05 from control by Kruskal Wallis non-parametric test. Error bars are ±1 standard deviations of the mean with a confidence level of 95%.

Aza4 also showed significant affinity and selectivity towards poly(dA)[poly(dT)]$_2$ and (dA)$_{32}$[(dT)$_{32}$]$_2$ triplex DNA structures with the average C_b/C_f values of 10.59 and 2.06 with the significance levels of p=0.015 and p=0.020, respectively, according to non-parametric Kruskal–Wallis test. It's binding affinity to poly(dA)[poly(dT)]$_2$ triplex DNA was very similar to Azamethyl's. On the other hand, its binding affinity to (dA)$_{32}$[(dT)$_{32}$]$_2$ triplex DNA was significantly lower than Azamethyl's. Additionally, its binding to 5'-$T_2G_{20}T_2$-3' quadruplex and poly(dA).poly(dT)-dsDNA was also significant according to our statistical analysis

with p=0.027 and p=0.038, respectively. Its binding to any other sequence was not statistically significant.

3.3.8. Aza5:

The fluorescence spectra of the Aza5 samples in each dialysis cassette were depicted in Figure 33. The concentration of Aza5 was also found to be different in each dialysis cassette Table 9. The average C_b/C_f values with the statistical analysis were plotted in Figure 34.

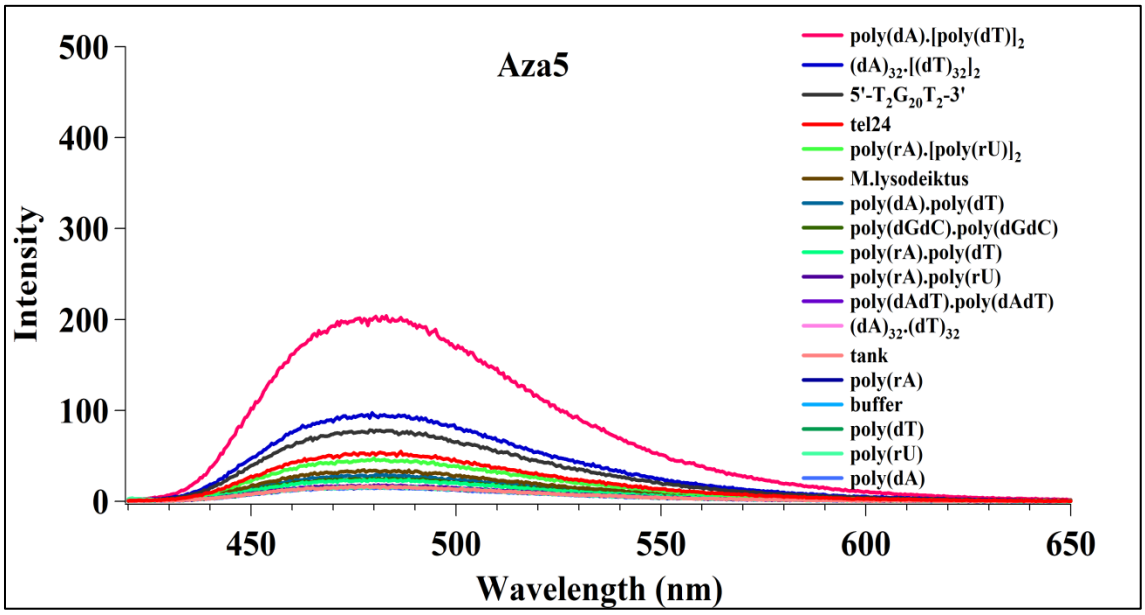

Figure 33. Average fluorescence spectra of Aza5. Measurements were obtained at the end of the 24 hours long competition dialysis against Aza5 from dialysis cassettes containing different nucleic acid structures

Table 9. Competition dialysis results for Aza5.

Oligonucleotides	Folds over buffer (C_b/C_f)			
	1st replicate	2nd replicate	Average	Standard deviation
poly(dA).[poly(dT)]$_2$ - triplex DNA	11.99	12.58	**12.29**	0.42
(dA)$_{32}$.[(dT)$_{32}$]$_2$ - triplex DNA	5.48	5.38	**5.43**	0.07
5'-T$_2$G$_{20}$T$_2$ – 3'- quadruplex DNA	4.07	4.13	**4.10**	0.04
poly(rA).[poly(rU)]$_2$ - triplex RNA	1.90	2.00	**1.95**	0.07
M.lysodeiktus - dsDNA	1.06	1.17	**1.11**	0.08
tel24 - quadruplex DNA	2.32	2.54	**2.43**	0.16
poly(dGdC).poly(dGdC) - dsDNA	0.49	0.64	**0.56**	0.11
poly(dA).poly(dT) - dsDNA	0.80	0.83	**0.82**	0.02
poly(rA).poly(dT) - DNA-RNA hybrid	0.29	0.51	**0.40**	0.16
poly(rA).poly(rU) - dsRNA	0.06	0.12	**0.09**	0.05
poly(dAdT).poly(dAdT) - dsDNA	0.03	0.14	**0.08**	0.08
(dA)$_{32}$.(dT)$_{32}$ - dsDNA	0.07	0.07	**0.07**	0.00
poly(rA) - ssRNA	0.01	-0.04	**-0.01**	0.04
poly(dT) - ssDNA	-0.04	-0.01	**-0.02**	0.02
buffer	0.00	0.00	**0.00**	0.00
tank	0.02	0.05	**0.04**	0.02
poly(dA) - ssDNA	-0.04	-0.06	**-0.05**	0.01
poly(rU) - ssRNA	-0.03	-0.02	**-0.03**	0.00

The ratio of the bound ligand to free ligand concentration (C_b/C_f) was determined by: $C_b/C_f=(C_t/C_f)-1$ where C_t (total ligand concentration) is the concentration of the ligand in each dialysis cassette and C_f (free ligand concentration) is the concentration of the ligand in a positive control dialysis cassette (buffer) that only includes 1X BPES buffer which typically did not significantly vary from initial small molecule concentration that was 1.0 μM in the solution (tank).

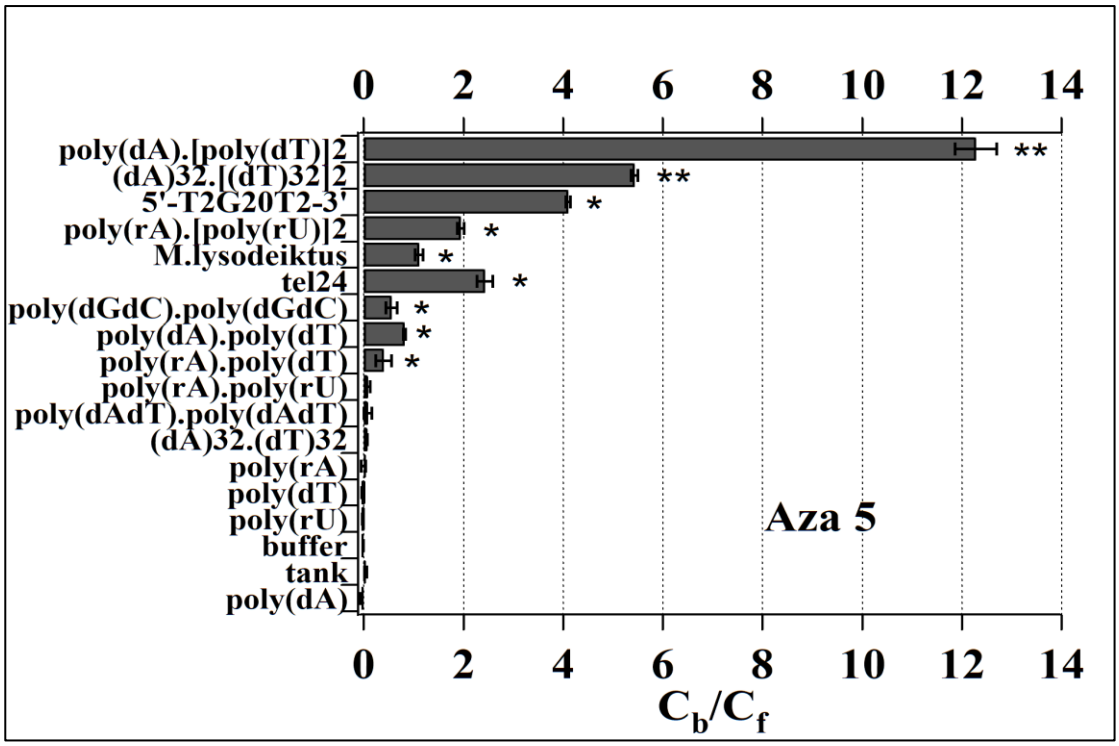

Figure 34. Competition Dialysis results for Aza5. **; p<0,01 from control by Kruskal Wallis non-parametric test. *; p<0,05 from control by Kruskal Wallis non-parametric test Error bars are ±1 standard deviations of the mean with a confidence level of 95%.

Our competition dialysis results revealed undoubtedly that Aza5 is also binding to triple helical structures of poly(dA).[poly(dT)]$_2$ and (dA)$_{32}$.[(dT)$_{32}$]$_2$ with very high affinity and selectivity (Figure 33-34, Table 9). The amount of Aza5 collected in the dialysis cassettes containing poly(dA).[poly(dT)]$_2$ and (dA)$_{32}$.[(dT)$_{32}$]$_2$ was substantial. The average C_b/C_f values of 12.29 and 5.43 with significance levels of p=0.007 and p=0.009, were obtained respectively, according to non-parametric Kruskal–Wallis test. Compared to Azamethyl, its binding affinity to poly(dA).[poly(dT)]$_2$ triplex DNA structure was slightly higher, whereas its binding affinity to (dA)$_{32}$.[(dT)$_{32}$]$_2$ was lower. Aza5 also showed statistically significant binding to 5'-$T_2G_{20}T_2$ -3' quadruplex, tel24,

poly(rA).[poly(rU)]$_2$ RNA triplex, *Micrococcus Lysodeiktus* duplex DNA, poly(dA).poly(dT) duplex DNA, poly(dGdC).poly(dGdC) duplex DNA, and poly(rA).poly(dT) DNA-RNA duplex hybrid with C_b/C_f values of 4.10, 2.43, 1.95, 1.11, 0.82, 0.56, and 0.40 respectively. Furthermore, Aza5 had no affinity towards single stranded nucleic acid structures under these conditions, where the obtained C_b/C_f values were within the experimental errors. Aza5 showed the highest selectivity towards triplex and quadruplex structures among all azacyanines studied here.

3.4. Conclusions:

Here we have examined the affinity and selectivity of eight azacyanines towards different nucleic acid sequences and structures. Six of them were benzimidazole derivatives differing in alky chain length and branching on the benzimidazole ring from each other. Two of them were benzothiazole derivatives differing in substitution on the sixth carbon of the benzimidazole ring from each other.

Our results revealed that Azamethyl, Azaethyl and Azapropyl possess high selectivity and binding affinity towards poly(dA).[poly(dT)]$_2$ – triplex DNA structure. Especially Azamethyl's affinity towards poly(dA).[poly(dT)]$_2$ was remarkable. C_b/C_f value was 11.7 ($p = 0.012$) meaning that 11.7 μM Azamethyl was accumulated to the dialysis cassette that contains poly(dA).[poly(dT)]$_2$ due to high binding affinity where the free Azamethyl concentration was only about 1.0 μM outside. Azabutyl was also binding poly(dA).[poly(dT)]$_2$ with relatively high affinity. However, it was not really selective towards poly(dA).[poly(dT)]$_2$. Its affinity towards poly(dA).[poly(dT)]$_2$ triplex DNA structure and 5'-$T_2G_{20}T_2$- 3' quadruplex DNA structure were similar. Overall, the affinity of benzimidazole derivatives towards poly(dA).[poly(dT)]$_2$ triplex DNA structure was decreasing with the increasing alky chain length. The order of affinity was Azamethyl > Azaethyl > Azapropyl > Azabutyl. In other words, the effect of molecular structure on binding ability of the small molecules to nucleic acid structures was crucial.

Also for these azacyanines with the linear alkyl chain length in the benzimidazole ring, we observed that their affinity towards DNA structures was higher than their affinity to RNA structures. Moreover, their affinity towards DNA-RNA hybrid structures was in between. We also observed that none of the azacyanines showed significant binding affinity towards any of the single stranded nucleic acid structures under these conditions.

Azaisopropyl and Azaisobutyl, which bear a branched alkyl chain in their benzimidazole ring, showed no significant binding affinity statistically to any of the nucleic acid structures examined. Especially, in the case of Azaisopropyl there was no binding at all. It was evident that the branching on the benzimidazole ring was detrimental, preventing these molecules from binding to any of the nucleic acid structures included in our assay.

Based on benzothiazole derivatives, our results revealed that Aza4 and Aza5 also possess high selectivity and binding affinity towards poly(dA).$[poly(dT)]_2$ – triplex DNA structure. Especially Aza5's affinity towards poly(dA).$[poly(dT)]_2$ was remarkable. C_b/C_f value was 12.3 ($p = 0.007$). Aza5 showed the most dramatic results in terms of its affinity and selectivity towards triplex poly(dA).$[poly(dT)]_2$ triplex DNA structure among all of the azacyanine derivatives.

Aza4 also showed high affinity and selectivity towards poly(dA).$[poly(dT)]_2$ triplex DNA structure. C_b/C_f value was 10.6 with the p value: 0.015. Furthermore, its binding to $(dA)_{32}.[(dT)_{32}]_2$ triplex DNA was also noteworthy with the C_b/C_f value 2.06 ($p = 0.020$).

Previously, using surface plasma resonance (SPR) spectroscopy it has been shown that the binding affinity of Azamethyl, Aza4 and Aza5 towards G-quadruplex- tel 24 structure were quite similar (Çetinkol *et al*., 2008). Furthermore, in term of their binding affinity to poly(A) at high drug concentrations, Azamethyl and Aza5 had similar binding affinities but the binding affinity of Aza4 was quite lower (Çetinkol & Hud, 2009). Moreover, in his studies Kim revealed that Aza5 showed the most

remarkable effect on yeast cells with $(GAA)_n$ repeats. In addition, Kim hypothesized that the effect they observed was due to the binding and the stabilizing effect of azacyanines to triple helical nucleic acids (Kim, 2009). Here, our results confirmed the studies of Kim that azacyanines were binding to poly(dA).$[poly(dT)]_2$ triplex DNA structure with high affinity and selectivity. Their affinity order was Aza5 > Azamethyl > Aza4 in an agreement with Kim's data (Kim, 2009). In terms of their binding abilities to tel24, even though their binding affinity is way lower compared to their affinity to poly(dA).$[poly(dT)]_2$ triplex DNA, we observed a very similar trend. Aza5 had slightly higher affinity than Azamethyl, and Azamethyl had slightly higher affinity than Aza4.

In conclusion, our competition dialysis results revealed that certain azacyanine molecules possess high affinity and selectivity towards triplex and quadruplex DNA structures. More specifically Aza5, Azamethyl, and Aza4 showed the most dramatic binding selectivity towards poly(dA).$poly(dT)_2$ triplex DNA structure. Their ability of binding to other triplex and quadruplex structures was also statistically significant. Moreover, our results showed that, among the benzimidazole derivatives, the binding affinity of the small molecules towards poly(dA).$poly(dT)_2$ triplex DNA was decreasing with the increasing alkyl chain length and branching. Especially the effect of branching on binding affinity of these molecules was significant. Neither Azaisopropyl nor Azaisobutyl showed significant binding affinity towards any of the nucleic acid structures included in our competition dialysis assay.

CHAPTER 4

THESIS CONCLUSION

4.1. Azamethyl, Aza4 and Aza5 Catalytically Inhibit Topo IIα:

Here, we first investigated the effect of different azacyanines on Topo IIα. Our results revealed that Azamethyl, Aza4, and Aza5 can decrease the catalytic activity of Topo IIα with high efficiency. More importantly, their efficiency was higher than the proven Topo IIα poison (Etoposide). Etoposide (also known as Toposar and VePesid) is one of the medications used in chemotherapy and included in the World Health Organization's "List of Essential Medicines" in 2015 as an anticancer drug (World Health Organization, 2015).

In our assay, we have observed that 50.0 μM Azamethyl decrease Topo IIα catalytic activity even more strongly than 500.0 μM of Etoposide. However, we have observed that Azamethyl affects Topo IIα catalytically. In other words, azacyanines cannot be considered as poisons, like Etoposide. This means that they are probably less toxic than the Etoposide. The lower toxicity of azacyanines might have a significant impact on their potential use in chemotherapy. Even though Etoposide is a commonly used medicine, it cannot be used in high doses due to its highly toxic side effects to normal cells which limit its effectiveness in chemotherapy (Marigny, Aubin, Burgot, Le Gall, & Gandemer, 2005). Therefore, azacyanines with low toxicity, meaning lower side effects, might also be good choices to inhibit Topo IIα in chemotherapeutic applications.

Unlike Azamethyl, Aza5, and Aza4; Azaethyl and Azaisobutyl did not change Topo IIα's activity. Surprisingly, they both strengthen the intensity of the bands belonging to decatenated DNA products in our gel. This indicates that they do not decrease the catalytic activity of Topo IIα enzyme but rather increase its activity. However, this outcome requires further detailed investigation.

The results obtained here provide an alternative insight about the mechanistic explanation of azacyanine derivatives' effects in yeast cells observed also by Kim (Kim, 2009) and demonstrate the potentials of Azamethyl, Aza4 and Aza5. However, their effect on different types of cancer cells should also be examined by in-vivo studies. Only after such examinations, their real potential as Topo IIα interfering molecules will be truly realized.

4.2. Azamethyl, Aza4, and Aza5 Bind to Triplex and Quadruplex Nucleic Acid Structures with High Affinity and Selectivity:

Our competition dialysis results showed that Azamethyl, Aza5, and Aza4 bind with high affinity and selectivity especially to poly(dA).$[poly(dT)]_2$ - triplex DNA and 5'- $T_2G_{20}T_2$- 3' - quadruplex DNA structures. In addition to these molecules, Azaethyl, Azapropyl, and Azabutyl also showed differential binding affinity towards the same triplex and quadruplex structures. On the other hand, Azaisopropyl and Azaisobutyl did not show any binding affinity towards any of the nucleic acid structures examined here.

In terms of their triplex binding affinity, Aza5 showed the highest binding affinity. Its C_b/C_f values were 12.3 (p=0.007) and 5.4 (p=0.009) towards poly(dA).$poly[(dT)]_2$ and $(dA)_{32}.[(dT)_{32}]_2$ triplex DNA structures respectively. This means that Aza5 binds to poly(dA).$poly(dT)_2$ triplex DNA sequence 12.3 folds more than our control (includes only buffer). Its affinity to quadruplex structures was also high with C_b/C_f values of 4.1 (p=0.011) and 2.43 (p=0.013) towards 5'- $T_2G_{20}T_2$ – 3' and tel24 quadruplex DNAs respectively. These findings are important because as explained in chapter 1.1, stabilizing triplex and quadruplex structures could be a promising strategy in cancer treatment.

Moreover, Azamethyl also showed high affinity and selectivity towards triplex and quadruplex DNA structures. Its C_b/C_f values were 11.7 (p=0.012) and 10.7 (p=0.014) towards poly(dA).poly$[(dT)]_2$ and $(dA)_{32}.[(dT)_{32}]_2$ triplex DNA structures, respectively. Furthermore, Aza4 also showed relatively high affinity towards triplex DNA structures. Azaethyl, Azapropyl, and Azabutyl also showed high affinity and selectivity towards poly(dA).poly$[(dT)]_2$ triplex DNA structure but their binding affinity and selectivity were not as high as Azamethyl's, Aza4's, or Aza5's. On the other hand, Azaisopropyl and Azaisobutyl showed no notable affinity towards any nucleic acid structures investigated here.

Among the benzimidazole derivatives (Azamethyl, Azaethyl, Azapropyl, Azabutyl, Azaisopropyl, and Azaisobutyl) investigated, it is obvious that the affinity and selectivity of these molecules towards poly(dA).poly$[(dT)]_2$ triplex DNA structure is highly dependent on the linear alkyl chain length and branching. With the increasing length of linear alkyl chain and/or branching, the binding ability of azacyanines to poly(dA).poly$[(dT)]_2$ triplex DNA structure was decreasing. To our knowledge, this is the first work displaying how the systematic change in molecular structure of the small molecule can alter the triplex binding affinity and selectivity.

Our competition dialysis results also provide an alternative explanation about the mechanism of azacyanines' effects on cells observed previously by Kim (Kim, 2009). He hypothesized that the reason behind the observed double stranded breaks in yeast cells might be due to the high binding affinity and selectivity of Azamethyl, Aza4 and Aza5 toward triplexes. Here, we have clearly demonstrated that all three molecules have high affinity and selectivity towards certain triplex structures.

4.3.Concluding Remarks:

In conclusion, we have found two probable explanations about the observed effects of Azamethyl, Aza4 and Aza5 in yeast cells demonstrated by Kim (Kim, 2009).

The first explanation is the ability of these molecules to change the catalytic activity of Topo IIα. Our results explicitly revealed that catalytic activity of Topo IIα decreased with Azamethyl, Aza4, and Aza5. Moreover, the effect was significantly higher than the inhibition ability of Etoposide which is a proven Topo IIα poison. Therefore, these molecules might have a high potential to be effective chemotherapeutic agents. However, further investigation on their effect in different cancer cell lines are needed to realize their full potential.

Our second explanation, which supports the findings and hypothesizes of Kim (Kim, 2009), is the fact that these molecules have high binding affinity and selectivity especially towards certain triplex DNA structures. They were also shown to have relatively high binding affinity towards certain quadruplex structures.

At this point we do not know exactly at which catalytic step (Figure 7) Topo IIα is affected, but we suspect that the binding of these molecules (Azamethyl, Aza4, and Aza5) to higher order nucleic acid structures might be the reason behind their effects on Topo IIα's catalytic activity. These molecules might be binding to enzyme binding sites on the DNA before the enzyme and therefore preventing the formation of an intact DNA-enzyme complex by changing the DNA conformation or they might be directly targeting the enzyme and blocking its binding to the DNA.

Overall, these molecules might have potential to be used in chemotherapy due to their negative effects on Topo IIα's catalytic activity and can also be used in gene targeting due to their triplex binding affinity. The findings presented in this thesis, inspire us to further investigate azacyanines' potentials.

REFERENCES

Andrews, C. A., Vas, A. C., Meier, B., Giménez-Abián, J. F., Díaz-Martínez, L. A., Green, J., Clarke, D. J. (2006). A mitotic topoisomerase II checkpoint in budding yeast is required for genome stability but acts independently of Pds1/securin. *Genes and Development*, *20*(9), 1162–1174.

Bachurin, S. S., Kletskii, M. E., Burov, O. N., & Kurbatov, S. V. (2018). Non-canonical DNA structures: Comparative quantum mechanical study. *Biophysical Chemistry*, *235*, 19–28.

Barros, F. W. A., Bezerra, D. P., Ferreira, P. M. P., Cavalcanti, B. C., Silva, T. G., Pitta, M. G. R., Pessoa, C. (2013). Inhibition of DNA topoisomerase I activity and induction of apoptosis by thiazacridine derivatives. *Toxicology and Applied Pharmacology*, *268*(1), 37–46.

Bau, J. T., Kang, Z., Austin, C. A., & Kurz, E. U. (2013). Salicylate, a catalytic inhibitor of topoisomerase II, inhibits DNA cleavage and is selective for the isoform. *Molecular Pharmacology*, *85*(2), 198–207.

Baudat, F., Manova, K., Yuen, J. P., Jasin, M., & Keeney, S. (2000). Chromosome synapsis defects and sexually dimorphic meiotic progression in mice lacking Spo11. *Molecular Cell*, *6*(5), 989–998.

Bax, B. D., Chan, P. F., Eggleston, D. S., Fosberry, A., Gentry, D. R., Gorrec, F., Gwynn, M. N. (2010). Type IIA topoisomerase inhibition by a new class of antibacterial agents. *Nature*, *466*(7309), 935–940.

Baxter, J., & Diffley, J. F. X. (2008). Topoisomerase II inactivation prevents the completion of DNA replication in budding yeast. *Molecular Cell*, *30*(6), 790–802.

Bergerat, A., De Massy, B., Gadelle, D., Varoutas, P. C., Nicolas, A., & Forterre, P. (1997). An atypical topoisomerase II from archaea with implications for meiotic recombination. *Nature*, *386*(6623), 414–417.

Bing, T., Zheng, W., Zhang, X., Shen, L., Liu, X., Wang, F., Shangguan, D. (2017). Triplex-quadruplex structural scaffold: A new binding structure of aptamer. *Scientific Reports*, *7*(1), 1–10.

Bissler, J. J. (2007). Triplex DNA and human disease. *Frontiers in Bioscience*, *12*, 4536–4546.

Bochman, M. L., Paeschke, K., & Zakian, V. A. (2012). DNA secondary structures: Stability and function of G-quadruplex structures. *Nature Reviews Genetics*, *13*(11), 770-780.

Chaires, J. B., Dattagupta, N., & Crothers, D. M. (1982). Studies on interaction of anthracycline antibiotics and deoxyribonucleic acid: Equilibrium binding studies on interaction of Daunomycin with deoxyribonucleic acid. *Biochemistry*, *21*(17), 3933–3940.

Chaires J.B. (1998). Drug-DNA interactions. *Current Opinion in Structural Biology*, *8*, 314-320.

Chaires, J. B., Ren, J., Henary, M., Zegrocka, O., Reid Bishop, G., & Strekowski, L. (2003). Triplex selective 2-(2-naphthyl)quinoline compounds: Origins of affinity and new design principles. *Journal of the American Chemical Society*, *125*(24), 7272–7283.

Champoux, J. J. (2001). DNA topoisomerases: structure, function, and mechanism. *Annual Review of Biochemistry*, *70*, 369–413.

Chen, Z., Zhang, H., Ma, X., Lin, Z., Zhang, L., & Chen, G. (2015). A novel fluorescent reagent for recognition of triplex DNA with high specificity and selectivity. *The Analyst*, *140*(22), 7742–7747.

Classen, S., Olland, S., & Berger, J. M. (2003). Structure of the topoisomerase II ATPase region and its mechanism of inhibition by the chemotherapeutic agent ICRF-187. *Proceedings of the National Academy of Sciences of the United States of America*, *100*(19), 10629–10634.

Cliby, W. A., Lewis, K. A., Lilly, K. K., & Kaufmann, S. H. (2002). S phase and G2 arrests induced by topoisomerase I poisons are dependent on ATR kinase function. *Journal of Biological Chemistry*, *277*(2), 1599–1606.

Coelho, P. A., Queiroz-Machado, J., Carmo, A. M., Moutinho-Pereira, S., Maiato, H., & Sunkel, C. E. (2008). Dual role of topoisomerase II in centromere resolution and aurora B activity. *PLoS Biology*, *6*(8), 1758–1777.

Conrad, N. K. (2014). The emerging role of triple helices in RNA biology. *Wiley Interdisciplinary Reviews: RNA*, 5(1), 15-29.

Corbett, K. D., & Berger, J. M. (2006). Structural basis for topoisomerase VI inhibition by the anti-Hsp90 drug radicicol. *Nucleic Acids Research*, *34*(15), 4269–4277.

Çetinkol, Ö. P., Engelhart, A. E., Nanjunda, R. K., Wilson, W. D., & Hud, N. V. (2008). Submicromolar, selective G-quadruplex ligands from one pot: Thermodynamic and structural studies of human telomeric DNA binding by azacyanines. *ChemBioChem*, *9*(12), 1889–1892.

Çetinkol, Ö. P., & Hud, N. V. (2009). Molecular recognition of poly (A) by small ligands: an alternative method of analysis reveals nanomolar, cooperative and shape-selective binding. *Nucleic Acids Research*, *37*(2), 611–621.

Diaz-Martinez, L. A., Gimenez-Abian, J. F., & Clarke, D. J. (2008). Chromosome cohesion - rings, knots, orcs and fellowship. *Journal of Cell Science*, *121*(13), 2107–2114.

Drolet, M., Bi, X., & Liu, L. F. (1994). Hypernegative supercoiling of the DNA template during transcription elongation in vitro. *Journal of Biological Chemistry*,

269(3), 2068–2074.

Drolet, M., Phoenix, P., Menzel, R., Massé, E., Liu, L. F., & Crouch, R. J. (1995). Overexpression of RNase H partially complements the growth defect of an Escherichia coli delta topA mutant: R-loop formation is a major problem in the absence of DNA topoisomerase I. *Proceedings of the National Academy of Sciences of the United States of America*, *92*(8), 3526–3530.

Dwyer, D. J., Kohanski, M. A., Hayete, B., & Collins, J. J. (2007). Gyrase inhibitors induce an oxidative damage cellular death pathway in Escherichia coli. *Molecular Systems Biology*, *3*(91), 1-15.

Edwards, M. J., Flatman, R. H., Mitchenall, L. A., Stevenson, C. E. M., Le Tung, B. K., Clarke, T. A., Maxwell, A. (2009). A crystal structure of the bifunctional antibiotic simocyclinone D8, bound to DNA gyrase. *Science*, *326*(5958), 1415–1418.

Escudé, C., Nguyen, C. H., Kukreti, S., Janin, Y., Sun, J.-S. S., Bisagni, E., Helene, C. (1998). Rational design of a triple helix-specific intercalating ligand. *Proceedings of the National Academy of Sciences*, *95*(7), 3591–3596.

Fay, M. M., Lyons, S. M., & Ivanov, P. (2017). RNA G-Quadruplexes in Biology: Principles and Molecular Mechanisms. *Journal of Molecular Biology*, *429*(14), 2127-2147.

Ferguson, L. R., & Baguley, B. C. (1994). Topoisomerase II enzymes and mutagenicity. *Environmental and Molecular Mutagenesis*, *24*(4), 245–261.

Fox, K. R., & Darby, R. A. J. (2004). Triple Helix-Specific Ligands. In M. Demeunynck, C. Bailly, & D. Wilson (Eds.), *Small Molecule DNA and RNA Binders*, chapter 14, 360–383.

Frank-Kamenetskii, M. D., & Mirkin, S. M. (1995). Triplex DNA structures. *Annual Review of Biochemistry*, *64*, 65–95.

Gacy, A. M., Goellner, G. M., Spiro, C., Chen, X., Gupta, G., Bradbury, E. M., McMurray, C. T. (1998). GAA instability in Friedreich's Ataxia shares a common, DNA-directed and intraallelic mechanism with other trinucleotide diseases. *Molecular Cell*, *1*(4), 583–593.

Gilmour, D. S., Pflugfelder, G., Wang, J. C., & Lis, J. T. (1986). Topoisomerase I interacts with transcribed regions in Drosophila cells. *Cell*, *44*(3), 401–407.

Goto, T., Laipis, P., & Wang, J. C. (1984). The purification and characterization of DNA topoisomerases I and II of the yeast Saccharomyces cerevisiae. *The Journal of Biological Chemistry*, *259*(16), 10422–10429.

Haddadin, M. J., Kurth, M. J., & Olmstead, M. M. (2000). One-step synthesis of new heterocyclic azacyanines. *Tetrahedron Letters*, *41*(30), 5613–5616.

Han, H., & Hurley, L. H. (2000). G-quadruplex DNA: A potential target for anti-cancer drug design. *Trends in Pharmacological Sciences*. *21*(4), 136-142.

Han, M. S., Lytton-Jean, A. K. R., & Mirkin, C. A. (2006). A gold nanoparticle based approach for screening triplex DNA binders. *Journal of the American Chemical Society*, *128*(15), 4954–4955.

Hanahan, D., & Weinberg, R. A. (2011). Hallmarks of cancer: The next generation. *Cell*, *144*(5), 646–674.

Harkness, R. W., & Mittermaier, A. K. (2017). G-quadruplex dynamics. *Biochimica et Biophysica Acta - Proteins and Proteomics*, *1865*(11), 1544-1554.

Hartsuiker, E., Mizuno, K., Molnar, M., Kohli, J., Ohta, K., & Carr, A. M. (2009). Ctp1CtIP and Rad32Mre11 nuclease activity are required for Rec12Spo11 removal, but Rec12Spo11 removal is dispensable for other MRN-dependent meiotic functions. *Molecular and Cellular Biology*, *29*(7), 1671–1681.

Helene, C., Thuong, N. T., & Harel, A. (1992). Control of gene expression by triple

helix-forming oligonucleotides. The Antigene strategy. *Annals of the New York Academy of Sciences*, *660*(1), 27–36.

Hornedo, J., & Van Echo, D. A. (1985). Amsacrine (m-AMSA): A new antineoplastic agent pharmacology, clinical activity and toxicity. *Pharmacotherapy: The Journal of Human Pharmacology and Drug Therapy*, *5*(2), 78–90.

Hu, Y., Cecconello, A., Idili, A., Ricci, F., & Willner, I. (2017). Triplex DNA nanostructures: from basic properties to applications. *Angewandte Chemie - International Edition*, 56(48), 15210-15233.

Huang, C. E., Milutinovich, M., & Koshland, D. (2005). Rings, bracelet or snaps: fashionable alternatives for Smc complexes. *Philosophical Transactions of the Royal Society B: Biological Sciences*, *360*(1455), 537–542.

Hurley L.H. (1989). DNA and associated targets for drug design. *Journal of Medicinal Chemistry, 32*, 2027-2033.

Ju, B. G., Lunyak, V. V., Perissi, V., Garcia-Bassets, I., Rose, D. W., Glass, C. K., & Rosenfeld, M. G. (2006). A topoisomerase IIβ-mediated dsDNA break required for regulated transcription. *Science*, *312*(5781), 1798–1802.

Ju, B. G., & Rosenfeld, M. G. (2006). A breaking strategy for topoisomerase IIβ/PARP-1-dependent regulated transcription. *Cell Cycle*, *5*(22), 2557–2560.

Keeney, S. (2008). Spo11 and the formation of DNA double-strand breaks in meiosis. *Genome Dynamics and Stability*, 2, 81-123.

Keeney, S., Giroux, C. N., & Kleckner, N. (1997). Meiosis-specific DNA double-strand breaks are catalyzed by Spo11, a member of a widely conserved protein family. *Cell*, *88*(3), 375–384.

Ketron, A. C., Denny, W. A., Graves, D. E., & Osheroff, N. (2012). Amsacrine as a topoisomerase II poison: Importance of drug-DNA interactions. *Biochemistry*,

51(8), 1730–1739.

Kim, H. M. (2009). Genome instability induced by triplex forming mirror repeats in S.cerevisiae, (May). Doctoral dissertation, *Georgia Institute of Technology*. Retrieved from: https://smartech.gatech.edu/bitstream/handle/1853/33874/kim_hyun-min_200905_phd.pdf?sequence=1&isAllowed=y

Kim, N., & Jinks-Robertson, S. (2017). The Top1 paradox: Friend and foe of the eukaryotic genome. *DNA Repair, 56*, 33–41.

Kohanski, M. A., Dwyer, D. J., Hayete, B., Lawrence, C. A., & Collins, J. J. (2007). A common mechanism of cellular death induced by bactericidal antibiotics. *Cell*, *130*(5), 797–810.

Laponogov, I., Pan, X. S., Veselkov, D. A., Mcauley, K. E., Fisher, L. M., & Sanderson, M. R. (2010). Structural basis of gate-DNA breakage and resealing by type II topoisomerases. *PLoS ONE, 5*(6), 1-8.

Larsen, A. K., Escargueil, A. E., & Skladanowski, A. (2003). Catalytic topoisomerase II inhibitors in cancer therapy. *Pharmacology & Therapeutics*, *99*(2), 167–181.

Lee, P. Y., Costumbrado, J., Hsu, C.-Y., & Kim, Y. H. (2012). Agarose gel electrophoresis for the separation of DNA fragments. *Journal of Visualized Experiments : JoVE*, (62), 1–5.

Lewis, R. J., Singh, O. M., Smith, C. V, Skarzynski, T., Maxwell, A., Wonacott, A. J., & Wigley, D. B. (1996). The nature of inhibition of DNA gyrase by the coumarins and the cyclothialidines revealed by X-ray crystallography. *The EMBO Journal*, *15*(6), 1412–1420.

Li, H., Wang, Y., & Liu, X. (2008). Plk1-dependent phosphorylation regulates functions of DNA topoisomerase IIalpha in cell cycle progression. *Journal of Biological Chemistry*, *283*(10), 6209–6221.

Li, H., Wang, Y., & Liu, X. (2008). Plk1-dependent phosphorylation regulates functions of DNA topoisomerase IIα in cell cycle progression. *Journal of Biological Chemistry*, *283*(10), 6209–6221.

Li, W., & Ma, H. (2006). Double-stranded DNA breaks and gene functions in recombination and meiosis. In *Cell Research* , *16*, 402–412.

Lipshultz, S. E., Scully, R. E., Lipsitz, S. R., Sallan, S. E., Silverman, L. B., Miller, T. L., Colan, S. D. (2010). Assessment of dexrazoxane as a cardioprotectant in doxorubicin-treated children with high-risk acute lymphoblastic leukaemia: long-term follow-up of a prospective, randomised, multicentre trial. *Lancet Oncology*, *11*(10), 950–961.

Liu, L. F. (1989). DNA Topoisomerase poisons as antitumor drugs. *Annual Review of Biochemistry*, *58*(1), 351–375.

Liu, L. F., & Miller, K. G. (1981). Eukaryotic DNA topoisomerases: two forms of type I DNA topoisomerases from HeLa cell nuclei. *Proceedings of the National Academy of Sciences of the United States of America*, *78*(6), 3487–3491.

Liu, L. F., & Wang, J. C. (1987). Supercoiling of the DNA template during transcription. *Proceedings of the National Academy of Sciences*, *84*(20), 7024–7027.

Lodisch, H., Berk, A., Zipursky, S. L., Matsudaira, P., Baltimore, D., & Darnell, J. (2000). Molecular Cell Biology. 4th edition. In *Molecular Cell Biology*, section 12.3, The role of topoisomerases in DNA.

Losada, A., & Hirano, T. (2005). Dynamic molecular linkers of the genome: The first decade of SMC proteins. *Genes and Development*, *19*(11), 1269-1287.

Lucas, I., Germe, T., Chevrier-Miller, M., & Hyrien, O. (2001). Topoisomerase II can unlink replicating DNA by precatenane removal. *EMBO Journal*, *20*(22), 6509–6519.

Lyu, Y. L., & Wang, J. C. (2003). Aberrant lamination in the cerebral cortex of mouse embryos lacking DNA topoisomerase IIbeta. *Proceedings of the National Academy of Sciences of the United States of America*, *100*(12), 7123–7128.

Marigny, K., Aubin, F., Burgot, G., Le Gall, E., & Gandemer, V. (2005). Particular cutaneous side effects with etoposide-containing courses: Is VP16 or etoposide phosphate responsible? *Cancer Chemotherapy and Pharmacology*, *55*(3), 244–250.

Martinez, R. and Chacon-Garcia, L. (2005). The search of DNA-intercalators as antitumoral drugs: What it worked and what did not work. *Current Medicinal Chemistry, 12*(2), 127-151.

McClendon, A. K., Rodriguez, A. C., & Osheroff, N. (2005). Human topoisomerase IIα rapidly relaxes positively supercoiled DNA: Implications for enzyme action ahead of replication forks. *Journal of Biological Chemistry*, *280*(47), 39337–39345.

Mergny J.L. and Helene C. (1998). G-quadruplex DNA: a target for drug design. *Nature Medicine, 4*, 1366-1367.

Michaelis, C., Ciosk, R., & Nasmyth, K. (1997). Cohesins: Chromosomal proteins that prevent premature separation of sister chromatids. *Cell*, *91*(1), 35–45.

Morham, S. G., Kluckman, K. D., Voulomanos, N., & Smithies, O. (1996). Targeted disruption of the mouse topoisomerase I gene by camptothecin selection. *Molecular and Cellular Biology*, *16*(12), 6804–6809.

Muñoz-Gámez, J. A., Quiles-Pérez, R., Ruiz-Extremera, A., Martín-Álvarez, A. B., Sanjuan-Nuñez, L., Carazo, A., Salmerón, J. (2011). Inhibition of poly (ADP-ribose) polymerase-1 enhances doxorubicin activity against liver cancer cells. *Cancer Letters*, *301*(1), 47–56.

Neale, M. J., Pan, J., & Keeney, S. (2005). Endonucleolytic processing of covalent protein-linked DNA double-strand breaks. *Nature*, *436*(7053), 1053–1057.

Ni, Z., Ye, T., Yu, Y., Gao, L., Fei, Y., Li, Q., Zeng, L. (2018). Triplex-forming oligonucleotide as a lighting-up switch for a DNA abasic site-binding fluorescent ligand. *Journal of Luminescence*, *198*(February), 193–197.

Nitiss, J. (2009). Targeting DNA topoisomerase II in cancer chemotherapy. *Nature Reviews Cancer*, *9*(5), 338–350.

Nitiss, J. L. (2009). DNA topoisomerase II and its growing repertoire of biological functions. *Nature Reviews Cancer*, *9*(5), 327–337.

Peciña, A., Smith, K. N., Mézard, C., Murakami, H., Ohta, K., & Nicolas, A. (2002). Targeted stimulation of meiotic recombination. *Cell*, *111*(2), 173-184.

Pommier, Y. (2013). Drugging topoisomerases: Lessons and Challenges. *ACS Chemical Biology*, *8*(1), 82–95.

Pommier, Y., & Cherfils, J. (2005). Interfacial inhibition of macromolecular interactions: Nature's paradigm for drug discovery. *Trends in Pharmacological Sciences*, *26*(3), 138–145.

Ragazzon, P. A., Garbett, N. C., & Chaires, J. B. (2007). Competition dialysis: A method for the study of structural selective nucleic acid binding. *Methods*, *42*(2), 173–182.

Rakoczy, P. E. (2001). Antisense DNA technology. *Methods in Molecular Medicine*, *47*, 89–104.

Ren, J., & Chaires, J. B. (1999). Sequence and structural selectivity of nucleic acid binding ligands. *Biochemistry*, *38*(49), 16067–16075.

Rigo, R., Palumbo, M., & Sissi, C. (2017). G-quadruplexes in human promoters: A challenge for therapeutic applications. *Biochimica et Biophysica Acta - General Subjects*, *1861*(5), 1399–1413.

Siddiqui-Jain, A., Grand, C. L., Bearss, D. J., & Hurley, L. H. (2002). Direct evidence

for a G-quadruplex in a promoter region and its targeting with a small molecule to repress c-MYC transcription. *Proceedings of the National Academy of Sciences*, *99*(18), 11593–11598.

Staker, B. L., Hjerrild, K., Feese, M. D., Behnke, C. A., Burgin, A. B., & Stewart, L. (2002). The mechanism of topoisomerase I poisoning by a camptothecin analog. *Proceedings of the National Academy of Sciences of the United States of America*, *99*(24), 15387–15392.

Thurston, D.E. (1999). Nucleic acid targeting: therapeutic strategies for the 21st century. *British Journal of Cancer*, *80*, 65-85.

Toscano-Garibay, J. D., & Aquino-Jarquin, G. (2014). Transcriptional regulation mechanism mediated by miRNA – DNA • DNA triplex structure stabilized by Argonaute. *Biochimica et Biophysica Acta - Gene Regulatory Mechanisms*, *1839*(11), 1079–1083.

Travers, A., & Muskhelishvili, G. (2015). DNA structure and function. *FEBS Journal*, *282*(12), 2279–2295.

Treszezamsky, A. D., Kachnic, L. A., Feng, Z., Zhang, J., Tokadjian, C., & Powell, S. N. (2007). BRCA1- and BRCA2-deficient cells are sensitive to etoposide-induced DNA double-strand breaks via topoisomerase II. *Cancer Research*, *67*(15), 7078–7081.

Tsai, F. T. F., Singh, O. M. P., Skarzynski, T., Wonacott, A. J., Weston, S., Tucker, A., Wigley, D. B. (1997). The high-resolution crystal structure of a 24-kDa gyrase B fragment from E. coli complexed with one of the most potent coumarin inhibitors, clorobiocin. *Proteins: Structure, Function and Genetics*, *28*(1), 41–52.

Tuduri, S., Crabbé, L., Conti, C., Tourrière, H., Holtgreve-Grez, H., Jauch, A., Pasero, P. (2009). Topoisomerase I suppresses genomic instability by preventing interference between replication and transcription. *Nature Cell Biology*, *11*(11),

1315–1324.

Uday Bhanu, M., & Kondapi, A. K. (2010). Neurotoxic activity of a Topoisomerase-I inhibitor, camptothecin, in cultured cerebellar granule neurons. *NeuroToxicology*, *31*(6), 730–737.

Van Dyke, M., & Nelson, L. (2013). Triple helix-interacting proteins and cancer. *OA Molecular Oncology*, *1*(1), 5.

Vos, S. M., Tretter, E. M., Schmidt, B. H., & Berger, J. M. (2011). All tangled up: How cells direct, manage and exploit topoisomerase function. *Nature Reviews Molecular Cell Biology*, *12*(12), 827-841.

Vrooman, L. M., Neuberg, D. S., Stevenson, K. E., Asselin, B. L., Athale, U. H., Clavell, L., Sallan, S. E. (2011). The low incidence of secondary acute myelogenous leukaemia in children and adolescents treated with dexrazoxane for acute lymphoblastic leukaemia: A report from the Dana-Farber Cancer Institute ALL Consortium. *European Journal of Cancer*, *47*(9), 1373–1379.

Wang, J. C. (1998). Moving one DNA double helix through another by a type II DNA topoisomerase: The story of a simple molecular machine. *Quarterly Reviews of Biophysics*, *31*(2), 107-144.

Wang, M., Yu, Y., Liang, C., Lu, A., & Zhang, G. (2016). Recent advances in developing small molecules targeting nucleic acid. *International Journal of Molecular Sciences*, *17*(6), 779.

Wang, X., Zhao, X., Malik, M., & Drlica, K. (2010). Contribution of reactive oxygen species to pathways of quinolone-mediated bacterial cell death. *Journal of Antimicrobial Chemotherapy*, *65*(3), 520–524.

Waring, M.J. and Wakelin, L.P. (2004). Forty Years On, in small molecule DNA and RNA binders (eds M. Demeunynck, C. Bailly and W.D. Wilson). doi:10.1002/3527601783.ch1.

Watson, J. D., & Crick, F. H. (1953). Molecular structure of nucleic acids; a structure for deoxyribose nucleic acid. *Nature*, *171*, 737–738.

Węsierska-Gądek, J., Schloffer, D., Gueorguieva, M., Uhl, M., & Skladanowski, A. (2004). Increased susceptibility of poly(ADP-ribose) polymerase-1 knockout cells to antitumor triazoloacridone C-1305 is associated with permanent G2 cell cycle arrest. *Cancer Research*, *64*(13), 4487–4497.

Winkler, D. (2011). Modelling topoisomerase i inhibition by minor groove binders. *Bioorganic and Medicinal Chemistry*, *19*(4), 1450–1457.

World Health Organization. (2015). WHO Model List of Essential Medicines - 19th List. *Essential Medicines*, (April), 1–45.

Wu, H. Y., Shyy, S., Wang, J. C., & Liu, L. F. (1988). Transcription generates positively and negatively supercoiled domains in the template. *Cell*, *53*(3), 433–440.

Wu, J., Phatnani, H. P., Hsieh, T. S., & Greenleaf, A. L. (2010). The phosphoCTD-interacting domain of Topoisomerase I. *Biochemical and Biophysical Research Communications*, *397*(1), 117–119.

Xu, H., Di Antonio, M., McKinney, S., Mathew, V., Ho, B., O'Neil, N. J., Aparicio, S. (2017). CX-5461 is a DNA G-quadruplex stabilizer with selective lethality in BRCA1/2 deficient tumours. *Nature Communications*, *8*, 14432. Doi: 10.1038/ncomms14432.

Yang, X., Li, W., Prescott, E. D., Burden, S. J., & Wang, J. C. (2000). DNA topoisomerase IIbeta and neural development. *Science (New York, N.Y.)*, *287*(5450), 131–134.

APPENDIX A

PREPARATION OF BUFFERS AND STOCK SOLUTIONS

1X BPES buffer (pH:7.0) solution for competition dialysis experiments:

6.0 mM Na_2HPO_4, 2.0 mM NaH_2PO_4, 1.0 mM Na_2EDTA, 185.0 mM NaCl.

Concentrations were arranged by using following equation;

$$M_1 \times V_1 = M_2 \times V_2$$

Thus for 1.0 L of 1X BPES buffer, following amounts of ingredients were mixed. Preparation of each ingredient will be given next.

- Na_2HPO_4 : 300 mM (stock) x V_1= 6 mM x 1000 mL; **V_1 = 20.0 mL,**
- NaH_2PO_4 : 400 mM (stock) x V_1= 2 mM x 1000 mL; **V_1 = 5.0 mL,**
- Na_2EDTA : 100 mM (stock) x V_1= 1 mM x 1000 mL; **V_1 = 10.0 mL,**
- NaCl : 500 mM (stock) x V_1= 185 mM x 1000 mL; **V_1 = 370.0 mL,**
- 500.0 mL deionized water added to 405.0 mL solution,
- pH was adjusted to 7.0 by NaOH and/or HCl,
- Total volume was arranged to 1.0 L with deionized (Millipore) water.

300 mM Na_2HPO_4 stock solution for 1X BPES buffer:

For 300.0 mM; 100.0 mL stock solution 4.26 gram was needed. Calculations are below;

n (mol) = molarity (M) x volume (L)

0.3 M x 0.1 L = 0.03 mol.

m = mol x M_w (141.96 g/mol for Na_2HPO_4)

0.03 x 141.96 = 4.26 g.

400 mM NaH_2PO_4 stock solution for 1X BPES buffer:

For 400.0 mM; 100.0 mL stock solution 4.80 gram was needed. Calculations are below;

n (mol) = molarity (M) x volume (L)

0.4 M x 0.1 L = 0.04 mol.

m = mol x M_w (119.98 g/mol for NaH_2PO_4)

0.04 x 119.98 = 4.80 g.

100 mM Na_2EDTA stock solution for 1X BPES buffer:

For 100.0 mM; 100.0 mL stock solution 3.72 gram was needed. Calculations are below;

n (mol) = molarity (M) x volume (L)

0.1 M x 0.1 L = 0.01 mol.

m = mol x M_w (372.24 g/mol for $Na_2EDTA.2H_2O$)

0.01 x 372.24 = 3.72 g.

pH of the solution must be 8.0 and arranged with concentrated NaOH and/or HCl.

500 mM NaCl stock solution for 1X BPES buffer:

For 500.0 mM; 1.0 L stock solution 29.22 gram was needed. Calculations are below;

n (mol) = molarity (M) x volume (L)

0.5 M x 1.0 L = 0.5 mol.

m = mol x M_w (58.44 g/mol for NaCl)

0.5 x 58.44 = 29.22 g.

10% (w/v) SDS stock solution for competition dialysis experiments:

10.0 g SDS (Sigma Aldrich, 862010) dissolved in 80.0 mL deionized water. Then volume was completed to 100.0 mL with deionized (Millipore) water.

1% Agarose Gel for Topoisomerase kit visualization:

1.00 g agarose (VWR-Amresco RA, N605) was dissolved in 100.0 mL of 1X TAE buffer in a microwave oven. After cooling down, 0.5 µg/mL of EtBr was added. Next, the gel was poured into "B2" Thermo Fischer Owl Easycast Mini Gel Electrophoresis system and left for the complete polymerization of agarose for about 30 to 40 minutes. 1X TAE buffer was poured on the gel and into the tray as a running buffer. Later, the samples were loaded into the wells. The gel was run at 100 Volt for 3 hours. Afterwards, the gel was stained with 1.0 µg/mL EtBr-water mixture for about 40 minutes followed by 30 minutes of de-staining with distilled water. Finally, the image of the gel was taken using BioRad XR+ molecular gel imager system.

1X TAE (Tris Acetate EDTA) buffer (pH:8.5) solution for agarose gel electrophoresis experiments:

40.0 mM Tris (pH: 7.6), 20.0 mM acetic acid, and 1.0 mM EDTA.

50X TAE buffer was prepared and diluted to 1X TAE buffer,

1X TAE buffer (1.0 L): 20 mL of 50X TAE buffer and 980 mL Millipore deionized water.

Preparation of 50X TAE buffer;

For 100.0 mL 50X TAE buffer, following amounts of ingredients were mixed. Preparation of ingredients will be given next.

- 24.20 g Tris base (M_w: 121.14 g/mol),
- 50.0 mL deionized water to dissolve Tris base,

- 5.71 mL glacial acetic acid,
- 10.0 mL; 0.5 M (pH:8.0) EDTA,
- Arrange pH around 8.5 using concentrated NaOH and/or HCl,
- Complete total volume to 100.0 mL with deionized water.

For 1X TAE buffer, dilute 20.0 mL of 50X TAE buffer with 980.0 mL deionized water.

0.5 M, pH: 8.0 EDTA solution for 50X TAE buffer:

For 500.0 mM; 100.0 mL stock solution 18.61 gram was needed. Calculations are below;

n (mol) = molarity (M) x volume (L)

0.5 M x 0.1 L = 0.05 mol.

m = mol x M_w (372.24 g/mol for $Na_2EDTA.2H_2O$)

0.05 x 372.24 = 18.61 g.

10.0 mM, pH: 7.5 Tris-HCl solution for drug dilutions:

For 10.0 mM; 100.0 mL stock solution 0.12 gram Tris and 20.0 µL 11.0 M HCl were needed. Calculations are below;

n (mol) = molarity (M) x volume (L)

0.01 M x 0.1 L = 0.001 mol.

m = mol x M_w (121.1 g/mol for Tris)

0.01 x 121.1 = 0.12 g. pH was arranged to 7.52 with HCl.

EtBr solution for staining of nucleic acids:

2.80 mg EtBr (Sigma Aldrich, E1510) was dissolved in 1.40 mL deionized water as a stock solution (2.0 µg/µL). To have 0.5 µg/mL EtBr in a gel and 1.0 µg/mL in staining water, following amounts of EtBr was added to the gel and staining water;

For 100.0 mL gel, we put 25.0 µL of EtBr stock solution into 100.0 mL 1X TAE buffer thus 50.0 µg EtBr will be in the gel. At the end, it makes 0.5 µg/mL.

For 400.0 mL staining water, we put 200.0 µL of EtBr into 400.0 mL distilled water therefore 400.0 µg EtBr will be in the water. At the end, it makes 1.0 µg/mL for staining.

APPENDIX B

OLIGONUCLEOTIDES USED IN COMPETITION DIALYSIS

Oligonucleotides given in Table B.1 were purchased from different companies and used throughout the competition dialysis experiments. Detailed instruction for preparation of double stranded oligonucleotides, DNA-RNA hybrid, RNA double stranded oligonucleotides, triplex DNA structures, and quadruplex DNA structures are given in chapter 3.2. Extinction coefficient values (ε) were either taken from the literature or purchased company. Monomoric units (nucleotide, base pair, triplet, and quartet) were used to prepare 75.0 μM of stock solutions.

Table B.1. Oligonucleotides used throughout the competition dialysis experiments.

Conformation	Index	Nucleic Acid	λ (nm)	ε ($M^{-1}cm^{-1}$)	Monomeric Unit	Company
Single-stranded DNA	1	poly(dA)	257	8600[a]	Nucleotide	Sigma-Aldrich P0887
	2	poly(dT)	264	8520[a]	Nucleotide	Sigma-Aldrich P6905
Single-stranded RNA	3	poly(rA)	258	9800[a]	Nucleotide	Merck
	4	poly(rU)	260	9350[a]	Nucleotide	Merck
Double-stranded DNA	5	$(dA)_{32}.(dT)_{32}$*	260	$(dA)_{32}$: 387400[b] $(dT)_{32}$: 259800[b]	Base pair	IDT
	6	poly(dA).poly(dT)	260	12000[a]	Base pair	Sigma-Aldrich P9764
	7	poly(dAdT).poly(dAdT)	262	13200[a]	Base pair	Sigma-Aldrich P0883
	8	poly(dGdC).poly(dGdC)	254	16800[a]	Base pair	Sigma-Aldrich P9389
	9	Micrococcus Lysodeikticus (72% GC)	260	13846[a]	Base pair	Sigma-Aldrich P8259
DNA-RNA Hybrid	10	poly(rA).poly(dT)*	258 264	poly(rA): 9800[a] poly(dT): 8520[a]	Base pair	Sigma-Aldrich

Double-stranded RNA	11	poly(rA).poly(rU)	260	14280[a]	Base pair	Sigma-Aldrich P1537
Triplex DNA	12	$(dA)_{32}.[(dT)_{32}]_2$*	260	$(dA)_{32}$: 387400[b] $(dT)_{32}$: 259800[b]	Triplet	IDT
	13	poly(dA).[poly(dT)]$_2$*	260 264	poly(dA).poly(dT): 12000[a] poly(dT): 8520[a]	Triplet	Sigma Aldrich
Triplex RNA	14	poly(rA).[poly(rU)]$_2$*	260	poly(rA).poly(rU): 14280[a] poly(rU): 9350[a]	Triplet	Sigma Aldrich & Merck
Quadruplex DNA	15	5'-$T_2G_{20}T_2$ -3' (OPC_2)	260	235600[b]	Quartet	IDT
	16	5'- TTGGG(TTAGGG)$_3$A -3' Tel24	260	244300[b]	Quartet	IDT

[a]from (Ragazzon *et al.*, 2007) ;[b]from Integrated DNA Technologies (IDT); *prepared from more than one nucleic acid – for detailed information see the section 3.2. Materials & Methods.

APPENDIX C

CONSTRUCTION OF STANDARD CURVES

C.1. Standard Curve Preparation:

The standard curves used in determination of the small molecule concentrations were prepared for each small molecule (azacyanine) using Fluorescence Spectroscopy.

For each small molecule, samples with varying concentrations of the small molecule were prepared from a stock solution of 50.0 μM. The concentration of the 50.0 μM stock solution was determined via UV-Vis spectroscopy using the calculated extinction coefficients for each molecule (Table 1). Samples were prepared by taking appropriate volumes of 50.0 μM small molecule stock solution, 1X BPES buffer, and 10%SDS. As shown in Table C1, all components (1X BPES buffer and 10%SDS) were kept at the same volume except the added small molecule stock solution. A representative calculation used in the preparation of the first and the second sample were given below. The concentrations of all the other samples were calculated the same way and the samples were prepared accordingly:

$$M_1 \times V_1 = M_2 \times V_2$$

- 50.0 μM x V_1 = 0.1 μM x 2000.0 μL; **V_1 = 4.0 μL**.
- 50.0 μM x V_2 = 0.2 μM x [2000+V_2 μL]; **V_2 = 8.0 μL –** 4.0 μL (already in the mixture) therefore **4.0 μL** from the stock is added to get a 0.2 μM sample.

Table C1. Preparation of samples for the standard curve construction:

	Concentration (µM)	Added drug volume (µL)	Total drug volume (µL)	10% SDS (µL)	1X BPES buffer (µL)	Total volume (µL)
Drug Stock Solution -50µM	0.1	**4.0**	4.0	32.0	1964.0	2000.0
	0.2	**4.0**	8.0	32.0	1964.0	2004.0
	0.3	**4.1**	12.1	32.0	1964.0	2008.1
	0.4	**4.1**	16.2	32.0	1964.0	2012.2
	0.5	**4.1**	20.3	32.0	1964.0	2016.3
	0.6	**4.2**	24.5	32.0	1964.0	2020.5
	0.7	**4.2**	28.7	32.0	1964.0	2024.7
	0.8	**4.2**	32.9	32.0	1964.0	2028.9
	0.9	**4.3**	37.2	32.0	1964.0	2033.2
	1.0	**4.3**	41.5	32.0	1964.0	2037.5
	1.1	**4.3**	45.8	32.0	1964.0	2041.8
	1.2	**4.4**	50.2	32.0	1964.0	2046.2
	1.3	**4.4**	54.6	32.0	1964.0	2050.6
	1.4	**4.4**	59.1	32.0	1964.0	2055.1
	1.5	**4.5**	63.6	32.0	1964.0	2059.6
	1.8	**11.1**	74.7	32.0	1964.0	2070.7
	2.1	**11.6**	86.3	32.0	1964.0	2082.3
	2.6	**23.3**	109.6	32.0	1964.0	2105.6
	3.2	**24.8**	134.4	32.0	1964.0	2130.4
	3.7	**26.0**	160.4	32.0	1964.0	2156.4
	4.3	**27.2**	187.5	32.0	1964.0	2183.5
	4.9	**28.4**	216.0	32.0	1964.0	2212.0
	5.5	**29.8**	245.8	32.0	1964.0	2241.8

Afterwards, the emission spectra for all samples were collected using Varian, Cary Eclipse fluorescence spectrometer using the parameters given below;

Azamethyl, Azaethyl, Azapropyl, Azabutyl, Azaisopropyl, and Azaisobutyl;

Excitation: 324 nm. Emission: 325-675 nm. Slits: 2.5/5.0. Scan rate: 300 nm/min.

Aza4;

Excitation: 389 nm. Emission: 390-650 nm. Slits: 2.5/5.0. Scan rate: 300 nm/min.

Aza5;

Excitation: 399 nm. Emission: 400-750 nm. Slits: 2.5/5.0. Scan rate: 300 nm/min.

Later, two standard curves were constructed for each small molecule using the fluorescence intensities at two different wavelengths (reference wavelengths). Two equations from "fluorescence intensity vs. the concentration" graphs were derived for each sample by performing linear regression. These equations were used to calculate the concentrations of the small molecules in the samples obtained from each of the competition dialysis cassettes (section 3.3). The concentrations obtained for a sample, by using both of the standard curves, are averaged out, and recorded as the final concentration.

The reason behind choosing two different wavelengths was to minimize our experimental errors. The first wavelength we choose was the wavelength where the maximum absorbance was occurring. However, at that wavelength the fluorescence intensity was out of range for our concentrated samples hence we could not observe any absorbance for the first chosen wavelength. Therefore, we chose another wavelength whose intensity was not out of range for the small molecule concentration we have examined.

Since all azacyanine molecules have different chemical structures (Figure 12), obtained spectra from fluorescence spectrophotometer were different for some of the molecules. Therefore, different excitation wavelengths were chosen as a reference for each molecule's standard curve constructions. Reference excitation wavelengths were 379 nm & 440 nm for Azamethyl, Azaethyl, Azapropyl, Azabutyl, Azaisopropyl, and Azaisobutyl, 445 nm & 465 nm for Aza4, and 475 nm & 520 nm for Aza5.

Small molecule concentrations of the samples obtained from 24 hours long competition dialysis (section 3.3) were calculated based on the equations obtained through the linear regression. Here, the measured fluorescence intensity belonging to a sample obtained from the dialysis cassette containing a certain nucleic acid structure was put in place of Y value on the equation after dilution corrections. Then, the concentrations corresponding to the X value on the equation were calculated.

C.2. Standard Curve for Azamethyl:

a.

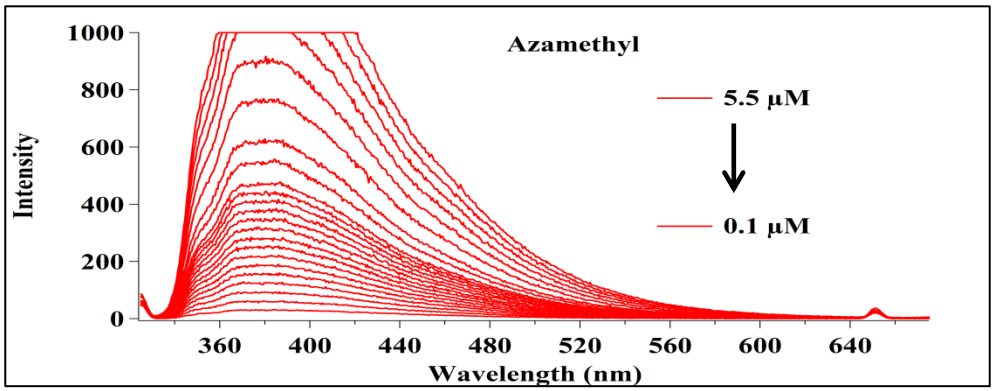

b.

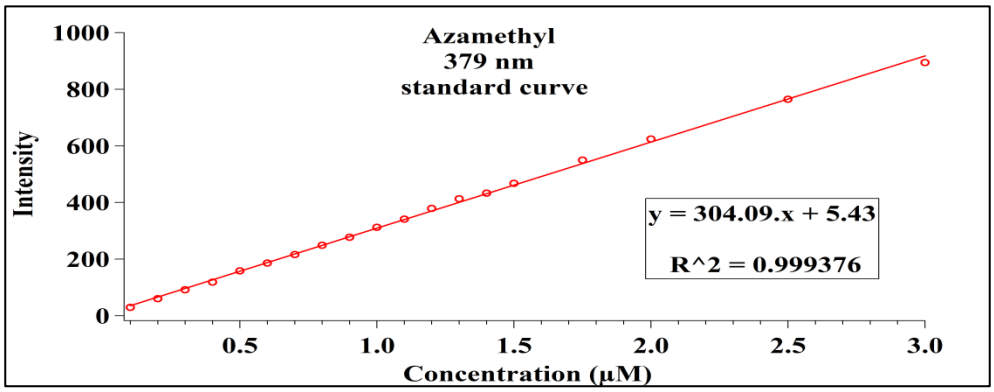

c.

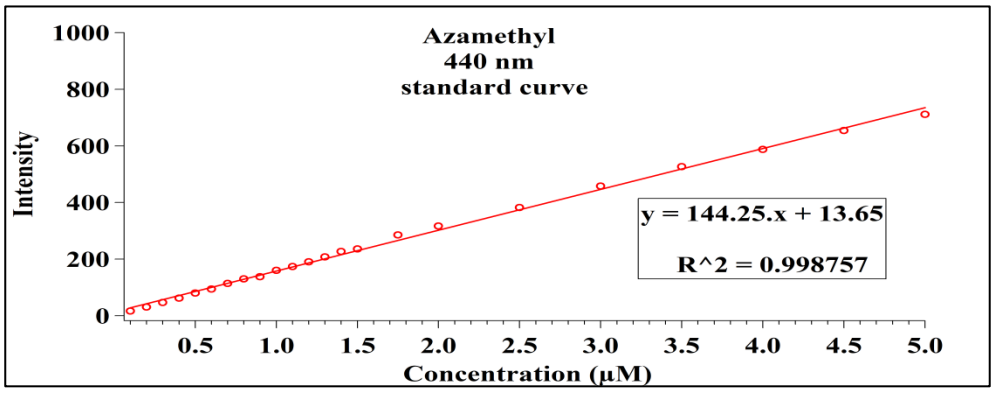

Figure C.1. Standard curve construction for Azamethyl. a. Fluorescence intensity vs wavelength measurements for different concentration of Azamethyl. b. The standard

curve using the fluorescence intensities at 379 nm vs concentration (circles). c. The standard curve using the fluorescence intensities at 440 nm vs concentration (circles). The linear regression lines and the obtained equations were also given on the graphs in b and c.

C.3. Standard Curve for Azaethyl:

a.

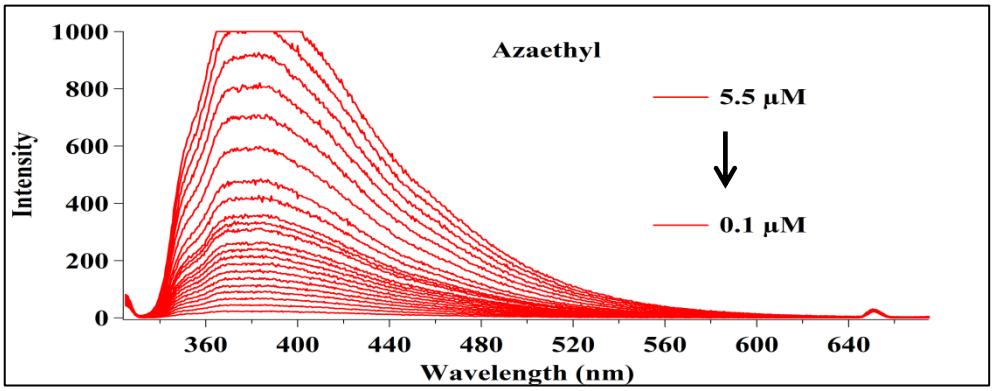

b.

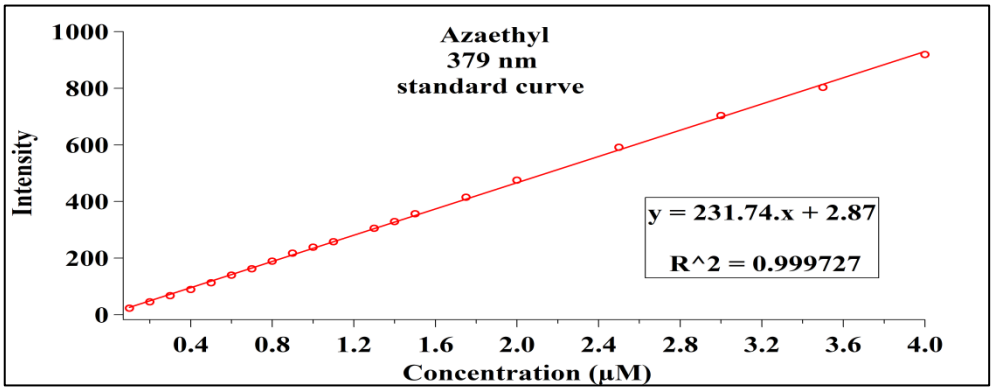

c.

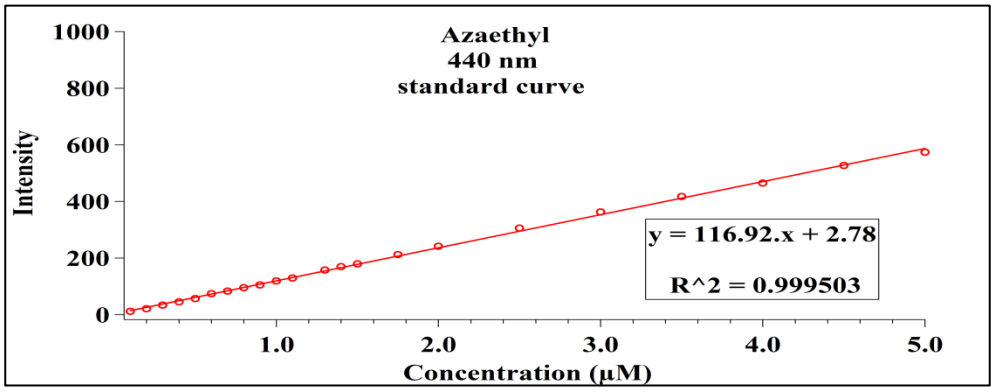

Figure C.2. Standard curve construction for Azaethyl. a. Fluorescence intensity vs wavelength measurements for different concentration of Azaethyl. b. The standard curve using the fluorescence intensities at 379 nm vs concentration (circles). c. The standard curve using the fluorescence intensities at 440 nm vs concentration (circles). The linear regression lines and the obtained equations were also given on the graphs in b and c.

C.4. Standard Curve for Azapropyl:

a.

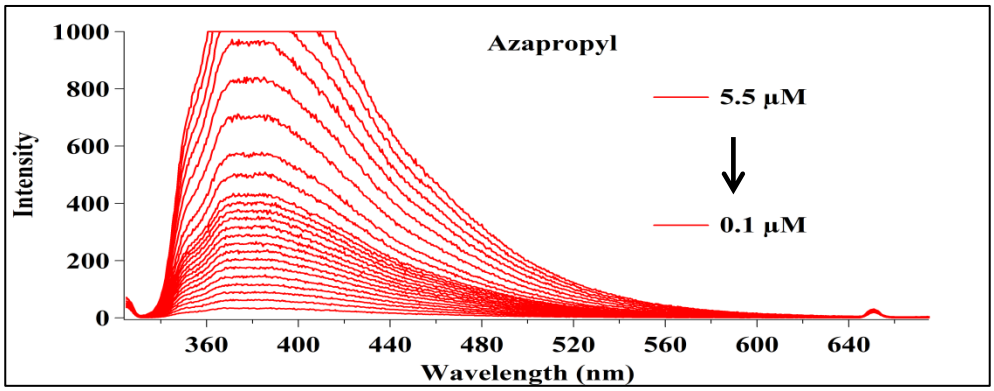

b.

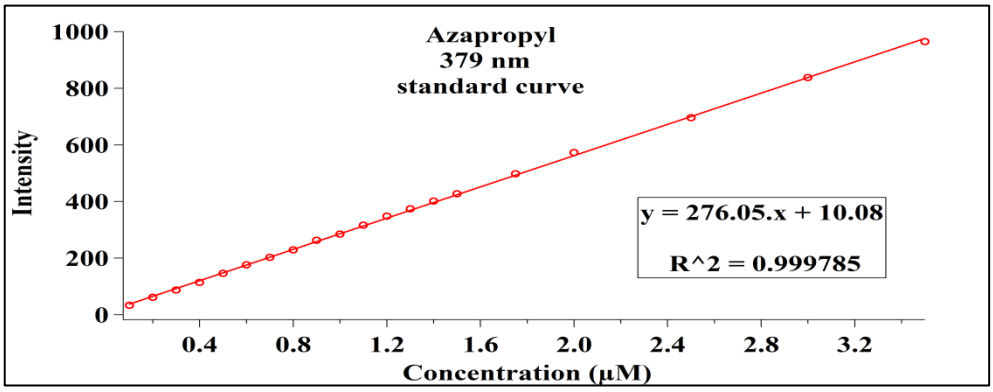

c.

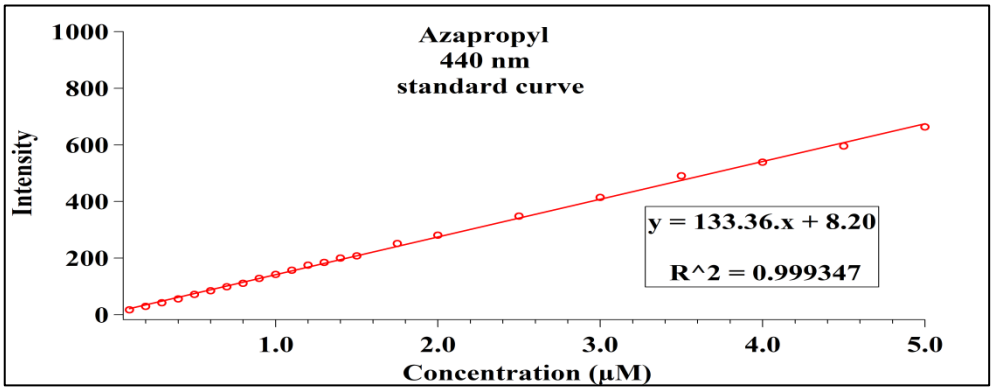

Figure C.3. Standard curve construction for Azapropyl. a. Fluorescence intensity vs wavelength measurements for different concentration of Azapropyl. b. The standard curve using the fluorescence intensities at 379 nm vs concentration (circles). c. The standard curve using the fluorescence intensities at 440 nm vs concentration (circles). The linear regression lines and the obtained equations were also given on the graphs in b and c.

C.5. Standard Curve for Azabutyl:

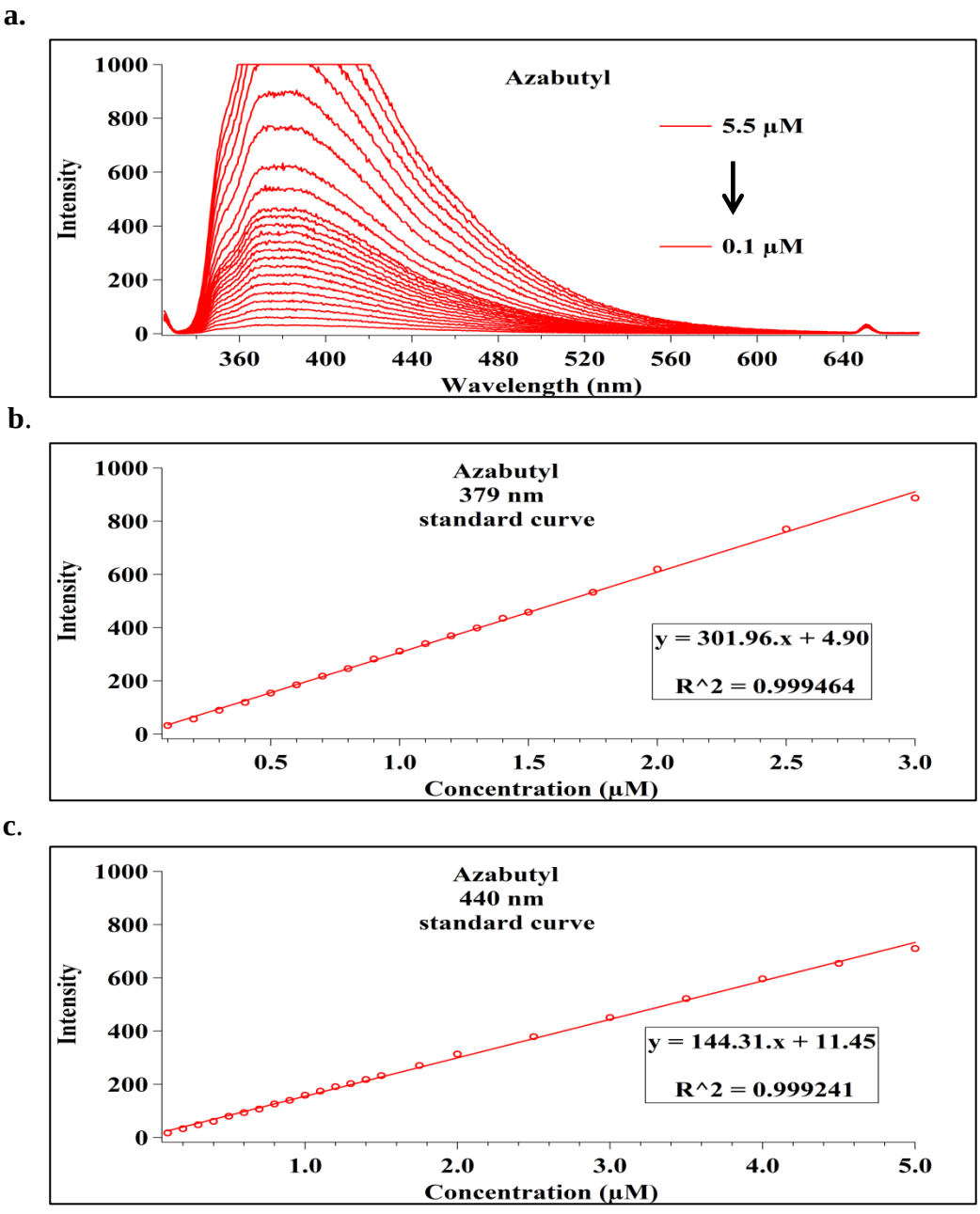

Figure C.4. Standard curve construction for Azabutyl. a. Fluorescence intensity vs wavelength measurements for different concentration of Azabutyl. b. The standard

curve using the fluorescence intensities at 379 nm vs concentration (circles). c. The standard curve using the fluorescence intensities at 440 nm vs concentration (circles). The linear regression lines and the obtained equations were also given on the graphs in b and c.

C.6. Standard Curve for Azaisopropyl:

a.

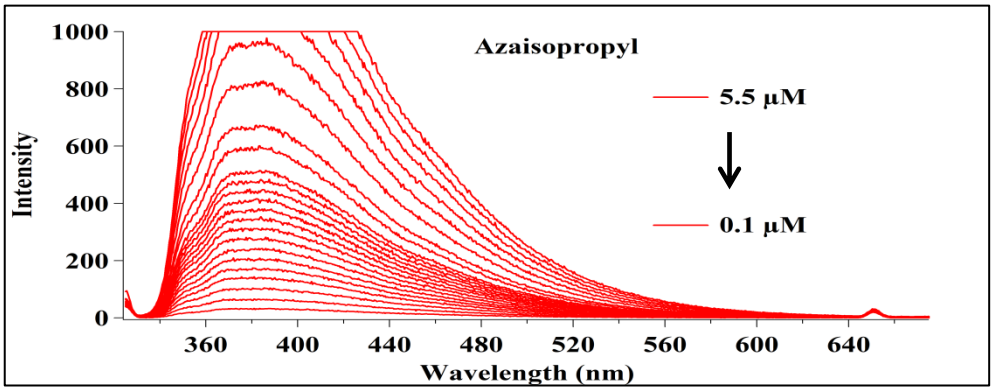

b.

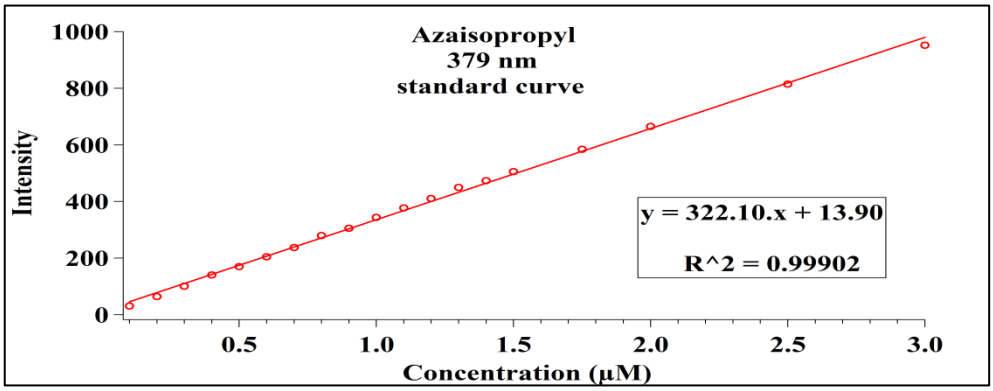

c.

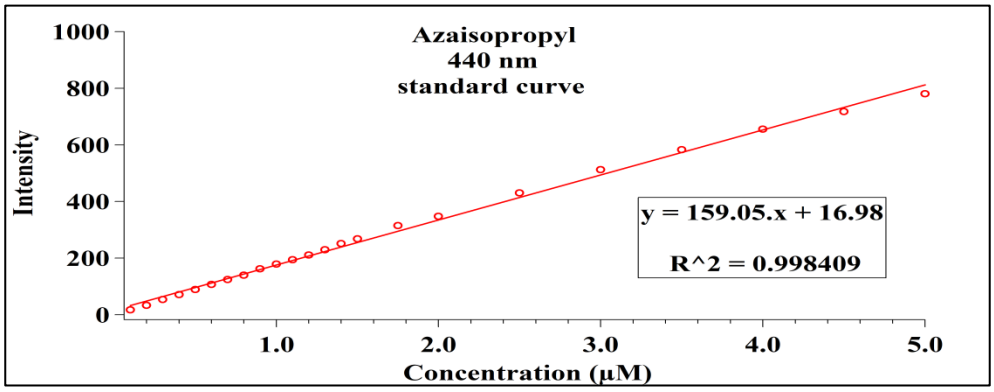

Figure C.5. Standard curve construction for Azaisopropyl. a. Fluorescence intensity vs wavelength measurements for different concentration of Azaisopropyl. b. The standard curve using the fluorescence intensities at 379 nm vs concentration (circles). c. The standard curve using the fluorescence intensities at 440 nm vs concentration (circles). The linear regression lines and the obtained equations were also given on the graphs in b and c.

C.7. Standard Curve for Azaisobutyl:

a.

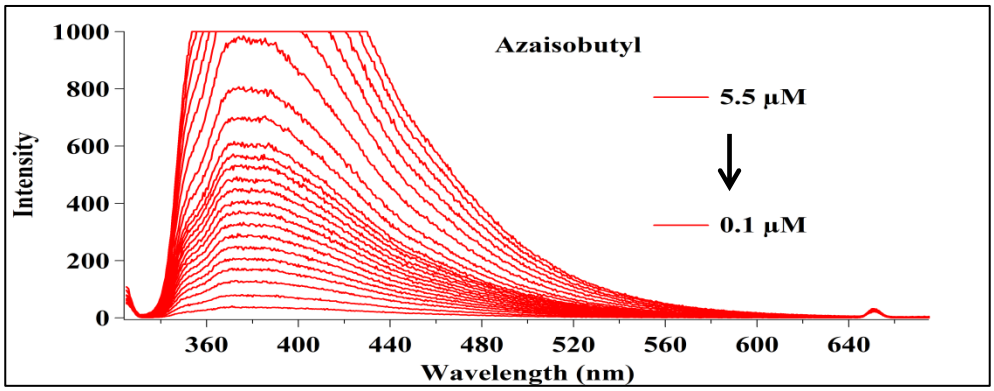

b.

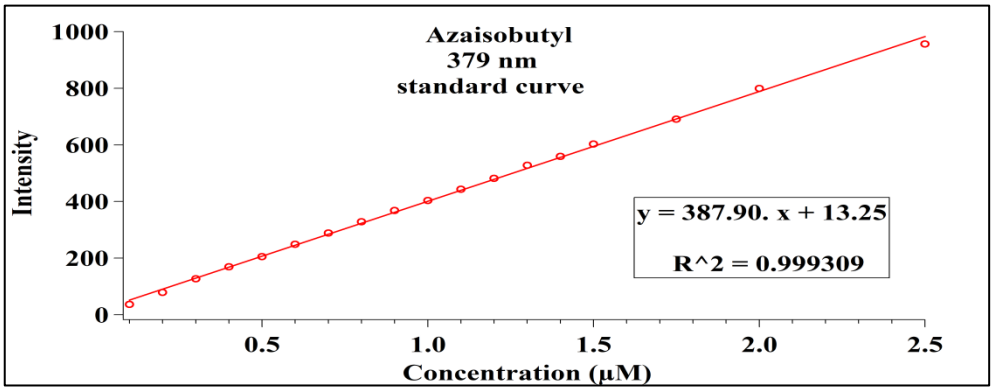

c.

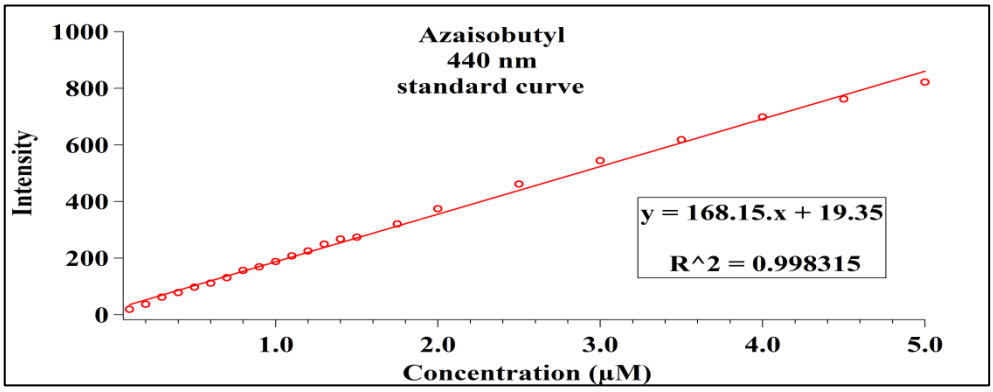

Figure C.6. Standard curve construction for Azaisobutyl. a. Fluorescence intensity vs wavelength measurements for different concentration of Azaisobutyl. b. The standard curve using the fluorescence intensities at 379 nm vs concentration (circles). c. The standard curve using the fluorescence intensities at 440 nm vs concentration (circles). The linear regression lines and the obtained equations were also given on the graphs in b and c.

C.8. Standard Curve for Aza4:

a.

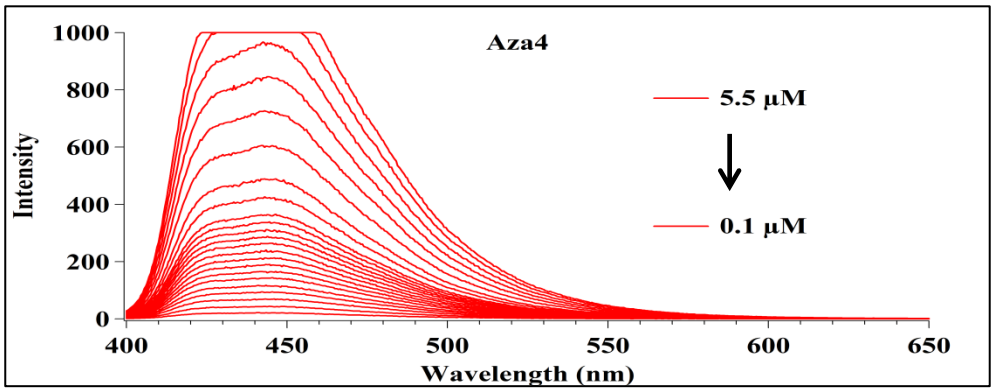

b.

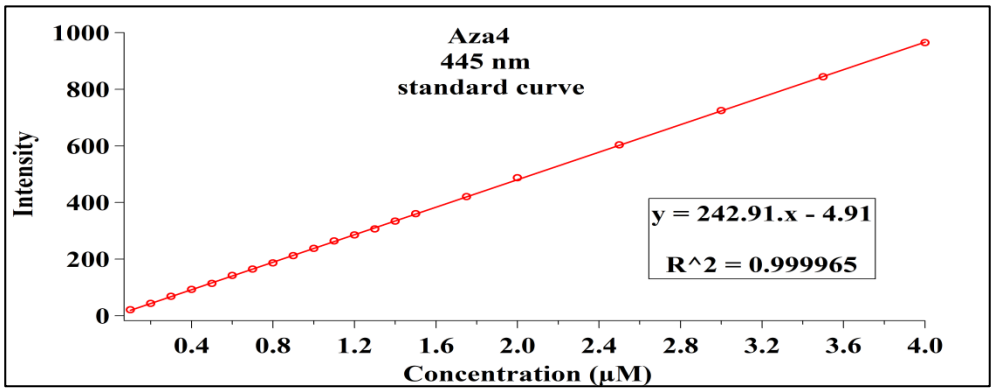

c.

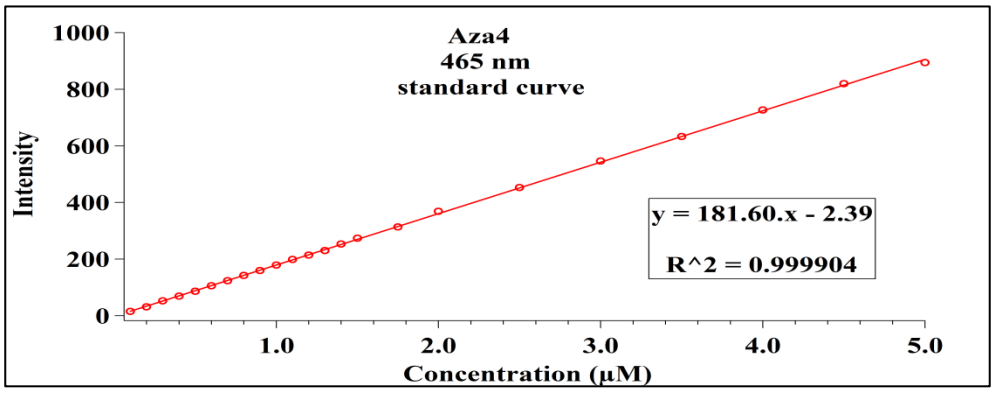

Figure C.7. Standard curve construction for Aza4. a. Fluorescence intensity vs wavelength measurements for different concentration of Aza4. b. The standard curve

using the fluorescence intensities at 445 nm vs concentration (circles). c. The standard curve using the fluorescence intensities at 465 nm vs concentration (circles). The linear regression lines and the obtained equations were also given on the graphs in b and c.

C.9. Standard Curve for Aza5:

a.

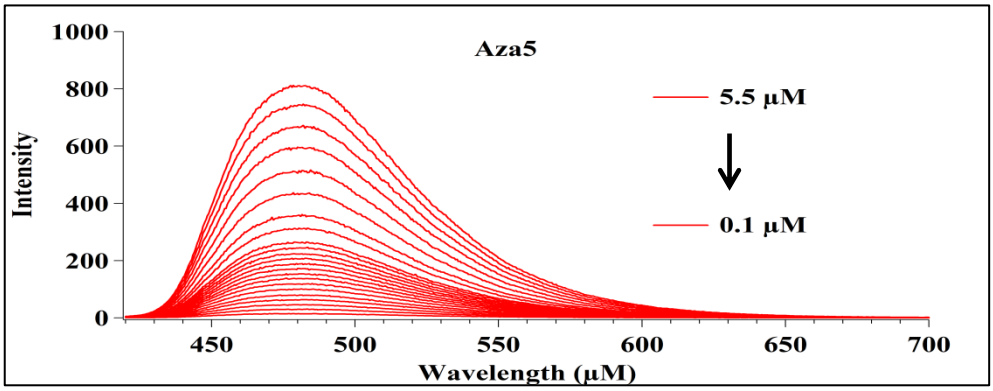

b.

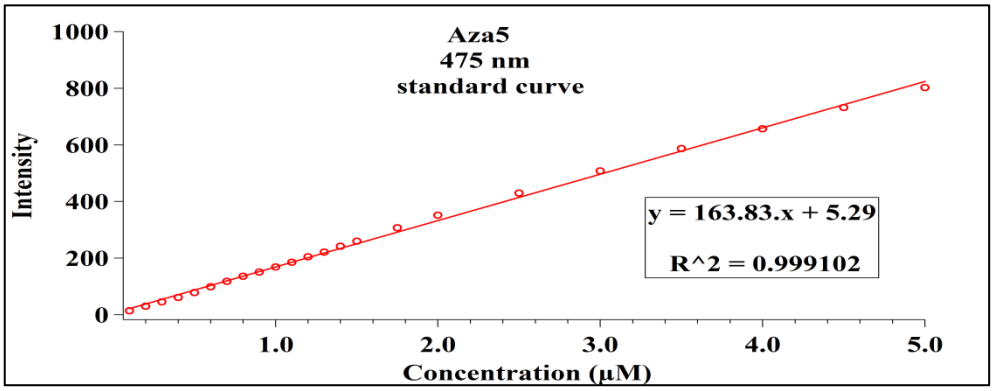

c.

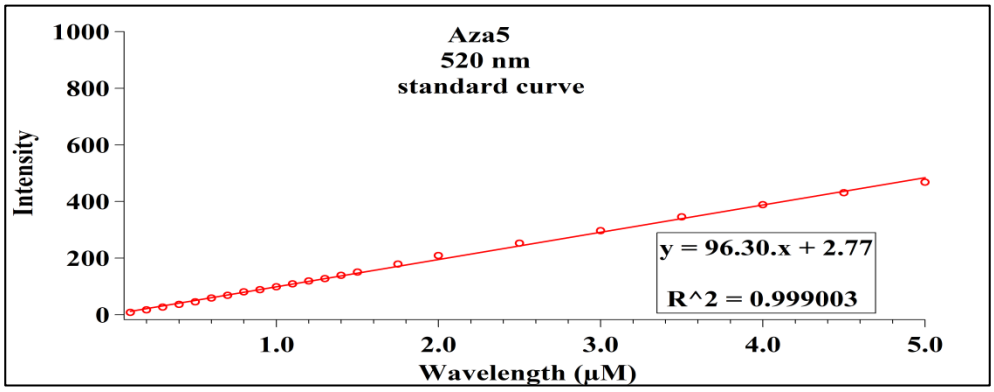

Figure C.8. Standard curve construction for Aza5. a. Fluorescence intensity vs wavelength measurements for different concentration of Aza5. b. The standard curve using the fluorescence intensities at 475 nm vs concentration (circles). c. The standard curve using the fluorescence intensities at 520 nm vs concentration (circles). The linear regression lines and the obtained equations were also given on the graphs in b and c.

Table C2. Equations derived from standard curves for each azacyanine molecule:

	379 nm	**440 nm**
Azamethyl	y = 304.09.x + 5.43	y = 144.25.x + 13.65
Azaethyl	y = 231.74.x + 2.87	y = 116.92.x + 2.78
Azapropyl	y = 276.05.x + 10.08	y = 133.36.x + 8.20
Azabutyl	y = 301.96.x + 4.90	y = 144.31.x + 11.45
Azaisopropyl	y = 322.10.x + 13.90	y = 159.05.x + 16.98
Azaisobutyl	y = 387.90.x + 13.25	y = 168.15.x + 19.35
	445 nm	**465 nm**
Aza4	y = 242.91.x – 4.92	y = 181.60.x – 2.39
	475 nm	**520 nm**
Aza5	y = 163.83.x + 5.29	y = 96.30.x + 2.77

APPENDIX D

STATISTICAL ANALYSIS

The statistical analysis of our competition dialysis data is given in Table D1. The competition dialysis data (C_b/C_f values) represented here is the mean of two independent experiments (see section 3.3). In our statistical analysis confidence levels were taken as 99% and 95%. $p<0.01$ and $p<0.05$ were considered as significantly different from the positive control that is small molecule concentration in the cassette containing only the buffer solution. The Kruskal Wallis non-parametric test was performed for all molecules except Azaisopropyl. Since the Azaisopropyl data showed a normal distribution (Kolmorogov-Smirnow: $p=0.200$ and Shapiro-Wilk: $p=0.620$) one-way ANOVA followed by Bonferronni and Sidak Post-Hoc tests were performed for it.

In the Table D1 statistical analysis results for the azacyanines that are found to be binding significantly to a certain nucleic acid structure are presented. If the statistical analysis results were not given in the table below, it signifies that the binding of the small molecule to that particular nucleic acid structure was not found statistically significant. “Dashes” on the Table D1 means that the p values exceeded 0.05 and therefore were found as non-significant.

Table D.1. Statistical analysis results of competition dialysis experiments:

	Azamethyl		**Aza4**		**Aza5**	
	C_b/C_f	p-value	C_b/C_f	p-value	C_b/C_f	p-value
poly(dA).[poly(dT)]$_2$ triplex DNA	**11.7**	**0.012**	**10.6**	**0.015**	**12.3**	**0.007**
(dA)$_{32}$.[(dT)$_{32}$)]$_2$ triplex DNA	**10.7**	**0.014**	**2.1**	**0.020**	**5.4**	**0.009**
5'-T$_2$G$_{20}$T$_2$-3' - quadruplex DNA	**2.5**	**0.017**	**0.9**	**0.027**	**4.1**	**0.011**
poly(rA).[poly(rU)]$_2$ triplexRNA	**1.7**	**0.021**	**-**	**-**	**1.9**	**0.016**
***Micrococcus Lysodeicticus*- dsDNA**	**1.3**	**0.026**	**-**	**-**	**1.1**	**0.021**
5'-TTGGG [TTAGGG]$_3$A - 3' quadruplexDNA	**1.1**	**0.032**	**-**	**-**	**2.4**	**0.013**
poly(dGdC).poly(dGdC)dsDNA	**1.1**	**0.038**	**-**	**-**	**0.6**	**0.033**
poly(dA).poly(dT) dsDNA	**0.9**	**0.047**	**0.7**	**0.038**	**0.8**	**0.026**

Table D.1. Statistical analysis results of competition dialysis experiments:

	Azaethyl		**Azapropyl**		**Azabutyl**		**Azaisopropyl**		**Azaisobutyl**	
	C_b/C_f	p-value	C_b/C_f	p-value	C_b/C_f	p-value	C_b/C_f	p-value	C_b/C_f	p-value
poly(dA).[poly(dT)]$_2$ triplex DNA	**6.9**	**0.026**	**5.2**	**0.024**	**4.9**	**0.016**	**-**	**-**	**-**	**-**
(dA)$_{32}$.[(dT)$_{32}$)]$_2$ triplex DNA	**1.4**	**0.033**	**0.8**	**0.041**	**-**	**-**	**-**	**-**	**2.5**	**0.198**
5'-T$_2$G$_{20}$T$_2$-3' - quadruplex DNA	**0.8**	**0.044**	**1.3**	**0.031**	**4.6**	**0.021**	**-**	**-**	**-**	**-**
poly(rA).[poly(rU)]$_2$ triplexRNA	-	-	-	-	-	-	-	-	-	-
***Micrococcus Lysodeicticus*-dsDNA**	-	-	-	-	**0.6**	**0.028**	-	-	-	-
5'-TTGGG [TTAGGG]$_3$A - 3' quadruplexDNA	-	-	-	-	**0.6**	**0.038**	-	-	-	-
poly(dGdC).poly(dGdC)dsDNA	-	-	-	-	-	-	-	-	-	-
poly(dA).poly(dT) dsDNA	-	-	-	-	-	-	-	-	-	-